THE TRANSLATIONAL NTPASE OLA1 IS AN RNA BINDING PROTEIN

JESSICA SEMMELROCK

Bachelor of Science, University of Lethbridge, 2020

A thesis submitted
in partial fulfilment of the requirements for the degree of

MASTER OF SCIENCE

in

BIOCHEMISTRY

Department of Chemistry and Biochemistry
University of Lethbridge
LETHBRIDGE, ALBERTA, CANADA

THE TRANSLATION NTPASE OLA1 IS AN RNA BINDING PROTEIN

JESSICA SEMMELROCK

Date of Defense: Jul 07, 2023

Dr. Hans-Joachim Wieden Dr. Trushar Patel Thesis Co-Supervisors	Professor Associate Professor	Ph.D. Ph.D.
Dr. Ute Kothe Thesis Examination Committee Member	Professor	Ph.D.
Dr. Borries Demeler Thesis Examination Committee Member	Professor	Ph.D.
Dr. Michael Gerken Chair, Thesis Examination Committee	Professor	Ph.D.

DEDICATION

To future Wieden lab members, I hope this is useful to you.

ABSTRACT

With ribosome-dependent protein synthesis being essential to life, previously overlooked components of the ribosome regulome can potentially become novel therapeutic targets. Obg-like ATPase 1 (OLA1) – or YchF in bacteria – is among several universally conserved guanosine nucleotide-dependent molecular switches, called GTPases, that interact with the ribosome throughout its life cycle and provide an important fitness advantage. However, OLA1's exact cellular role and molecular mechanism of action are poorly understood. Structural modelling reveals that OLA1 can form a tRNA-bound complex in the ribosomal A site, overall mimicking the structure of the Elongation Factor-Tu ternary complex (EF-Tu•GTP•aminoacyl-tRNA) and several other translational GTPases. Using electrophoretic mobility shift assays (EMSAs) and nitrocellulose filtration, I reveal that human OLA1 can bind tRNA independent of the ribosome. Integration of these results with previous studies suggests a role for OLA1 in ribosome maintenance.

LAY SUMMARY

All cells require proteins, which are made by a large biomolecular machine called the ribosome, in a process referred to as translation. There are still many details to learn about the creation, function, and recycling of ribosomes for the goal of developing therapeutics. For example, Obg-like ATPase 1 (OLA1) is believed to help with ribosome function and is involved in stress response, infection, and cancer. Yet, OLA1 is poorly understood. By comparing the structure of OLA1 to other better-defined proteins also involved in translation, I hypothesize that OLA1 interacts with a type of molecule called tRNA. This study uses biochemistry to define the interaction between OLA1 and tRNA. OLA1 from humans and *E. coli* differ in how they bind to tRNA. Combining these results with what has been reported previously suggests that OLA1's cellular role is likely associated with ribosome maintenance.

ACKNOWLEDGEMENTS

Thank you to everyone who enabled me to pursue my love of science. To my mom, who noticed my inquisitive mind early on and who inspired me with her flurry of creative projects. To my dad, an S-tier role model for steadfast work ethic and healthy living. To my stepdad, an all-around homie. And, of course, my siblings, who helped make me who I am today. To Cass and our LRC pals. To Abbie, Maya, Miranda, Theo, Simon, the Lysyk family, and many more. I love you all!

Thank you to Nehal and Joe for supporting me through my first independent-study experience in my undergraduate days. HJ, thank you so much for opening the doors to an exciting world of RNA and translation research and for accepting me into your lab as a graduate student. Thank you, Trushar, for agreeing to be my co-supervisor and for the valuable help over the years. Thank you to Ute and Borries. You two have been inspiring role models. I am glad for every one of our conversations.

I am incredibly grateful to my past and present Wieden, Kothe, Patel, Demeler, and Thakor lab colleagues. Especially Harland, a talented scientist and mentor who taught me everything he could. And the wonderful Fan and Sarah, who I would not have been able to complete this project without. To my summer students, Shayne and Maria, you were both joyous to mentor. To the iGEM teams I've been a part of, I am so proud of our hard work. Emily, I enjoyed witnessing your inspiring willpower. Luc and Amy, thanks for lending a hand when I was recovering from my ACL tear and surgery. Thanks to Davi, Julia, Fabian, Kristi, Marcel, Syd, Amanda, Dora, Maduni, Hope, Tim, Daniel, and Gayatri for the much-needed coffee chats and hangouts. I cherish all the laughs, all the constructive criticism, all the nerding out, and all the fun times.

Finally, I would like to thank the UofL administrative and janitorial staff. The jobs you do lay the foundation of our institution. I appreciate your exceptional work, especially through the pandemic. I wouldn't be where I am without you. Thank you so much.

TABLE OF CONTENTS

DEDICATION iii

ABSTRACT iv

LAY SUMMARY v

ACKNOWLEDGEMENTS vi

TABLE OF CONTENTS vii

LIST OF TABLES x

LIST OF FIGURES xi

LIST OF ABBREVIATIONS xii

CHAPTER 1: INTRODUCTION 1

General Overview 1

The Central Dogma of Biology 1

The Ribosome 3

Overview of the Ribosome Cycle 4

Biogenesis of Ribosomes, tRNA, and mRNA 4

Translation Initiation 6

Elongation 8

Termination and Ribosome Recycling 9

Auxiliary Translation Factors: GTPases 11

The Conserved Nucleotide Binding Domain 12

GTPase Activating Factors (GAFs) 12

Guanine Exchange Factors (GEFs) 14

Molecular Mimicry Between GTPases 14

A History and Analysis of OLA1, A Universally Conserved NTPase 16
OLA1 Provides a Fitness Advantage Across the Domains of Life 16
OLA1 Structure and Translation Factors: Intra- and Inter-Similarities 17
Promiscuous Nucleotide Binding 24
Nucleic Acid Binding as Suggested by Molecular Mimicry 26
Existing OLA1 Hypotheses 26
A Hypothesis Built on Molecular Mimicry 30
Objectives I and II 31
CHAPTER 2: MATERIALS AND METHODS 33
Buffers and Reagents. 33
Plasmid DNA Maxiprep. 33
In Vitro Transcription and Purification of $tRNA^{Lys}$ and $tRNA^{Phe}$. 34
Protein Purification. 36
Ribosome Isolation. 37
Nondenaturing Electrophoretic Mobility Shift Assays (EMSAs). 37
Silver Staining of Proteins and Nucleic Acids. 38
Aminoacylation of $tRNA^{Lys}$ and $tRNA^{Phe}$ 38
Nitrocellulose Filtration Assays. 39
Microscale Thermophoresis Helicase Assays. 40
Microscale Thermophoresis RNA and Protein Affinity Check. 41
CHAPTER 3: RESULTS 43
3.1 Objective 1: tRNA Binding 43
Aminoacylation of tRNA. 43

Deacylated tRNA Forms a Complex with OLA1 43

*Ec*OLA1 Does Not Increase the Fraction of Deacylated tRNA on Vacant Ribosomes..... 48

3.2 Objective 2: RNA Remodeling 49

RNA Remodeling Activity on the *E. coli* Sarcin-Ricin Loop. 49

CHAPTER 4: DISCUSSION..... 53

4.1 Objective 1: tRNA Binding..... 53

Correlation Between tRNA Structure and Function 54

Differences in tRNA Binding Between hOLA1 and *Ec*OLA1..... 54

Ribosome-Aided Stabilization of OLA1-tRNA Complexes..... 56

Experimental Limitations 57

4.2 Objective 2: RNA Remodeling 58

Experimental Limitations 59

4.3 OLA1 and Translation: A Holistic View 60

Differences Between Bacteria and Eukaryotes: A Hybrid Hypothesis..... 60

CHAPTER 5: CONCLUSIONS AND FUTURE DIRECTIONS..... 63

5.1 An Update to the Proposed Functional Cycle of OLA1..... 63

5.2 Future Directions: Advancing Our Understanding of the OLA1 Functional Cycle. 64

BIBLIOGRAPHY 67

APPENDIX I. SUPPLEMENTAL MATERIALS TO CHAPTER 3 86

Objective 1: tRNA Binding..... 86

Objective 2: RNA Remodeling 88

LIST OF TABLES

Table 1. Primers for the amplification of $tRNA^{Lys}$ and $tRNA^{Phe}$ 35

Table 2. SRL, ASF, and RD RNA and complementary DNA oligos 40

Table 3. Dissociation constants (K_D's) 47

LIST OF FIGURES

Figure 1. The central dogma of biology illustrates the flow of genetic information 2

Figure 2. The general cycle of the ribosome 4

Figure 3. Mature tRNA folds into a distinct structure 6

Figure 4. Structural mimicry of complexes formed by trGTPases 15

Figure 5. The structure of OLA1 is similar across the domains of life 18

Figure 6. OLA1 shares domains with tRNA-binding proteins 20

Figure 7. Multiple sequence alignment of OLA1 homologs summarizing conserved motifs. 24

Figure 8. Aminoacylation of tRNA indicates correct folding of $tRNA^{Phe}$ 43

Figure 9. Comparison of $tRNA^{Phe}$ binding to TruB, EF-Ts, and GST-hOLA1•*Ec*tRNA or *Ec*OLA1 45

Figure 10. Concentration dependence of $tRNA^{Phe}$ binding 47

Figure 11. *Ec*OLA1 does not increase the fraction of $tRNA^{Phe}$ retained by 70S ribosomes 48

Figure 12. Helicase assay substrate and workflow 50

Figure 13. Changes in normalized fluorescence 52

Figure 14. The proposed functional cycle of OLA1 63

SFigure 1. Human and E. coli OLA1 co-elute with rRNA and tRNA 86

SFigure 2. Silver staining of RNA and protein 86

SFigure 3. EcOLA1 does not shift the migration of IVT $tRNA^{Phe}$ 87

SFigure 4. The (A) SRL and (B) ASF conformations 88

SFigure 5. Alternate helicase assay substrate 88

SFigure 6. Helicase assay results 89

SFigure 7. MST binding affinity results 89

LIST OF ABBREVIATIONS

5P-Seq	5′ monophosphate sequencing
aa	Amino acid
aaRS	Aminoacyl-tRNA synthetase
ABCE1	ATP-binding cassette subfamily E member 1
ADP	Adenosine diphosphate
ArfA/B	Alternative rescue factor A/B
ASF	A-site finger
A-site	Aminoacyl-site
*At*OLA1	*Arabidopsis thalia* OLA1
ATP	Adenosine triphosphate
BARD1	BRCA1 associated RING domain 1
BRCA1	Breast cancer gene 1
BSA	Bovine serum albumin
CPA1	Carbamoyl phosphate synthetase A1
cryo-EM	Cryogenic electron microscopy
DNA	Deoxyribonucleic acid
DOC45	DNA damage-regulated overexpressed in cancer 45
dsDNA	Double-stranded DNA
*Ec*OLA1	*Escherichia coli* OLA1
EF	Elongation factor
EF-Ts	Elongation factor thermal stable
EF-Tu	Elongation factor thermal unstable
EMSA	Electrophoretic mobility shift assays
E-site	Exit-site
GAF	GTPase activating factor
GAP1	GTPase activating protein 1
GBP45	GTP-binding protein with a molecular weight of 45 kD
G-domain	Guanine domain
GDP	Guanosine diphosphate
GEF	Guanine exchange factors
GTBP9	GTP-binding protein 9
GTP	Guanosine triphosphate
GTPases	Guanosine triphosphatase hydrolyzing enzymes
*Hi*OLA1	*Haemophilus influenzae* OLA1
hOLA1	Human OLA1
IF	Initiation factors
IRES	Internal ribosome entry site
i-tRAP	Individual tRNA acylation PCR
LSU	Large subunit
mRNA	Messenger RNA
MST	Microscale thermophoresis
Nano-tRNAseq	Nanopore-based tRNA sequencing
ncRNA	Noncoding RNA
NTPases	Nucleoside triphosphatase hydrolyzing enzymes
OLA1	Obg-like ATPase 1
*Pf*OLA1	*Plasmodium falciparum* OLA1
*Ph*OLA1	*Pyrococcus horikoshii* OLA1
P_i	Inorganic phosphate
P-loop	Phosphate loop
poly-A tail	Poly-adenine tail
P-site	Peptidyl-site
Pth	Peptidyl-tRNA hydrolase
qPCR	Quantitative polymerase chain reaction

RACK1	Receptor of activated protein C kinase 1
Rbg1	Ribosome interacting GTPase 1
RD	RNA duplex
RF	Release factor
RNA	Ribonucleic acid
RNases	Ribonucleases
r-proteins	Ribosomal proteins
RRF	Ribosome recycling factor
rRNA	Ribosomal RNA
RSH	RelA/Spot homologs
S/N	Signal-to-noise ratio
*Sc*OLA1	*Saccharomyces cerevisiae* OLA1
SelB	Selenocysteine B
SIMBI	Signal recognition particle, MinD, and BioD
smFRET	Single-molecule fluorescence resonance energy transfer
SmpB	Small protein B
SmrB	Small MutS related B
SRL	Sarcin-ricin loop
SSU	Small subunit
*Tc*OLA1	*Trypanosoma cruzi* OLA1
TGS	ThrRS, GTPase, and SpoT
tmRNA	Transfer-messenger RNA
TRAFAC	Translation factor
trGTPases	Translational GTPases
tRNA	Transfer RNA
TruB	tRNA pseudouridine synthase B
UTR	Untranslated region
wt	Wildtype

CHAPTER 1: INTRODUCTION

General Overview

Protein biosynthesis is essential to life. As such, interfering with the function of proteins and RNA components necessary for translation *in vivo* is a valuable antimicrobial strategy (Wilson, 2009, 2014). Antimicrobial resistance is "one of the top ten global public health threats facing humanity" (World Health Organization, 2021). Some "noncanonical" translation components (*i.e.,* outside the textbook overview) confer antimicrobial tolerance (Fishbein et al., 2020; Koller et al., 2022; Rudra et al., 2020). Thus, it is prudent to understand each step of protein biosynthesis at the molecular level, including noncanonical steps, as these details can be exploited for the design of therapeutics for which resistance mechanisms do not yet exist.

One noncanonical translation component is Obg-like ATPase 1 (OLA1), often studied for its association with cancer (Balasingam et al., 2020). OLA1's role in translation is not fully defined, with no clear molecular explanation for how or why it interacts with the ribosome. Recent preliminary data indicates that tRNA is important for OLA1's function (Wieden lab, unpublished), but none of the currently discussed hypotheses regarding OLA1's cellular role and mechanism consider this. The work reported here aims at characterizing OLA1's affinity to tRNA and whether it can remodel ribosomal RNA.

This chapter aims to provide an overview of the central dogma and translation, describe molecular mimicry observed between OLA1 and translation factors that bind RNA, review current hypotheses for OLA1's cellular role, and establish a hypothesis for the role of OLA1 regarding putative RNA interactions.

The Central Dogma of Biology

The central dogma of biology describes the interplay between deoxyribonucleic acid (DNA), ribonucleic acid (RNA), and proteins (figure 1). DNA, the hereditary material of all organisms, can be replicated into DNA or transcribed into RNA by DNA or RNA polymerases. A small portion of this RNA, called messenger (m)RNA, is a transient form of hereditary information and serves as a template for making proteins via ribosome-dependent translation (Chapeville *et al.*, 1962; Hubé &

Francastel, 2018). During translation, nucleotide triplets are read as codons by the ribosome, with each codon corresponding to one of the 21 canonical amino acids (including selenocysteine) that are subsequently added to the growing polypeptide chain (Hatfield & Gladyshev, 2002). Proteins carry out many functions within cells, fulfilling the requirements for life, like compartmentalization (Chen & Silver, 2012), metabolism (Yuan et al., 2013), as well as sensing and responding to the environment (Cretel et al., 2008; Narayan et al., 2019). Proteins, such as polymerases and ribosomal (r-)proteins, even play roles in reproduction throughout the central dogma and through cell division (Aze & Maiorano, 2018; Steitz, 1999).

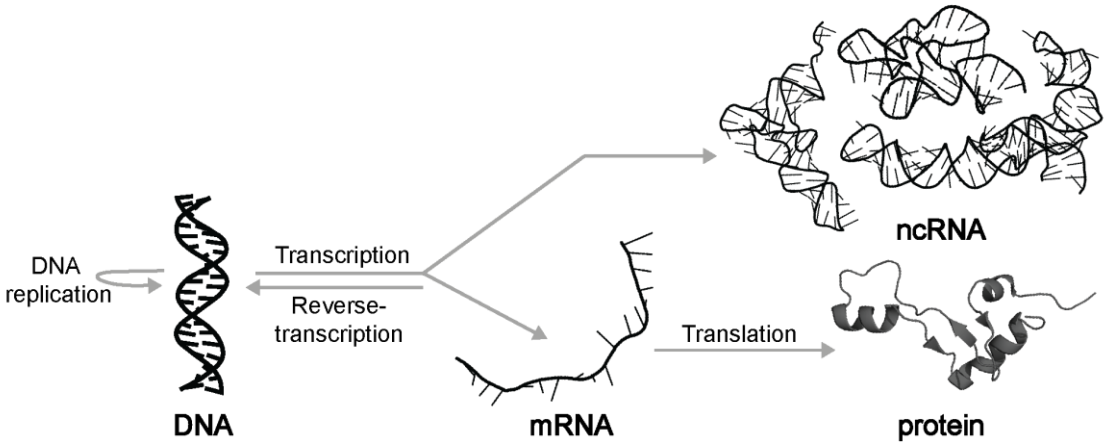

Figure 1. The central dogma of biology illustrates the flow of genetic information. DNA can be made from either DNA replication or reverse transcription of RNA. DNA is transcribed to either mRNA or ncRNA. Through translation, mRNA is decoded to synthesize proteins. Protein and ncRNA are both capable of structural and enzymatic functions. The RNA and protein structures shown here in cartoon form are from PDB 6BU8.

Once thought to be a unidirectional, linear process, the central dogma of biology has expanded to include reverse transcription (Koonin, 2012; Lescot *et al.*, 2016; Temin, 1985) and ever more roles for RNA (Brosius & Raabe, 2016; Eddy, 2001). Many different classes of functional RNAs exist, some straddling the line between coding and noncoding (nc)RNA (Brosius & Raabe, 2016; Hubé & Francastel, 2018). One example of RNA function outside of encoding proteins is in the peptidyl-transferase center of the ribosome; ribosomal (r)RNA is a structural and catalytic

component of translation (Liu & Fredrick, 2016; Ramakrishnan, 2002). Decoding the information stored in mRNA into the corresponding protein also requires transfer-(t)RNAs that serve as adaptor molecules by carrying an amino acid (aa) specific to the anticodon sequence on the opposite end of the 3D tRNA structure (Assmann et al., 2023; Wohlgemuth et al., 2011). A summary of what is known about translation is provided below, with some remaining research questions highlighted.

The Ribosome

Ribosomes are sophisticated ribonucleoprotein nanomachines that facilitate the mRNA-directed synthesis of proteins (reviewed in Bowman et al. (2020)). With concentrations between 36 000 to 55 000 ribosomes per *Escherichia coli* cell, translation components are highly abundant, including their many auxiliary factors (Bakshi et al., 2012). Ribosomes are composed of two complex subunits named the 30S and 50S subunits in prokaryotes and the 40S and 60S subunits in eukaryotes (Jüttner & Ferreira-Cerca, 2022). Independent of the organism, they are referred to as the small subunit (SSU) and large subunit (LSU), respectively. Each SSU combines with an LSU during initiation to form the 70S ribosome in bacteria and archaea and an 80S ribosome in eukaryotes (Jüttner & Ferreira-Cerca, 2022; Kisly & Tamm, 2023). “S” stands for Svedberg, a unit for sedimentation coefficients and, by proxy, size (Harding, 2018). Prokaryotic ribosomes are about 2.5 MDa in size, containing three rRNAs and over 50 proteins each (Byrgazov et al., 2013). Eukaryotic ribosomes are about 40% larger (~4.3 MDa) due to expanded RNA segments, an additional rRNA, and over 30 additional proteins (Weisser & Ban, 2019; Yusupova & Yusupov, 2015). The exact rRNA and protein composition is dependent on the specific organism, with only 33 universally conserved r-proteins (Melnikov et al., 2018). Please note that S/LSU r-proteins will be labelled as per Ban *et al.* (2014), where the prefixes e- (archaeal/eukaryotic), b- (bacterial), and u- (universal) denote the levels of conservation unless otherwise stated. The term “universally conserved” is applied when representatives exist in each primary line of descent throughout the kingdoms of life. Some auxiliary factors for translation, consisting of proteins and RNA, are also universally conserved. They assist with ribosome assembly, quality control, translation, and stress response (Brandman & Hegde, 2016; Jiang *et al.*, 2007; Karamyshev & Karamysheva, 2018).

Overview of the Ribosome Cycle

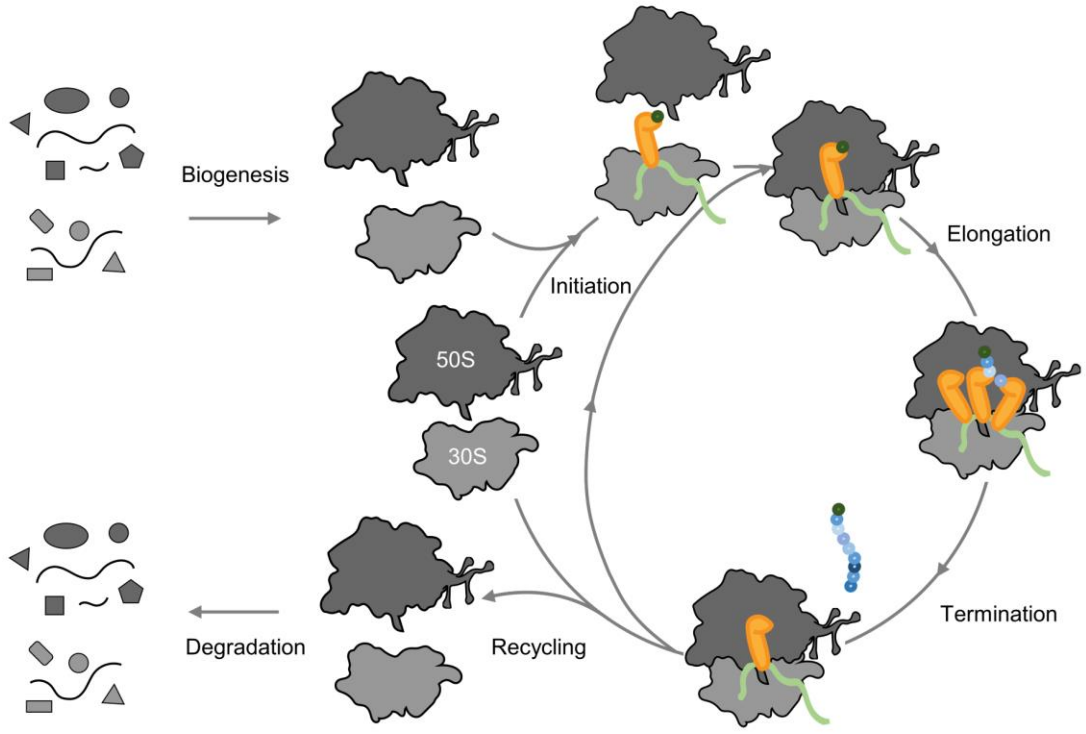

Figure 2. The general cycle of the ribosome. The phases of biogenesis, initiation, elongation, termination, recycling, degradation as well as continuous quality control occur in all organisms. This image is adapted from Brandon (2021).

Biogenesis of Ribosomes, tRNA, and mRNA

The general phases of the ribosome cycle (figure 2) are universal, but specific steps and factors differ between the domains of life. This is the case with ribosome biogenesis, which encompasses the cooperative, sequential processes of creating, maturing, and combining individual ribosomal components into ribosomal subunits (Jüttner & Ferreira-Cerca, 2022). The complete process is resource intensive. For example, in eukaryotes, making the rRNA and r-protein mRNA requires three different polymerases (Dörner *et al.*, 2023). Each pre-rRNA is processed, modified, and folded into complex tertiary structures. There are hundreds of biogenesis factors in eukaryotes alone, including but not limited to ribonucleases (RNases), chaperones, helicases, structural

proteins, modifications enzymes, and RNA-protein complexes (Dörner et al., 2023; Weisser & Ban, 2019).

Along with ribosome maturation, mRNA and tRNA maturation is another translation prerequisite. In eukaryotes, the pre-mRNA is matured by adding a 5' 7-methylguanosine cap, a 3' poly-adenine(A) tail, and in some cases, RNA splicing (Bentley, 2014). Different transcript isoforms are created depending on the transcription and maturation of mRNA, each with unique translation profiles depending on the sequence, structure, nucleotide modifications, and binding of additional proteins (Sonneveld et al., 2020). In addition to making multiple mRNA isoforms from the same DNA template, mRNA processing also protects against degradation (Gagliardi & Dziembowski, 2018). In prokaryotes, newly transcribed mRNA and mRNA in the process of being transcribed rapidly diffuses (~1s) to ribosome-rich regions where translation is carried out, partially protecting against degradation and allowing for co-transcriptional translation to occur (Bakshi *et al.*, 2012). Save for a recent finding of pseudo-5' capping on bacterial mRNA, mRNA processing is considered unique to eukaryotes (Vasilyev et al., 2019). On the other hand, tRNA maturation occurs in all domains of life (Phizicky & Hopper, 2010). After pre-tRNA is transcribed, they are cleaved at the 5' and 3' ends and given a 3' CCA tail (Assmann et al., 2023; Kunzmann et al., 1998). Additionally, each tRNA is modified by multiple enzymes (TruB, TrmA, etc.), many of which act as RNA chaperones as well, enabling a mature tRNA structure (Lorenz et al., 2017; Porat et al., 2021; Schultz & Kothe, 2020). Mature tRNA has a cloverleaf secondary structure with a D-arm/loop, anticodon arm/loop, variable loop, and TΨC-arm/loop (listed 5'-3') with the termini forming the acceptor stem (figure 3). Properly folded tRNA forms an L-shaped tertiary structure that is esterified to a cognate aa at the 3' CCA end by a corresponding aminoacyl-tRNA synthetase (aaRS) (Rubio Gomez & Ibba, 2020).

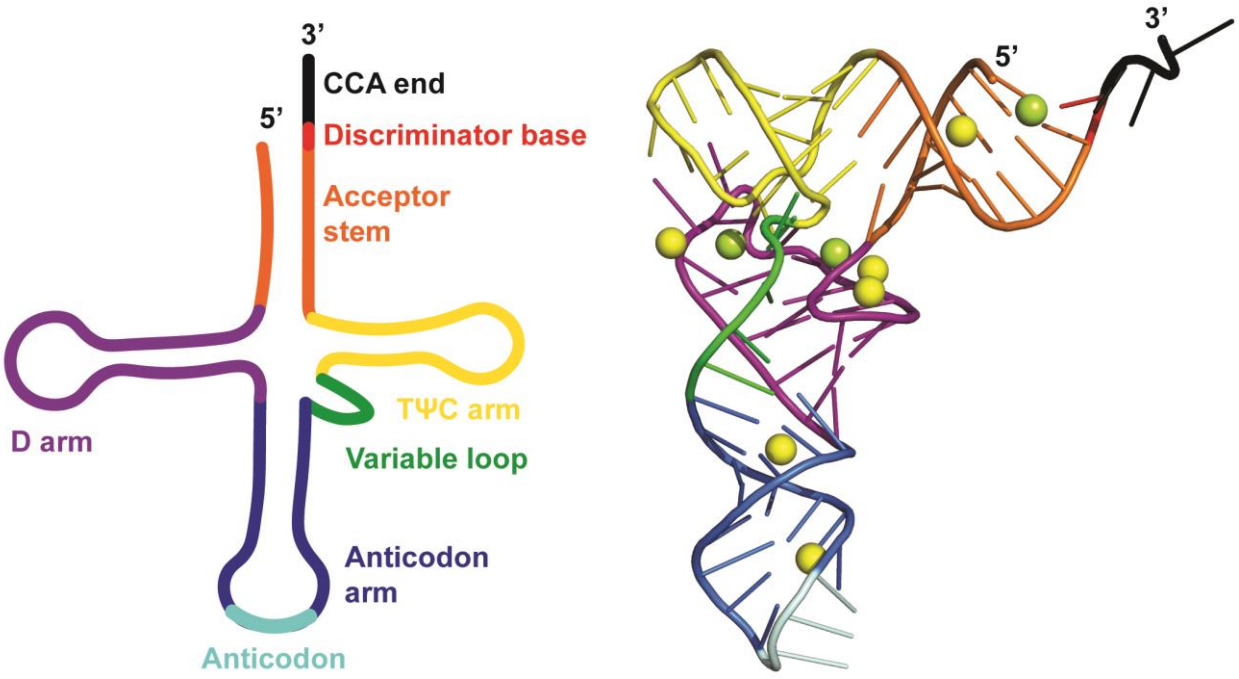

Figure 3. Mature tRNA folds into a distinct structure. On the left is the cloverleaf secondary structure, depicting the arrangement of the tRNA bases. On the right is the cartoon L-shaped tertiary structure (PDB 1EHZ). The tRNA colour coding is consistent between the figures. Mg^{2+} and Mn^{2+} cations are shown as yellow and lime spheres, respectively.

In a “standard” mRNA, there is a 5’ untranslated region (UTR) and one or more coding regions (a ribosome binding site, start codon, in-frame codons, and a stop codon) before a 3’ UTR. In addition to standard mRNA, there are mRNA lacking ribosome binding sites, mRNA lacking 5’ UTRs, and eukaryotic mRNA with internal ribosome entry sites (IRESs). For instance, organisms from all domains of life have leaderless mRNA, which possesses a start codon close to the 5’ end but lacks both a 5’ UTR and a ribosome-binding site (Grill et al., 2000; Rodnina, 2018). The vast array of different types of mRNA can provide adaptational strength under cellular stress.

Translation Initiation

Initiation is fine-tuned to ensure that the correct proteins are made at the appropriate quantities and times (Kudla et al., 2009; Reeve et al., 2014; Shah et al., 2013). These mechanisms are considered the most diverse of the ribosome cycle phases across the domains of life. The

similarities will be highlighted here throughout an overview of bacterial translation initiation. Initiation requires mRNA, initiation factors (IFs), and the SSU binding to form a pre-initiation complex. In bacteria, there are three IFs: IF3, which prevents LSU and elongation-tRNA association until the initiator-tRNA and favourable mRNA regions are in place; IF2, which binds the initiator Met-tRNA$_i^{Met}$; and IF1, which assists IF2 and IF3 (Basu et al., 2022; Rodnina, 2018; Yamamoto et al., 2016). Eukaryotes and archaea have additional IFs, some functionally equivalent but not homologous to bacterial IFs (Schmitt *et al.*, 2020). For example, archaeal (a) and eukaryotic (e)IF2 behave similarly to prokaryotic IF2, although (a/e)IF5B is the true IF2 homolog (Schmitt *et al.*, 2020).

During the prokaryotic initiation of standard mRNA, a ribosome-binding site called the Shine-Dalgarno (SD) sequence base pairs with a complementary segment of the 16S rRNA (Shine & Dalgarno, 1975). A start codon 5-13 nucleotides (nt) downstream of the SD sequence is recognized in the peptidyl (P)-site of the 30S subunit (Milón & Rodnina, 2012). Universally, the most common start codon is AUG (for methionine) but alternative start codons such as a CUG (leucine) or GUG (valine) are occasionally used *in vivo* (Ingolia et al., 2011). Following start codon positioning, the 70S initiation complex is formed through binding of the LSU, concomitant with IF1 and IF3 release and the formation of inter-ribosomal-subunit bridges. Many intersubunit bridges are universally conserved, such as the aminoacyl-site finger (ASF) rRNA, often referred to as bridge (B)1a (Komoda *et al.*, 2006). Finally, Met-tRNA$_i^{Met}$ is accommodated through GTP hydrolysis by IF2 (Rodnina, 2018). Eukaryotic initiation achieves a similar goal through more complexity, with even canonical initiation using multiple routes (Sonenberg & Hinnebusch, 2009).

Noncanonical initiation mechanisms serve as valuable adaptations to fight stress or facilitate infection. The universally conserved leaderless mRNA can bind directly to 70S/80S ribosomes or SSUs, sometimes without IFs (Akulich et al., 2016; Udagawa et al., 2004; Yamamoto et al., 2016). Ribosomes can also participate in “scanning initiation,” where a ribosome continues onto a start codon ~30 nt downstream of a stop-codon without first dissociating (Milón & Rodnina, 2012; Yamamoto *et al.*, 2016). Similar is “termination-reinitiation,” where the SSU reinitiates on a start codon close to – or sometimes partially overlapping with – the stop codon (Huber *et al.*, 2019).

With initiation on internal ribosome entry sites (IRESs), the need for eukaryotic IFs that enable ribosome scanning towards the start codon is forgone through RNA structure, reminiscent of the Shine-Dalgarno•16S interaction (Sonenberg & Hinnebusch, 2009). Despite not occurring in prokaryotes, it was found that as long as an IRES has a start codon, a 70S ribosome with RNA helicase S1 can still translate it (Roberts & Wieden, 2022), suggesting the presence of a start codon is the most uniting factor of initiation.

Elongation

Following the formation of the initiation complex, the ribosome can enter the elongation phase, a cyclic process involving the decoding of the codon present at the ribosomal A-site, peptide bond formation, and subsequent, concomitant translocation of the mRNA and tRNAs. Most aminoacyl (aa)-tRNA are delivered to the ribosome by elongation factor thermal unstable (EF-Tu) in bacteria or the eukaryotic/archaeal homolog, (e/a)EF1A (Pape et al., 1998; Xu et al., 2021). One exception is selenocysteine (Sel)B or (e/a)EFSec for binding Sec-tRNA^{Sec} (Copeland & Howard, 2021; Meng et al., 2022). EF-Tu forms a ternary complex with GTP and aa-tRNA. EF-Tu can bind to every aa-tRNA with comparable affinity through "thermodynamic compensation," meaning the binding strength for tRNA and the corresponding aa towards EF-Tu compensate one another (LaRiviere et al., 2001). Rapid sampling of ternary complexes at the ribosomal aminoacyl (A)-site occurs in search of a cognate tRNA (*i.e.,* matching of the corresponding codon-anticodon sequence) (Geggier *et al.*, 2010; Morse *et al.*, 2020). EF-Tu gates the accommodation of the cognate aa-tRNA and subsequently dissociates, allowing for peptide bond formation and translocation. The peptide bond is an amide bond formed between the growing peptide on the P-site tRNA to the A-site tRNA aa. In the particular case of peptide bond formation between prolines, EF-P or (e/a)IF5A interacts through the exit (E)-site to alleviate ribosome stalling (Hummels & Kearns, 2020; Ude *et al.*, 2013).

Throughout translocation, the ribosome undergoes significant conformational changes, including rotation of the two subunits relative to one another and swivelling of the SSU head relative to the body. In a non-rotated state, the peptidyl-tRNA is in an A/A position, and the newly deacylated tRNA is in a P/P position; in the rotated state, they are in A/P and P/E positions,

respectively (Rundlet *et al.*, 2021). EF-G in bacteria (or (e/a)EF2 in eukaryotes and archaea) engages the rotated ribosome, “unlocking” the A-site codon-anticodon interaction, accelerating movement of the peptidyl-tRNA into the P/P position and deacylated tRNA movement to the E/E site (Carbone et al., 2021; Rodnina et al., 2019). The ribosome simultaneously progresses along the mRNA with a counter-clockwise SSU head swivel motion, placing a new codon in the A-site. EF-G and the deacylated tRNA then dissociate, allowing another round of elongation (Rundlet *et al.*, 2021).

Typically, 5.6 or 20 aa can be incorporated into the growing polypeptide chain per second in eukaryotes and prokaryotes, respectively (Hummels & Kearns, 2020; Ingolia *et al.*, 2011). The number of polypeptides synthesized at a given time is increased through multiple ribosomes consecutively assembling on a single mRNA, forming a polysome. Some brief instances of pausing are necessary during elongation to enable the ribosome-nascent chain complex to bind co-translational chaperones (Ingolia *et al.*, 2011). Interestingly, brief pause sites do not result in ribosome collisions. During extended pauses, stress responses can be engaged. For example, when deacylated tRNA has accumulated far above the standard ~15% of total tRNA in gram-negative bacteria, the stringent response is triggered by the binding of the GTP pyrophosphatase RelA to deacylated tRNA at the A-site (Brown et al., 2016; Wendrich et al., 2002). Through this interaction, RelA synthesizes one of two hyperphosphorylated nucleotide signalling molecules collectively called (p)ppGpp (*i.e.,* alarmone) that downregulate transcription of translation-related genes and upregulate transcription of stress response genes (Brown et al., 2016; Kushwaha et al., 2019). Some stress responses allow the ribosomes to continue translation post-stress and terminate on a stop codon, while others lead to premature termination.

Termination and Ribosome Recycling

In canonical translation, a stop codon (UAA, UAG, or UGA) is eventually positioned in the ribosomal A-site, indicating the completion of the synthesized polypeptide. In bacteria, either release factor (RF)1 or RF2 will succeed in binding the ribosome at a stop codon in place of a ternary complex (Buskirk & Green, 2017; Rodnina, 2018). An additional factor, RF3, helps RF1 or RF2 dissociate after hydrolysis of the ester bond between the peptidyl-tRNA and the polypeptide chain (Adio *et*

al., 2018). Eukaryotes only have eRF1 and eRF3, which are distantly related to their bacterial counterparts (Buskirk & Green, 2017). In archaea, termination is carried out by an a(RF1/Pelota)•aEF1α heterodimeric complex, resembling the EF-Tu ternary complex (Kobayashi et al., 2010; Kobayashi et al., 2012).

After canonical termination, recycling of the post-termination ribosome proceeds. In bacteria, subunit splitting is facilitated by ribosome recycling factor (RRF), EF-G, and IF3. RRF and EF-G bind at the A-site to disrupt intersubunit bridge B2a, and IF3 prevents subunit reassociation (Rodnina *et al.*, 2019). Eukaryotic and archaeal ribosome recycling requires an additional protein called ATP-binding cassette subfamily E member 1 (ABCE1) to interact with eRF1, promoting subunit splitting (Nürenberg-Goloub *et al.*, 2020; Pisarev *et al.*, 2010; Rodnina, 2018). As with initiation, termination, and recycling mechanisms clearly differ between domains of life. However, they all typically culminate in a complete protein, as well as free ribosomal subunits that can feed back into the ribosome cycle.

There are a few cases of premature termination across all organisms. For example, when a truncated mRNA lacks a stop-codon, small protein B (SmpB) and the hybrid transfer-messenger (tm)RNA aminoacylated with alanine are bound by EF-Tu•GTP to rescue the ribosome in a process termed “trans-translation” (Ivanova et al., 2004; Saito et al., 2022). The tmRNA mimics an mRNA•tRNA complex while SmpB mimics an anticodon stem-loop, allowing for the addition of an 11-aa degradation signal to the aberrant polypeptide chain (Bessho *et al.*, 2007; Ivanova *et al.*, 2004). When ribosomes are stalled on intact mRNA and collide to form disomes, the endonuclease small MutS-related B (SmrB) binds and cleaves upstream mRNA, allowing trans-translation to commence (Saito *et al.*, 2022). The essential SMR domain of SmrB is found in all sampled eukaryotes and some archaea, suggesting high conservation of this rescue pathway. When trans-translation is insufficient for the frequency of ribosome stalling in *E. coli*, a similar mechanism is engaged by alternative rescue factor A (ArfA) and RF2 (Chadani *et al.*, 2011; Demo *et al.*, 2017). Additionally, ArfB assists in peptide release from stalled ribosomes through its peptidyl-tRNA hydrolase activity (Carbone et al., 2020).

During the recycling of stalled ribosomes or after the incorporation of a noncognate aa into the growing polypeptide chain, peptidyl-tRNA dissociates from the ribosome. Peptidyl-tRNA hydrolase (Pth) enzymes free the tRNA by cleaving the ester bond between the tRNA and the peptide (Das & Varshney, 2006). Peptidyl-tRNA-bound ribosomes that are stalled on a nonstop mRNA, which lack a stop-codon, are rescued by YaeJ and its homologs; the YaeJ C-terminus mimics a stop codon, and the N-terminal GGQ motif is used to hydrolyzes the peptidyl-tRNA (Gagnon et al., 2012). In cases where translation is prematurely terminated, the defective mRNA and resulting polypeptides are degraded (Karousis & Mühlemann, 2019).

Auxiliary Translation Factors: GTPases

It is imperative for the cell that protein synthesis is carried out with high fidelity because aberrant proteins can be toxic (Drummond & Wilke, 2009; Radman, 2020; Tawde et al., 2022). An additional layer of quality control during translation comes from guanosine nucleotide-dependent molecular switches, also called guanosine triphosphatase hydrolyzing enzymes (GTPases). The GTPase superclass is subdivided into two classes, the translation factor (TRAFAC) class and the signal recognition particle, MinD, and BioD class (SIMBI, not discussed here) (Leipe et al., 2002). TRAFAC members are involved in translation, signal transduction, cell motility, and intracellular transport. Here, the focus will be on the translational (tr)GTPases that directly interact with the ribosome (Verstraeten et al., 2011), such as IF2, EF-Tu, EF-G, RF3, and their archaeal/eukaryotic counterparts, mentioned above. All GTPase molecular switches cycle between an “active” triphosphate bound state; an “inactive” diphosphate bound state; and the empty or *apo* state. Typically, GTPases are known to have slow intrinsic GTPase activity (<1 min^{-1}) and rapid nucleotide dissociation (>60 min^{-1}) (Buglino et al., 2002; Vetter & Wittinghofer, 2001), discouraging them from hydrolyzing GTP when free from their GTPase activating proteins or factors (GAPs or GAFs). Conformational changes upon the irreversible step of GTP hydrolysis are coupled to downstream biological functions. In this way, GTPases gate the transitions between each phase of translation and maintain a specific order of events relative to one another. Further regulation is achieved during stringent response by the highly abundant ppGpp binding GTPases in place of GTP, preventing their hydrolysis-dependant functions (Dworkin, 2023).

The Conserved Nucleotide Binding Domain

All GTPases contain a structurally conserved α/β fold called the guanosine binding (G)-domain first described over 40 years ago (Kabsch et al., 1977; Morikawa et al., 1978; Verstraeten et al., 2011). Their sequences vary, save for the G motifs (Caldon et al., 2001). Though the G motif order is typically 1 through 5 from N to C-terminus, rearrangement to G4-5-1-2-3 still maintains a functional GTP-binding site (Anand et al., 2006). The G1 motif (phosphate (P)-loop or Walker A motif), $GX_4GK(S/T)$, enfolds the α and β phosphate of bound nucleotide without restructuring upon nucleotide hydrolysis (Sprang, 1997). G2, X(T/S)X, together with G3, DXXG, forms the Walker B motif that coordinates a magnesium ion, facilitating nucleotide binding through interaction with the β and γ phosphates (Sprang, 1997; Verstraeten *et al.*, 2011). Interestingly, G1 and G3 are found in many nucleotide-binding proteins, like ATPases (Saraste et al., 1990; Sprang, 1997). G2 is less conserved, with notable variation between GTPase subfamilies (Caldon et al., 2001; Paduch et al., 2001). GTP specificity through recognition of the guanine ring is dictated by the G4 and G5 motifs, (N/T)KXD and (T/G)(C/S)A, respectively (Sprang, 1997). G2 also partially influences the interaction between G4 and the purine ring. Notably, G5 is the least conserved among the G motifs, making G4 the primary guanine differentiator (Verstraeten *et al.*, 2011). Ribosome-binding TRAFAC GTPases typically have an α-helix between G4 and G5 used for recruitment by the stalk proteins to the ribosome (*vide infra*). Switch I (the effector loop) and switch II commonly overlap with the G2 and G3 motifs, respectively (Lin *et al.*, 2023). The switches act as nucleotide sensors, both undergoing conformational changes during GTP hydrolysis, which can affect the overall configuration of the protein (Wittinghofer & Vetter, 2011). Variations within the G-domain, especially the G motifs, dictate the intrinsic nucleotide binding properties of GTPases, thus, affecting their biological function.

GTPase Activating Factors (GAFs)

The ribosome functions as the GAF for IF2, EF-Tu, EF-G, and RF3, increasing the rate of hydrolysis by several orders of magnitude (Carlson et al., 2017; Mohr et al., 2002). The ribosome facilitates its GAF function in two ways: through the ribosomal stalk proteins and the rRNA sarcin-ricin loop (SRL). The bacterial ribosome stalk is composed of uL10, uL11, multiple copies of bL7/12

(bL12 is an acetylated bL7), and an interacting segment of the 23S (e28S) (Diaconu *et al.*, 2005). Eukaryotes and archaea have homologous P0 for uL10, L12 for uL11, and nonhomologous yet functionally similar P1/P2 instead of bL7/12. A helix-loop-helix motif in the bL7/12 CTD binds an α-helix in the inter-G4-5 regions of EF-Tu (helix D), EF-G (G'), and RF3 (G') to facilitate their binding to the ribosomal A-site (Carlson et al., 2017; Ge et al., 2018; Helgstrand et al., 2007; Wieden et al., 2001). In contrast, the IF2 interaction with the stalk is used in subunit association, increasing it 40-fold (Ge *et al.*, 2018). The ribosome stalk is hypothesized to catalyze GTP hydrolysis by stabilizing a favourable G-domain conformation (Mohr *et al.*, 2002). For example, bL7/12 increases the binding of EF-Tu•GTP•Phe-tRNA^{Phe} to the ribosome over 10-fold and the rate of GTP hydrolysis by over 2,500-fold (from 0.2 to >500 s^{-1}) (Diaconu *et al.*, 2005). Likewise, the GTPase activity of EF-G is increased from 0.4 to 250 s^{-1} in the presence of the bL7/12 CTD stalk (Diaconu *et al.*, 2005). Interestingly, the ribosome stalk is not limited to binding trGTPases as it is involved in the recruitment and ATPase activity of ABCE1 in eukaryotes (Imai *et al.*, 2018).

The SRL is the other contributor to stimulate GTPase activity in IF2, EF-Tu, EF-G (Caldon et al., 2001; Clementi et al., 2010; Koch et al., 2015) and possibly RF3 (Graf *et al.*, 2018). SRL nucleotides act by positioning and stabilizing switch II residues (typically histidine) in the transition state (Aleksandrov & Field, 2013; Pape et al., 1998; Shi et al., 2012; Voorhees et al., 2010). Unlike the ribosome stalk proteins, the SRL discriminates against GDP-bound IF2 and EF-G (Mitkevich *et al.*, 2012). This mechanism for increasing the likeliness of active, GTP-containing IF2 or EF-G complexes to bind the ribosome works for two reasons. First, because neither preferentially binds GDP; IF2 has similar affinities to GDP and GTP (*e.g.,* $K_{D,IF2}$ = 11 µM for GTP, 5 µM for GDP at 25°C (Hauryliuk *et al.*, 2009)) and EF-G preferentially binds GTP (*e.g.,* $K_{D,EFG}$ = 9.1 µM for GTP, 16.7 µM for GDP at 37°C (Hauryliuk *et al.*, 2008)). Secondly, there is a higher GTP: GDP ratio in healthy cells (*e.g.,* 8:1 in *E. coli* during mid-log growth), so GTP will outcompete GDP for binding to these enzymes (Becker et al., 2012; Buckstein et al., 2008; Sprang, 1997). Interestingly, the GTP hydrolysis activity of the IF2 homolog eIF2 is stimulated by eIF2B, not the ribosome (Schmitt *et al.*, 2020).

Guanine Exchange Factors (GEFs)

GTPases with a higher affinity for GDP than GTP, like EF-Tu, require a guanine exchange factor (GEF). The GEF for EF-Tu is EF-Thermal stable (Ts); it binds the same region of EF-Tu as the ribosome stalk, decreasing potential interference with productive EF-Tu•GTP•aa-tRNA and inhibiting noncognate aa-tRNA accommodation (Kolberg et al., 1997; Wieden et al., 2002; Wieden et al., 2001). The GEF for RF3 is the ribosome in complex with RF1 or RF2; upon hydrolysis of the peptidyl-tRNA ester bond, GDP is exchanged for GTP on RF3, and hydrolysis occurs, causing dissociation of all RFs (Zavialov et al., 2001). In other words, the nucleotide specificity of RF3 prevents RF removal before polypeptide release, further exemplifying how GEFs are important regulators of GTPase function and timing.

Molecular Mimicry Between GTPases

Commonalities in structure and function are collectively thought of as molecular mimicry. Molecular mimicry is exploited by RNA and proteins alike to share binding sites for their various, occasionally overlapping functions. Mimicry can be structural through the conservation of shape and charge distribution, as seen by the evolutionarily distinct bL7/12 CTD and EF-Ts; they share a motif whose interaction with EF-Tu is mutually exclusive (Kolberg *et al.*, 1997; Wieden *et al.*, 2002; Wieden *et al.*, 2001). More drastically, EF-G, IF2•IF1, RF3•RF1/2, and EF-Tu•aa-tRNA all appear to structurally mimic one another's general 3D shape (figure 4), as previously hypothesized (Grill *et al.*, 2000; Nyborg *et al.*, 1996; Nyborg *et al.*, 1997). On the other hand, molecular mimicry can be functional, as seen with the nonhomologous IFs between domains of life (*vide supra*).

Molecular mimicry driven hypotheses for trGTPases have been informative for their characterization (Brock et al., 1998; Caldon et al., 2001; Moore, 1995; Nissen et al., 1995) and often based on EF-Tu, as it is the most abundant and best-studied translation factor. For instance, in *E. coli* there are 8-14 EF-Tu molecules per ribosome depending on the growth phase of the cell, whereas EF-G exists in a 1:1 ratio with ribosomes (Furano, 1975). Also, EF-Tu was the model protein in one of the first descriptions of the G-domain (Kabsch *et al.*, 1977). The differences in

affinities to nucleotides and other binding partners by IF2, EF-Tu, EF-G, and RF3 enable the synchrony required for binding to the ribosomal A-site at the appropriate times.

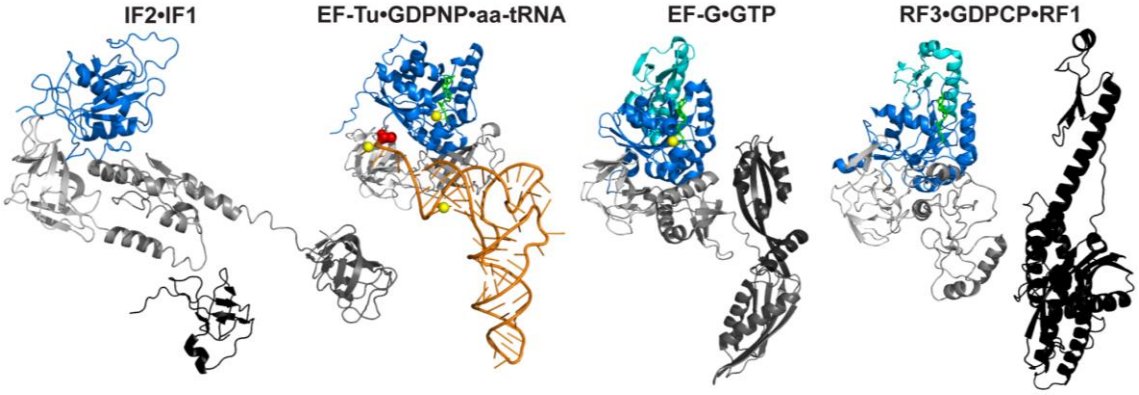

Figure 4. Structural mimicry of complexes formed by trGTPases. IF2•IF1 (PDB 1ZO1), EF-Tu•GDPNP•aa-tRNA (PDB 1B23), EF-G•GTP (PDB 2DY1), and RF3•GDPCP•RF1 (PDB 6GXN) are shown in cartoon form with each G-domain in blue, G' insertions in cyan, domains C-terminal of the G-domain in darkening shades of grey, and tRNA in orange. Additional proteins, IF1 and RF1, are black. Nucleotides are green, magnesium is yellow, and the cysteine on the charged tRNA is shown as red spheres.

There are additional universally conserved trGTPases, such as Obg-like ATPase 1 (OLA1), that somehow fit into the ribosome functional cycle but whose exact functions in translation are poorly understood. OLA1 is not strictly required for translation but provides a fitness advantage under various stressors. OLA1 has gained attention for its implicated role in cancer progression (Balasingam et al., 2020; Bian et al., 2022; Dong et al., 2021; Huang et al., 2020; Liu et al., 2022; S. Lu et al., 2021; Sun et al., 2010; Xu et al., 2016; Zhang et al., 2009), Down's Syndrome (Shin et al., 2004), and virulence (Chen & Chung, 2011; Cheung et al., 2016; Fernebro et al., 2008; J. Lu et al., 2021; Polkinghorne et al., 2006). However, understanding OLA1's effects on the ribosome needs further investigation. I propose that OLA1 can be better understood through testing molecular mimicry driven hypotheses (*vide infra*).

A History and Analysis of OLA1, A Universally Conserved NTPase

OLA1 Provides a Fitness Advantage Across the Domains of Life

OLA1 was first mentioned in the literature under the ordered locus name MG024 as belonging to the smallest known genome of all free-living organisms (*Mycoplasma genitalium*) (Fraser *et al.*, 1995). Because *ola1* is also conserved in *Haemophilus influenzae*, *ola1* was included in the minimal gene set proposed by Mushegian and Koonin (1996). Likewise, *ola1* was included among 206 genes in another hypothetical minimal protein-coding gene core (Gil et al., 2004), among the 79 core translation genes (Grosjean *et al.*, 2014), and as one of 75 nuclear markers conserved across vertebrates (Fong & Fujita, 2011). The name OLA1 is used here, but other names include GBP45, GTBP9, DOC45, PTD004, EngD, YyaF, Ybr025c, and in bacteria, YchF. Interestingly, Adékambi *et al.* (2011) concluded that a phylogenetic tree derived from the combination of *ychF*, *rpoB*, and *secY* is more robust than one derived from 16S rRNA. Since then, *ychF* has been used as a housekeeping gene for sequencing by Wang *et al.* (2019) and Tamura et al. (2012). In 2004, Galperin and Koonin listed YchF/OLA1 as a target to be prioritized for experimental study because of its high conservation and implicated role in translation (*vide infra*).

Even though *ola1* is part of the minimum gene core, it is not essential in all organisms. For instance, *M. genitalium* were found to tolerate putative disruption of *ola1* by transposon insertion, suggesting redundancy of function in the cell or a role in some conditions not yet tested (Glass *et al.*, 2006). Likewise, OLA1 is not essential for *Mycoplasma pneumoniae* or *Bacillus subtilis* under ideal growth conditions (Hutchison *et al.*, 1999; Morimoto *et al.*, 2002). Under heat stress (42°C), the deletion of *ola1* has been reported to cause filamentous growth in *E. coli* and a decrease of translation initiation in *Saccharomyces cerevisiae*; OLA1 is not essential for either organism (Dannenmaier et al., 2021; Dassain et al., 1999). Furthermore, *E. coli* lacking OLA1 is rapidly outcompeted by wildtype (wt) cells under ideal conditions (Wieden lab unpublished, Landwehr *et al.* 2021), a phenotype exacerbated under cold stress (16°C) (Wieden lab unpublished, Wenk *et al.*, 2012). There are only a few cases where OLA1 is critical. For example, OLA1 knockdown by antisense RNA causes 3-logs of growth inhibition in *Staphylococcus aureus* in comparison to wt cells (Forsyth *et al.*, 2002), RNAi against *ola1* inhibits cell proliferation of the parasite *Trypanosoma*

brucei (Gradia *et al.*, 2009), and OLA1 is required for *Vibrio vulnificus* growth in iron-limited conditions (Chen & Chung, 2011).

Studies have implicated OLA1 in iron metabolism (Chen & Chung, 2011; Danese et al., 2004), protein degradation (Gradia et al., 2009; Guerrero et al., 2006; Schultz et al., 2019), oxidative stress response (Gradia *et al.*, 2009; Hannemann *et al.*, 2016; Wenk *et al.*, 2012), neuronal differentiation (Oh *et al.*, 2007), centrosome regulation/cell proliferation (Ding et al., 2016; Matsuzawa et al., 2014; Otsuka et al., 2020; Xie et al., 2020; Yoshino et al., 2019), mediation of temperature stress (Mao *et al.*, 2013; Wallace *et al.*, 2015; Zhu *et al.*, 2020), atherosclerosis (Liu et al., 2022), and as previously mentioned, cancer, virulence, and ribosome-dependent protein synthesis. The difficulty in characterizing the exact cellular function of OLA1 may be partially attributed to the overlap in function with other proteins proposed by Glass *et al.* (2006).

One of the best-defined and integrated interaction pathways for OLA1 is in centrosome regulation. Briefly, human (h)OLA1 is localized to the centrosome by BRCA1 and participates in a complex with RACK1, BRCA1, γ-tubulin, BARD1, and an additional unknown factor, likely a small RNA, to enable centriole duplication and microtubule elongation. BARD1 binds hOLA1•ATP and allosterically activates nucleotide hydrolysis. These studies show that hOLA1-E168Q, a variant linked to breast cancer, can bind BARD1 but not BRCA1. Interestingly, residue E168 is highly conserved (figure 7) and may also be necessary for OLA1's role in RNA binding. The focus henceforth will be on the intersection of OLA1 and ribosome-dependent protein synthesis (translation) through RNA interactions.

OLA1 Structure and Translation Factors: Intra- and Inter-Similarities

OLA1 is considered a monomeric protein. However, there is one report of *Ec*OLA1 forming dimers via a cysteine bridge in response to oxidative stress (Hannemann *et al.*, 2016). Besides this report, dimerization has not been observed, and the purification of several OLA1 homologs in the Wieden lab shows OLA1 to be a monomer.

The first atomic OLA1 model was a 2.4 Å X-ray crystallography structure from *Haemophilus influenzae* (Teplyakov *et al.*, 2003). The bacterial and eukaryotic OLA1 structures

that have been solved since are highly similar. Structural alignments of human, *Schizosaccharomyces pombe*, *Thermus thermophilus*, *Oryza sativa*, and *H. influenzae* (*Hi*)OLA1 yield RMSDs of 1.9-3.4 Å for all Cα atoms (Cheung *et al.*, 2016; Koller-Eichhorn *et al.*, 2007). Interestingly, a structure very similar to these was deposited in the protein data bank (PDB) as "GTP-binding protein" from the archaea *Pyrococcus horikoshii OT3* (PDB 1WXQ) and has not yet been annotated as another OLA1 homolog. *P. horikoshii* (*Ph*)OLA1 has a low (30%) sequence identity with *Hi*OLA1 and enough structural difference that *Hi*OLA1 could not be used to solve the *Ph*OLA1 by molecular replacement (Lokanath et al., 2005), although, its overall structure resembles bacterial and eukaryotic OLA1 (figure 5). All atomic models of OLA1, including *Ph*OLA1, are comprised of an N-terminal G-domain with an α-helical insertion and a C-terminal TGS domain (named for its presence in ThrRS, GTPase, and SpoT), as shown in figure 5.

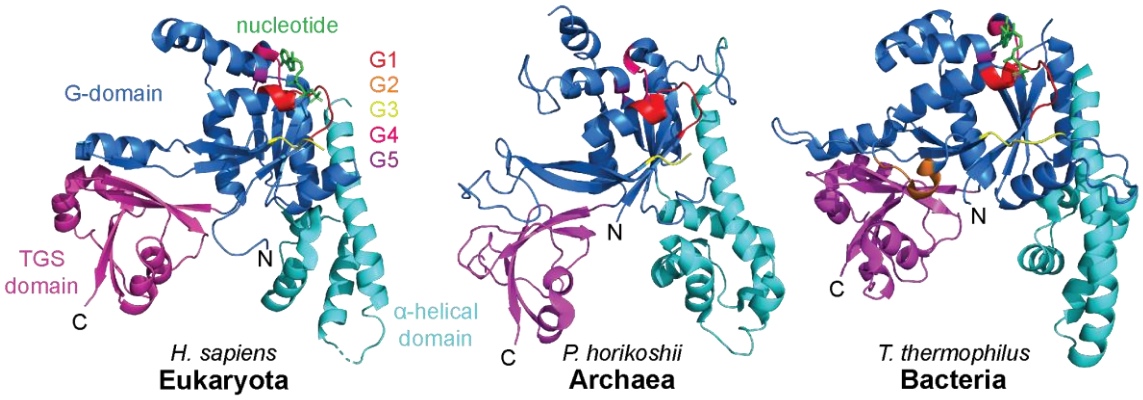

Figure 5. The structure of OLA1 is similar across the domains of life. Structures for *H. sapiens* (PDB 2OHF), *P. horikoshii* (PDB 1WXQ), and *T. thermophilus* (PDB 2DBY) OLA1 homologs were used as representatives from each domain of life. For each homolog, the G-domain is blue and the G motifs 1-5 are red, orange, yellow, pink, and purple, respectively (if resolved). The α-helical extension is cyan, the TGS domain is magenta, and the bound nucleotide is green.

The α-helical insertion is a coiled-coil domain commonly found in DNA-binding proteins (Pabo & Sauer, 1984). It is used for tRNA binding by several amino-acyl tRNA synthetases (aaRS), including ValRS, SerRS, and PheRS (figure 6A). The C-terminal coiled-coil of ValRS interacts electrostatically and hydrophobically with the tRNA elbow region's D- and TΨC -loops (Fukai *et al.*,

2003). SerRS's antiparallel α-helical domain contacts the TΨC loop and variable arm of the tRNA, appearing to curve around the tRNA (Biou et al., 1994). The N-terminal coiled-coil domain of PheRS binds the anticodon side of the tRNA elbow and the variable arm through backbone-mediated contacts (Moor et al., 2006). These examples constitute the first argument for molecular mimicry between OLA1 and tRNA binding proteins.

The second observation of molecular mimicry concerns the TGS domain, which is also present in ribosome binding GTPase 1 (Rbg1), ThrRS, and RelA (figure 6B). The GTPase Rbg1 binds A-site tRNA but not through its TGS domain. Instead, the TGS domain and an additional protein Tma46 are required for polysome binding (Francis et al., 2012; Zeng et al., 2021). On the other hand, ThrRS and RelA both associate with tRNA via their TGS domain and of these two, only RelA binds the ribosome (Brown *et al.*, 2016; Sankaranarayanan *et al.*, 1999). The ThrRS TGS domain is not known to be critical in tRNA specificity. Likewise, the RelA TGS domain binds a range of tRNA by forming electrostatic interactions between conserved basic residues (R, K, H) and the tRNA phosphate backbone (Brown *et al.*, 2016). Interestingly, RelA can bind aminoacylated and deacylated tRNA off the ribosome, but aminoacylated tRNA prevents the binding of RelA and the isolated TGS-helical domain segment to the ribosome (Takada *et al.*, 2021). An amino acid is sterically occluded by the RelA TGS β5-strand (Brown *et al.*, 2016). Work by Winther and coworkers found that RelA binding to deacylated tRNA is a prerequisite for ribosome binding in *E. coli* and that the RelA His432 stacks between the universally conserved C74 and C75 of tRNA (Winther et al., 2018). Thus, it is possible that the TGS domain of OLA1 forms sequence-independent contacts with deacylated tRNA and participates in ribosome binding as part of its functional cycle but may also bind aa-tRNA off the ribosome.

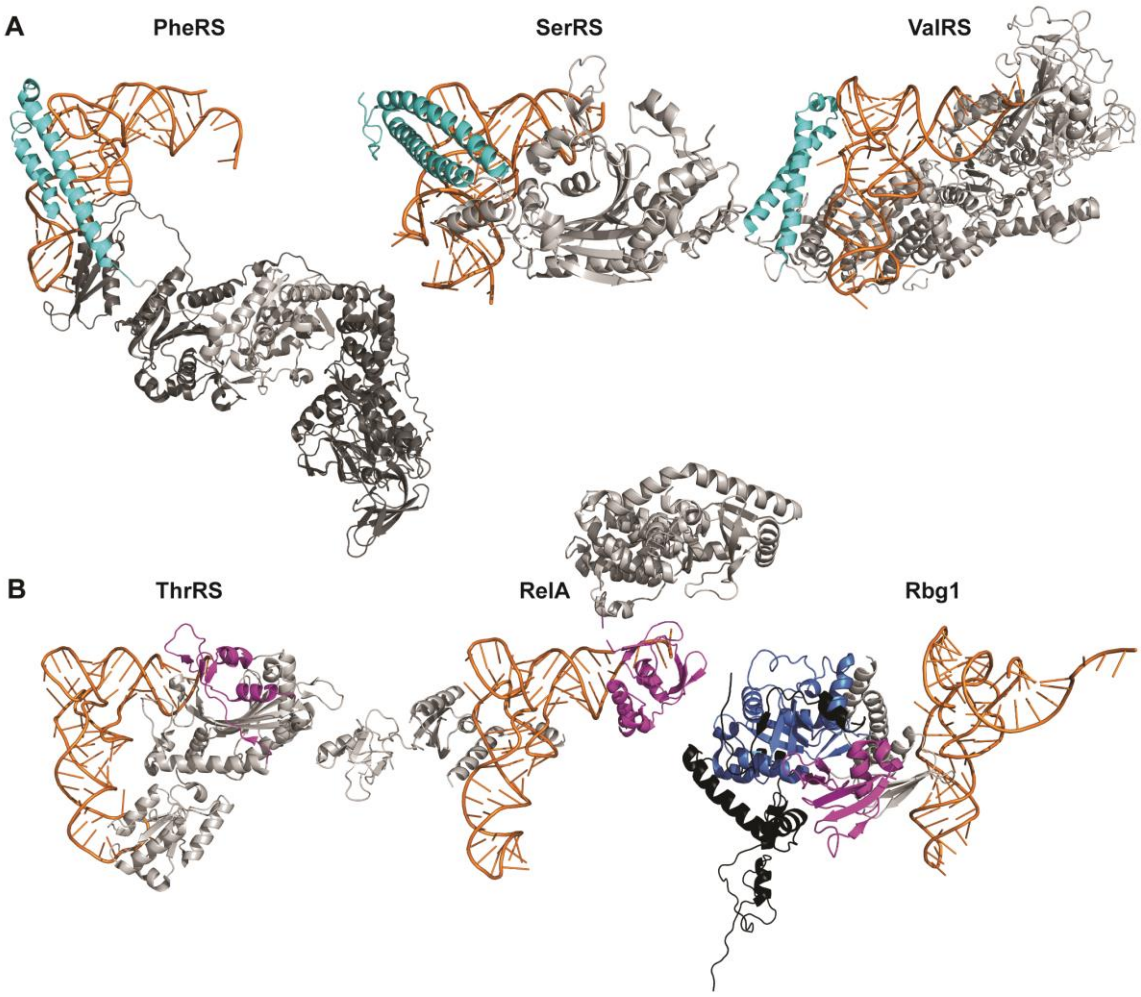

Figure 6. OLA1 shares domains with tRNA-binding proteins. (**A**) PheRS (PDB 2IY5), SerRS (PDB 4RQE), and ValRS (PDB 1IVS) use their α-helical domains (cyan) to bind tRNA. (**B**) ThrRS (PDB 4YYE), RelA (PDB 5IQR), and Rbg1•Tma1 (PDB 7RR5) use their TGS domains (magenta) to bind tRNA or the ribosome. tRNA is coloured orange, additional domains are grey, and Tma1 is black.

The tRNA binding proteins that share domains with OLA1 – the aaRS's, Rbg1, and RelA – all utilize GTP or ATP for their function, separate from tRNA binding. SerRS, ValRS, and PheRS bind deacylated tRNA and utilize ATP to form aa-tRNA, though tRNA can bind before or after ATP hydrolysis depending on the synthetase (Rubio Gomez & Ibba, 2020). Rbg1 requires nucleotide binding and the zinc-finger domain of Tma46 for its function on the ribosome but can bind the A-site with both GDP and GTP (Daugeron et al., 2011; Zeng et al., 2021). RelA requires both ATP

and GTP/GDP for synthesizing (p)ppGpp (Winther *et al.*, 2018). However, nucleotide binding is not known to dictate RelA's ability to interact with tRNA. Together, this suggests that tRNA can interact with OLA1 independent of the bound nucleotide, although a specific molecular mechanism involving tRNA may be nucleotide dependent.

OLA1's G-domain is evolutionarily conserved among ribosome-binding trGTPases like IF2, EF-Tu, EF-G, and RF3 (figures 4 and 5). It maintains the typical G motifs 1-3 and 5 but has noticeable differences in the G4 motif (NXXE instead of (N/T)KXD). The α-helical and TGS domains are positioned on either side of the G-domain with positive charges along the cleft between them. It was proposed by Teplyakov *et al.* (2003) that movement of the alpha-helical and TGS domains – putative nucleic acid binding domains – are each influenced by conformational changes in the G-domain switches upon the transition from the triphosphate to the diphosphate form. Rearrangement of the two G-domain switches into the diphosphate conformation is described as a loaded-spring or lever mechanism that regulates binding to interaction partners in other trGTPases like EF-Tu, EF-G, and IF2 (Vetter & Wittinghofer, 2001). ATP-binding motor proteins like kinesin and myosin also have switch regions that couple sensing of the γ-phosphate presence to mechanical energy transduction to support their cellular role. Thus, nucleotide binding and hydrolysis are likely coupled to a regulatory aspect of OLA1's nucleic-acid binding. So far, pre-steady-state measurements from Rosler et al. (2015) show that ATP-bound *Ec*OLA1 adopts two conformations, one of which likely positions the catalytic histidine near the bound ATP.

Consistent with a tRNA-dependent function of OLA1 on the ribosome, 2.6 Å cryogenic electron microscopy (cryo-EM) structures from *P. falciparum* (*Pf*) show *Pf*OLA1 bound in complex with deacylated tRNA at the 80S ribosomal A-site were recently reported (A. Amunts, unpublished). Samples were obtained from the lysate of *P. falciparum*-infected erythrocytes, supporting *in vivo* relevance of the respective complexes. Of note, *P. falciparum* is a eukaryotic, unicellular parasite that causes severe malaria in humans (Brazier et al., 2017). Like many TRAFAC GTPases, *Pf*OLA1 is oriented at the A-site with the nucleotide-binding pocket near the SRL and the ASF. The unstructured C-terminal tail of *Pf*OLA1 is nestled between two 18S rRNA segments that form an inter-helix-4-5 duplex. This SSU rRNA structure is a putative contact site for EF-Tu and EF-G that

is conserved in bacteria (Bowman *et al.*, 2020). Furthermore, several residues from r-proteins uS12, uL11, and P1 are found in proximity to OLA1 (A. Amunts, unpublished). The *Pf*OLA1 interactions with tRNA are similar to the interactions by RelA and Phe/SerRS; the TGS domain is bound to the CCA-end of the tRNA, while the α-helical domain contacts its TΨC loop and variable arm, appearing to curve slightly. Interestingly, His333 of *Pf*OLA1 forms a stacking interaction between C45 and C46 of tRNA, as is seen with RelA.

A multiple sequence alignment of OLA1 sequences for which structures have been obtained is presented below (figure 7), illustrating the conservation of sequence features across homologs. Because of the high conservation of OLA1's structure and sequence (*vide supra*), it is likely that OLA1 also has a conserved function across the domains of life. Thus, results from all homologs will continue to be discussed collectively, and only key differences will be highlighted.

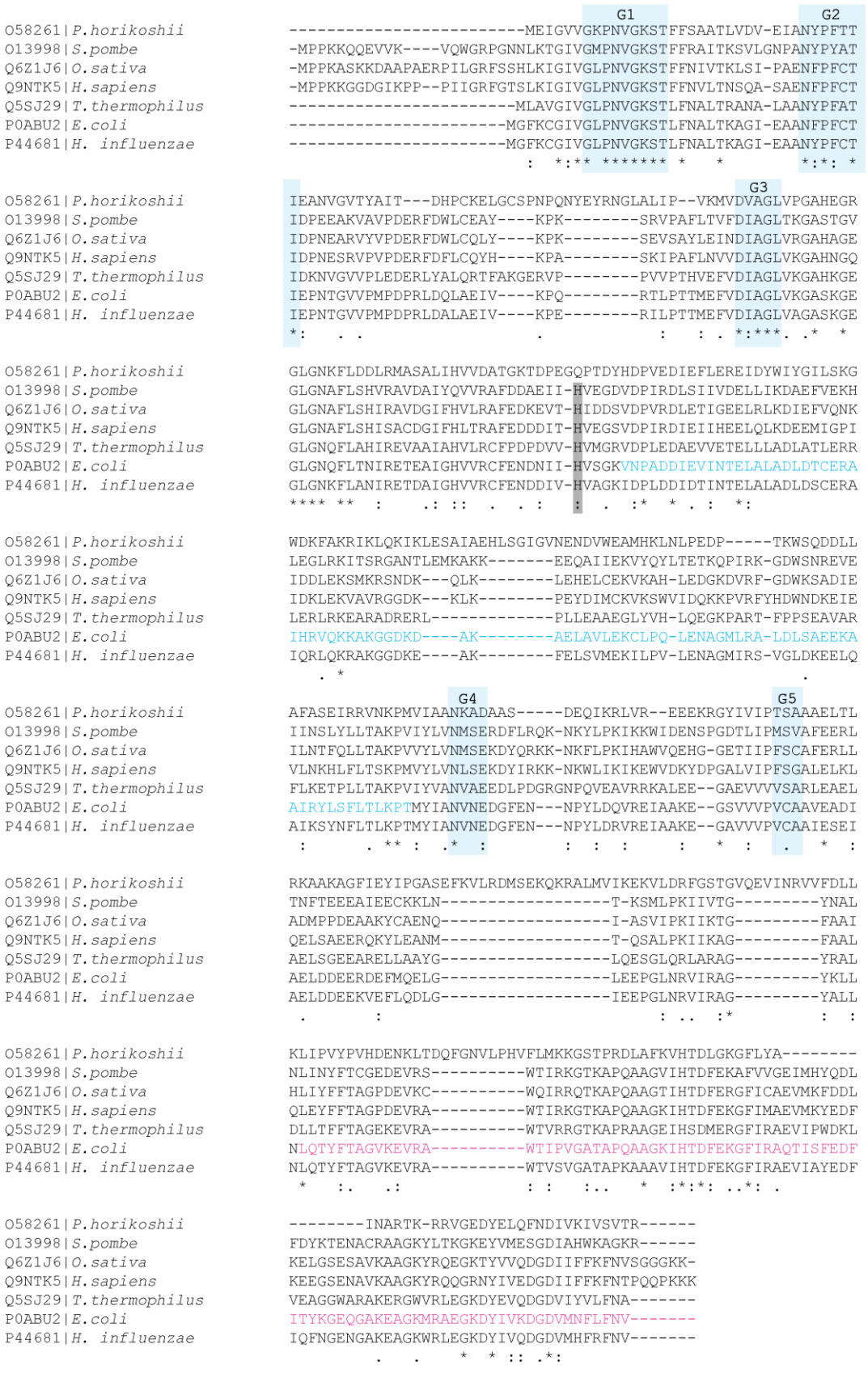
G1
G2
G3
G4
G5
O58261|P.horikoshii
O13998|S.pombe
Q6Z1J6|O.sativa
Q9NTK5|H.sapiens
Q5SJ29|T.thermophilus
P0ABU2|E.coli
P44681|H. influenzae

Figure 7. Multiple sequence alignment of OLA1 homologs summarizing conserved motifs. Sequences of all homologs for which a structure has been reported (*P. horikoshii*, *S. pombe*, *O. sativa*, H. sapiens, *T. thermophilus*, *H. influenza* sequences) and *E. coli* were aligned using CLUSTAL MUSCLE with default settings (Madeira *et al.*, 2022). The G motifs are labelled in blue boxes, and the catalytic histidine in a grey box. In the *P. horikoshii* OLA1 sequence, glutamine is found in the position of histidine. The *E. coli* OLA1 α-helical domain residues are cyan, and the TGS domain residues are magenta.

Promiscuous Nucleotide Binding

The unique OLA1 G4 motif prompted the discovery of OLA1's relaxed nucleotide binding specificity, setting it apart from other trGTPases. Some OLA1 homologs (*E. coli*, *H. influenzae*, *S. cerevisiae*, *etc*.) have preferential binding to adenine nucleotides (Becker *et al.*, 2012; Koller-Eichhorn *et al.*, 2007). In humans, OLA1 is typically an ATPase but a GTPase when phosphorylated at Thr325 (Sidlowski *et al.*, 2023). Other OLA1 homologs can bind GTP or ATP for different cellular functions without any known modifications, such as in *Oryza sativa* and *Arabidopsis thaliana* (Cheung *et al.*, 2010). Switching nucleotide preference may benefit situations where ATP concentrations can decrease by over half, as sometimes occurs in stressed cells (Bajerski *et al.*, 2018). Recently the *A. thaliana* OLA1 was reported to bind and hydrolyze ppGpp, an alarmone nucleotide, with lower affinity and a third of the maximum velocity compared to A/GTP ($V_{max} \approx 35$ vs ~93 nmol/min) (Cheung et al., 2022). Alarmones are likely inhibitors of OLA1, as they are with other trGTPases such as IF2, EF-Tu, and EF-G (Diez et al., 2020; Mitkevich et al., 2010; Rojas et al., 1984).

trGTPases (henceforth called trNTPases) contain a conserved catalytic histidine downstream of the G3 motif. In OLA1, this conserved histidine (H113, *E. coli* numbering) is found within the α-helix or disordered loop immediately preceding the α-helical domain (Rosler *et al.*, 2015). Interestingly, in the *P. horikoshii* (*Ph*)OLA1, glutamine (Gln119) is in the position of this histidine (figure 7), flanked by two histidines on either side of the disordered loop region. *Ph*OLA1

also has a canonical GTPase G4 motif, NKAD. The archaeal OLA1 may have a different nucleotide binding and hydrolysis mechanism than its bacterial and eukaryotic counterparts.

Because nucleotide binding is an essential determinant for trNTPase's interaction with the ribosome, the nucleotide specificity was investigated for OLA1. *E. coli* (*Ec*)OLA1 interacts with the 50S ribosomal subunit and 70S ribosomes in the presence of 2 mM ADP, ATP, and ADPNP, a nonhydrolyzable ATP analog (Becker et al., 2012; Tomar et al., 2011). Therefore, like EF-G, *Ec*OLA1 can interact with the ribosome in an "on" and "off" state, as defined by the bound nucleotide. Although OLA1•ADPNP has the highest binding affinity towards 70S ribosomes, it is unknown if ADPNP induces an OLA1 conformation that more closely resembles the ATP or ADP•P_i-bound state. Interestingly, *A. thaliana* OLA1 does not bind 26S rRNA in the presence of ppGpp, suggesting the alarmone inhibits ribosome binding by OLA1 (Cheung *et al.*, 2022). This further implies that the OLA1•ribosome interaction is ATP dependent to some extent.

The intrinsic OLA1 ATPase activity is low (< 1 min^{-1}) (Becker *et al.*, 2012; Koller-Eichhorn *et al.*, 2007) and still lower when OLA1 is dimerized (Hannemann *et al.*, 2016). Like EF-Tu, EF-G, and other TRAFAC members, OLA1's hydrolysis activity is enhanced by GAFs, such as the 70S ribosome. When *Ec*OLA1•ATP binds to the 70S ribosome, hydrolysis is stimulated ~10-fold (Becker *et al.*, 2012). It is likely that the ribosomal stalk and SRL are responsible for stimulating hydrolysis similar to other trNTPases. Consistent with this analogy to the canonical trNTPases, the stalk proteins are in proximity of the G-domain of OLA1 in the *P. falciparum* 80S structure (A. Amunts, unpublished). No additional data to support their direct role in catalysis has been reported. Interestingly, a modest stimulation of the OLA1 NTPase activity by approximately an order of magnitude through a potential allosteric effect has been reported for the *O. Sativa* GTPase-activating protein (GAP)1 and human BRCA1 associated RING domain (BARD)1 (Chen et al., 2022; Cheung et al., 2010; Cheung et al., 2008). The proposed mechanisms of GAP1 and BARD1 involve binding to the TGS domain, not the G-domain. Interaction between GAP1 and OLA1 also curiously prevents OLA1 from binding to LSU rRNA in rice (Cheung *et al.*, 2010). If GAP1 and

BARD1 interact similarly with OLA1, they could provide an additional layer of regulation for ribosome binding by OLA1 in rice and humans, respectively.

Nucleic Acid Binding as Suggested by Molecular Mimicry

OLA1 binds to a wide range of nucleic acids. The first demonstration of OLA1 binding to nucleic acid was with double-stranded DNA (Teplyakov *et al.*, 2003). In line with this, the ordinarily cytosolic hOLA1 localizes to the nucleus upon phosphorylation, enhancing the transcription of genes for mitochondrial proteins (Sidlowski *et al.*, 2023). The phosphorylation of conserved residue T325 results in conformational changes that expose DNA-binding motifs. Cheung and colleagues (2010) have shown that *O. sativa* OLA1's TGS domain binds 26S rRNA but not the 5.8S or 18S rRNAs, suggesting some target discrimination. If the interaction with nucleic acids is similar to other proteins with α-helical and TGS domains, it is most likely not sequence-specific; either a particular recognition motif is being overlooked, or OLA1 has structure-specificity concerning its nucleic acid binding activity. Interestingly, Teplyakov *et al.* (2003) noted that a more flexible nucleic acid, like RNA rather than DNA, would better wrap around the curved patch of polar residues of the α-helical domain, as is seen by tRNA in the *P. falciparum* structure (A. Amunts, unpublished). Overall, the nucleic acid specificity of OLA1 is not yet fully understood, with a detailed understanding of the role of tRNA binding particularly lacking.

Existing OLA1 Hypotheses

A role for OLA1 in translation was initially proposed based on its presence in multiprotein complexes with translation factors such as eEF1 in *S. cerevisiae* (Gavin *et al.*, 2002) and being co-transcribed with the gene for Pth in enterobacteria like *E. coli* (Cruz-Vera et al., 2002). Since then, OLA1 has been shown to interact with ribosomes in various organisms (Becker et al., 2012; Chen et al., 2015; Tomar et al., 2011), leading to many hypotheses on why and how exactly this occurs. Despite OLA1 structures hinting at nucleic acid binding, only Cheung *et al.* (2010) and Brandon (2021) investigate the interaction between OLA1 and RNA. Over the years, many hypotheses have been brought forth to explain select OLA1-related observations, not many of which involve a clear role for tRNA. Each of the following paragraphs contains proposed roles for OLA1 in translation, some of which overlap.

In 2009, Gradia *et al.* performed polysome profiling and located OLA1 in the ribosomal subunit and polysome fractions of cell lysates from *Trypanosoma cruzi* (*Tc*), a parasitic euglenoid, by immunoblotting. Immunoprecipitation further showed that *Tc*OLA1 interacts with eS7 and uL24, as well as the proteasome subunit RPN10 (in agreement with the Guerrero *et al.* (2006) yeast study). *Tc*OLA1 no longer associates with ribosomes in the presence of puromycin, a translation-inhibiting antibiotic that destabilizes polysomes (Kedersha *et al.*, 2000), suggesting *Tc*OLA1 engages during active translation. OLA1 also binds to ribosomes and polysomes in humans, specifically HEK293T (embryonic kidney) and A549 (lung carcinoma) cells (Chen et al., 2015). Together, these observations prompt the hypothesis that OLA1 participates in active translation in eukaryotes, perhaps assisting in the degradation of aborted proteins (Gradia *et al.*, 2009; Guerrero *et al.*, 2006).

Interestingly, several findings contradict *Pf*OLA1 binding to the ribosomal A-site. As previously mentioned, Gradia *et al.* (2009) showed the binding of *Tc*OLA1 to eS7 (located near the ribosomal E-site) and uL24 (near the polypeptide exit tunnel). Additionally, crosslinking of *Ec*OLA1(N20pBpa) by Landwehr *et al.* (2021) revealed the OLA1 N-terminus to be within 10Å of uL29, another r-protein near the polypeptide exit tunnel, perhaps because of a crowded polysome environment. The other *Ec*OLA1(N20pBpa) crosslinks are on the center of the SSU exterior (bS1uS2, uS3, uS5, uS8, uS10, uS11, bS18, bS21), with IF3, and with bL7/12. The authors suggest that the distribution of contacts is an artifact caused by the 10 Å crosslinking range of pBpa and possibly OLA1 dimerization, but neither was investigated further. Landwehr *et al.* (2021) also compared protein synthesis from different mRNA constructs *in vivo* in the presence and absence of OLA1. The presence of OLA1 correlated with impairment of leaderless mRNA translation. Coupled with the observation that OLA1 crosslinks to uS11 and IF3, it is suggested that OLA1 somehow promotes the binding of IF3 to the ribosome to encourage the translation of canonical mRNA instead of leaderless mRNA.

A gene deletion study by Samanfar *et al.* (2014) in *S. cerevisiae* (*Sc*) adds to the pool of potential interactions. Gene deletion of either uL11 (stalk protein), eL15 (binds 5.8S rRNA), Gcn1, or eEF2 (translocation) in combination with deletion of OLA1 leads to a significant decrease in

fitness, suggesting an overlap of their functions (in agreement with Glass *et al.* (2006)). Furthermore, the authors found that overexpression of *Sc*OLA1 compensates for the absence of uS17 (mRNA exit tunnel), eS8 (bridges 40S and 60S), and arginine-specific carbamoyl phosphate synthetase A1 (CPA1) in the presence of subinhibitory concentrations of the translocation inhibitor cycloheximide (45 ng ml^{-1}). This OLA1 gene deletion in *S. cerevisiae* increases the translation rate and decreases stop codon recognition. In other words, OLA1 is thought to promote premature stop codon bypass (Samanfar *et al.*, 2014). With Gcn1 now recognized for suppressing frameshifting (Houston et al., 2022), the overlap with OLA1 proposed by Samanfar *et al.* (2014) is clearer. Still, whether these observations result from the direct interaction of OLA1 with translation machinery or from OLA1-induced effects on other translation factors is unknown.

A year later, Chen et al. (2015) found that OLA1 suppresses canonical but not IRES-mediated initiation in human cells. Chen et al. (2015) also reported that the formation of the initiation ternary complex (eIF2•GTP•Met-$tRNA_i^{Met}$) is affected by different hOLA1 variants *in vitro*. Specifically, initiation ternary complex formation is suppressed by 80% in the presence of equimolar wt hOLA1, 15% with hOLA1**(**N230A) that lacks nucleotide binding, 50% with ΔTGS-hOLA1, and 0% with hOLA1•GDPNP. Chen et al. (2015) propose that OLA1 binds eIF2 and hydrolyzes available GTP, creating a GDP "cloud" that prevents eIF2 from binding the GTP it needs for initiation ternary complex formation. A direct interaction between hOLA1 and aIF2α was predicted using ZDOCK, but the model did not include tRNA. Given that an OLA1•nt•tRNA complex forms in eukaryotes, I propose that OLA1•nt could outcompete eIF2 for tRNA binding rather than binding eIF2 directly. However, this alternative explanation depends on OLA1 being able to bind aa-tRNA, which is yet to be tested. One certainty from Chen et al. (2015) is that GTP hydrolysis is required for OLA1 to inhibit eIF2.

OLA1 was designated a biogenesis factor due to "careful domain analysis, observed homology to bacterial ribosome biogenesis factors, and their detection in the ribosomal fractions" by Olinares et al. (2010). Specific details about the domain analysis and observed homology are lacking. However, mass spectrometry revealed a low abundance of OLA1 (relative abundance of 300 vs EF-Tu's 17 800 copies) and that OLA1 associates with a low amount of mono- or polysomes

(~6%) in the plant *Arabidopsis thalia* (Olinares *et al.*, 2010). In line with this, *Ec*OLA1 was observed to co-elute with an RNA helicase involved in rRNA maturation, RhlE, and to bind only ~30% of 70S ribosomes during immunoprecipitation (Becker *et al.*, 2012). *Ec*OLA1 is most abundant during exponential growth when ribosome biogenesis is high (Wieden, unpublished). Notably, OLA1 depletion in *E. coli* does not change ribosome composition (Gibbs *et al.*, 2020; Landwehr *et al.*, 2021). If OLA1 is involved in ribosome biogenesis, the interaction surface is likely exposed on mature ribosomes, perhaps enabling additional "inspection" by OLA1 during translation. Despite the proposed biogenesis function, it is not clear whether OLA1 targeting specific ribosomes is related to the ribosome structure, to the translated mRNA (e.g., leaderless mRNA), or both.

Lastly, a hypothesis tangentially related to the proposed OLA1•eIF2α interaction, translation of noncanonical mRNA, and various Δ*ola1* stress responses: perhaps OLA1 acts as a placeholder in the A-site to reversibly pause translation during stress, including during localization to stress granules in eukaryotes. When translation is stalled due to suboptimal conditions like oxidation, heat, cold, *etc.*, in eukaryotes, translation factors and 40S subunits are sequestered into stress granules (Hofmann et al., 2021). The exact stress granule assembly mechanisms discovered so far are sorted into types, with type I being the best studied. Type I involves a decrease in initiation through at least 20-30% removal of active eIF2α, canonically through eIF2α phosphorylation (Tweedie & Nissan, 2021). Not only is OLA1 suggested to prevent eIF2α dependant initiation but OLA1 also seems to localize to stress granules in *S. cerevisiae* during heat stress (46°C) (Wallace *et al.*, 2015). Two similar studies using different quantification techniques noted *Sc*OLA1 to have the most substantial transition from soluble to insoluble fraction upon heat stress (>98% insoluble and 13.0 ± 4.3-fold enrichment) (Cherkasov *et al.*, 2015; Zhu *et al.*, 2020). Without *Sc*OLA1, there is less translation upon heat shock recovery and higher *de novo* synthesis of proteasomal subunits (Dannenmaier *et al.*, 2021). Interestingly, OLA1 is not found in the stable core of mammalian or yeast stress granules (Jain *et al.*, 2016), suggesting that OLA1 is located near their edge. Furthermore, I propose that the translation product must be degraded when OLA1 cannot pause translation reversibly. Though highly speculative, this interplay could explain the relationship between OLA1, the proteasome, and translation mentioned above.

A Hypothesis Built on Molecular Mimicry

OLA1 is not abundant in the cell, especially compared to EF-Tu, which raises the question of how OLA1 can outcompete EF-Tu for binding to an overlapping site on the ribosome. Concentrations of OLA1 are ~0.4 to 4 μM in *E. coli* and ~0.2 μM in human USO2 cells, whereas EF-Tu concentrations are ~34 μM and ~10 μM in the same organisms, respectively (Calculated from Ishihama *et al.* (2008) and Beck *et al.* (2011)). Despite OLA1 concentrations being an order of magnitude lower than EF-Tu concentrations, OLA1 is bound to tRNA at the A-site in a cryoEM structure (A. Amunts, unpublished), coinciding with other biochemical data (*vide supra*). Similar to other A-site binding proteins, there must be some differentiator at the binding site allowing OLA1 to compete with EF-Tu. For instance, EF-G binds when a peptidyl-tRNA blocks the EF-Tu ternary complex. It is unclear if, like EF-G, OLA1 binds when a tRNA is already at the A-site. Alternatively, OLA1 could help recruit tRNA to the ribosome as part of a ternary complex, like EF-Tu. The identity and acylation state of the target tRNA are also of interest, as they reflect different phases of translation and the presence of stress. trNTPases interact with Met_i-, aa-, and peptidyl-tRNA, whereas RelA appears to bind a range of deacylated tRNA during amino acid starvation (Winther *et al.*, 2018). Interestingly, the results from Becker *et al.* (2012) clearly show that the empty 70S ribosome acts as a GAF towards OLA1. Thus, tRNA is not a prerequisite for ribosome binding *in vitro*. Nevertheless, nucleotide hydrolysis is typically indicative of critical regulatory roles. This leads to the overarching question of what tRNA and OLA1 do together at the A-site and if it requires ATP.

I propose that OLA1 can circumvent RNA misfolding at the A-site that otherwise prevents the interaction of EF-Tu and other translation factors. Within this context, OLA1 has been proposed as a ribosome biogenesis factor (Becker *et al.*, 2012; Olinares *et al.*, 2010), and preliminary helicase assay results suggest that OLA1 remodels RNA (Brandon, 2021). In line with the hypothesis that OLA1 performs ribosomal maintenance during biogenesis and that the EF-Tu and tentative OLA1 ternary complexes are similar, the tRNA may be required to ensure a restored binding site before OLA1 dissociates. Nucleotide hydrolysis both gates and enables movement in

the roles of trNTPases. In the proposed OLA1 model, ATPase activity would facilitate OLA1 dissociation from the remodelled A-site.

Results from previous studies support the proposed hypothesis of OLA1 being a ribosome maintenance protein. OLA1 provides a fitness advantage during cold stress (Wieden lab unpublished, Wenk *et al.*, 2012), when rRNA may become trapped in unproductive conformations, and during heat stress where there may be thermally induced local unfolding (Dannenmaier *et al.*, 2021; Dassain *et al.*, 1999). *Ec*OLA1 is expressed most highly during exponential growth when ribosome concentrations also increase for vigorous translation, but *Ec*OLA1 is moderately present at all stages of growth (Wieden lab unpublished). Ribosome maintenance by OLA1 could explain how OLA1 seems to be involved in every phase of translation – from ribosome biogenesis and initiation to stop codon recognition (Chen et al., 2015; Gradia et al., 2009; Landwehr et al., 2021; Samanfar et al., 2014) – as well as stress granule regulation (Cherkasov *et al.*, 2015; Zhu *et al.*, 2020). Furthermore, it does not exclude moonlighting activities involving other nucleic acid sequences from the functional cycle of OLA1. Moonlighting roles in DNA replication, RNA splicing, and amino-acid biosynthesis are not uncommon for tRNA-binding proteins (Lechler & Kreutzer, 1998; Mateyak & Kinzy, 2010; Zhou et al., 2015).

Objectives I and II

To enable a comprehensive investigation into OLA1's role on the ribosome, I aim to identify OLA1's affinity to deacylated tRNA (objective 1) and if OLA1 can unwind rRNA (objective 2).

Deep sequencing of RNAs that co-elute with *Ec*OLA1 during affinity chromatography and size exclusion chromatography showed all tRNAs to be enriched at least 4-fold in comparison to other short ncRNAs (<100 nt) (Brandon, 2021). $tRNA^{Phe}$ was enriched over 20-fold, while $tRNA^{Lys}$ was the least enriched tRNA. Thus, $tRNA^{Phe}$ and $tRNA^{Lys}$ are excellent candidates for biochemically measuring the binding affinity between OLA1 and tRNA. To explore if the role of OLA1 is conserved across domains of life, it is also important to compare both prokaryotic and eukaryotic OLA1 homologs (hOLA1 and *Ec*OLA1) when investigating their tRNA binding. Thus, the *first* objective of my thesis is to characterize the binding of hOLA1 and *Ec*OLA1 to $tRNA^{Phe}$ and $tRNA^{Lys}$ using

electrophoretic mobility shift assays (EMSAs) and nitrocellulose filter binding. Radiolabelling is used, as it does not compromise the three-dimensional structure of the ligand, which is a strength over methods that require conjugation to a fluorophore. This will establish whether OLA1 can bind tRNA in the absence of the ribosome.

The *second* objective of my thesis relates to a potential role for OLA1 on the ribosome. If OLA1 is a ribosome maintenance protein that remodels rRNA, it may also be able to remodel rRNA off the ribosome. The RNA remodelling activity of *Ec*OLA1 will be tested for rRNA using a Microscale Thermophoresis (MST) helicase assay described in Nelson et al. (2020). MST is advantageous because the change in size-dependent thermophoresis is largely independent of fluorophore location. In contrast, fluorescent microscopy requires more optimization of the fluorophore location to ensure an adequate signal change upon ligand binding.

The outcomes of this research are summarized in the conclusion, and future perspectives are laid out directly afterwards.

CHAPTER 2: MATERIALS AND METHODS

Buffers and Reagents.

All solvents and reagents were purchased from Thermo Fisher Scientific, Bio Basic Inc., VWR, and J.T. Baker. Biochemicals and corresponding buffers were purchased from Thermo Fisher Scientific and New England BioLabs. Nucleotides ((A/U/C/G)TP, d(A/T/C/G)TP, and ADP) were obtained from Sigma-Aldrich. Radiochemicals were purchased from PerkinElmer®. *E. coli* BL21(DE3), *E. coli* DH5α, and *E. coli* MRE600 cells were purchased from New England BioLabs. Total *E. coli* tRNA was purchased from Roche Diagnostics.

All buffers were filtered and degassed using sterile 0.45 µm nitrocellulose membrane filters (GE Healthcare) prior to use.

Plasmid DNA Maxiprep.

E. coli DH5α cells containing pCFO encoding the $tRNA^{Phe}$ gene were grown in 500 mL Lysogeny Broth (LB) supplemented with antibiotic (100 µg/mL ampicillin) overnight at 37°C and 220 rpm. Cells were subsequently harvested by centrifugation (5000xg, 10 min). The resulting cell pellet (typically 1-2.5 g) was gently resuspended in 6 mL Alkaline Lysis Solution I (ALSI; 50 mM glucose, 25 mM Tris-Cl, 10 mM EDTA, 8.0 pH) with 20 µg RNase A (Bio Basic; Cat. No. RB0473), incubated at room temperature for 10 minutes with 5 mg lysozyme (Bio Basic; Cat. No. LDB0308) and incubated 10 minutes on ice in 12 mL ALS II (0.2N NaOH, 1% (w/v) SDS). Then 9 mL cold ALS III (3 M K-acetate, 11.5% (v/v) acetic acid) was added for another 10-minute incubation on ice. The cell debris was pelleted using centrifugation (4500xg, 15 min, 4 ºC), strained through a Kimwipe™, and the DNA therein was extracted from the supernatant using phenol: chloroform extraction.

Equal volumes of a 1:1 acidic phenol (pH < 5): chloroform solution was combined with the respective nucleic acid containing solution and mixed by vortexing for 15 s. The aqueous and organic phases were separated by centrifugation (5800xg, 2 min). The upper aqueous phase was transferred into a new tube, washed with an equal volume of chloroform, and then centrifuged again (5800xg, 2 min). The aqueous phase was transferred to a new tube once more, then washed

with an equal volume of chloroform. Following a final centrifugation step (5 800xg, 2 min), the nucleic acid was ethanol precipitated.

To precipitate the contained nucleic acid, 3 M KOAc (pH 5.2) was added to the aqueous phase from the previous step to a final concentration of 0.3 M KOAc. Next, three volumes of ice-cold ethanol and glycogen (1 µg/µL) were added, and the resulting solution was incubated overnight at 4°C. All precipitated nucleic acid was pelleted by centrifugation (5 800xg, 20 min, 4°C) and the supernatant was removed. The resulting pellet was washed once with 3 mL ice-cold 70% ethanol (5800xg, 5min). Following the ethanol wash the pellet was air dried, then resuspended in 4 mL 20 mM Tris-HCL (pH 8.0), treated with 0.05 mg/mL RNase I (Thermo Scientific™; Cat. No. EN0601) at room temperature overnight, ethanol precipitated (0.1 vol. 3M NaOAc pH 5.2, 2 vol. cold ethanol), and finally resuspended in 400 µL milliQ H_2O.

***In Vitro* Transcription and Purification of tRNA^{Lys} and tRNA^{Phe}.**

The DNA for each tRNA was obtained using two slightly different protocols. For tRNA^{Phe}, *E. coli* DH5α containing the pCFO plasmid with the gene coding for *E. coli* tRNA^{Phe} was gifted by U. Kothe (Sampson & Uhlenbeck, 1988; Wright et al., 2011). This plasmid was maxi-prepped (described above, 2.2) and stored at -20°C for future use. The DNA template for the *in vitro* transcription of *E. coli* tRNA^{Phe} was touchdown PCR amplified from the pCFO plasmid as in Wright *et al.* (2011) using primers 1 and 2 (table 1). Following PCR, the reaction was incubated for 1 hr with DpnI (Thermo Scientific™; Cat. No. ER1701) at 37°C to remove the plasmid DNA. Subsequently, a Monarch® PCR & DNA Cleanup Kit (#T1030) was used to purify and concentrate the DNA template prior to use in *in vitro* transcription (IVT). For tRNA^{Lys}, the gene was first constructed by overlap extension PCR using primers 3 and 4 (table 1). The resulting PCR product was purified using gel extraction (EZ-10 Spin Column DNA Cleanup Kit, Bio Basic, Cat. No. BS367). The extracted template was then PCR amplified using primers 5 and 6 (table 1). Prior to use as an IVT template, the PCR product was purified with the Monarch® PCR & DNA Cleanup Kit.

Table 1. Primers for the amplification of $tRNA^{Lys}$ and $tRNA^{Phe}$

Primer	Sequence (5' to 3')
1	TAATACGACTCACTATAGGG
2	mUmGGTGCCCGGACTCG
3	TAATACGACTCACTATAGGGTCGTTAGCTCAGTTGGTAGAGCAGTTGACTTTTAATC
4	TGGTGGGTCGTGCAGGATTCGAACCTGCGACCAATTGATTAAAAGTCAACTGCTCTA
5	TAATACGACTCACTATAGGG
6	mUmGGTGGGTCGTGCAGGAT

Each IVT (50 µL test IVT / 1 mL preparative IVT) contained 10 mM DTT, 3 mM NTPs (ATP, UTP, CTP, and GTP), 5 mM GMP, 0.01 U/µL inorganic pyrophosphatase (Sigma-Aldrich®; Cat. No. 9024-82-2), 0.3 µM T7 RNA polymerase (in-house), 0.12 U/µL RiboLock RNase inhibitor (Thermo Scientific™; Cat. No. EO0381), and 1-2 ng/µL DNA template in transcription buffer (40 mM Tris-Cl, 15 mM $MgCl_2$, 2 mM spermidine, 10 mM NaCl, pH 7.5). IVTs were carried out at 37°C for a minimum of 3 hours. Each reaction was digested with 1 U/µL DNase I (Thermo Scientific™; Cat. No. EN0521) for 1 hr at 37°C. The enzymes were then heat-inactivated (70°C, 10 min) prior to phenol: chloroform extraction and ethanol precipitation of the generated RNA. The phenol: chloroform extraction and ethanol precipitation follow the same steps as those used during the DNA maxiprep (described above) except for the exclusion of the RNase treatment. Following precipitation, the tRNA was isolated by size exclusion chromatography (using a Superdex™ 200 Increase 10/300 GL or Superdex™ 75 10/300 GL depending on column availability) in RNA buffer (20 mM Hepes, 100 mM NaCl, 5 mM $MgCl_2$, pH 7.5). Fractions containing tRNA were identified using 15% 8M Urea-PAGE, pooled, and ethanol precipitated. The supernatant was discarded, and the resulting RNA pellet was resuspended in 100 µL H_2O. The concentration of each tRNA was determined spectroscopically by measuring the absorbance at 260 nm using the following molecular extinction coefficients: $\varepsilon_{260}=5\times10^5\ M^{-1}\ cm^{-1}$ for $tRNA^{Phe}$ (Peterson & Uhlenbeck, 1992); and the theoretical value $\varepsilon_{260}=7.5\times10^5\ M^{-1}\ cm^{-1}$ for $tRNA^{Lys}$.

Uniformly [5-^{3}H]UTP-labelled $tRNA^{Phe}$ was a gift from Dr. Ute Kothe (Wright *et al.*, 2011).

Protein Purification.

TruB and PheRS were generously donated by Schultz, S., from the laboratory of Dr. U. Kothe. N-terminally His_6-tagged wildtype *E. coli* OLA1 was readily available from previous lab member Dr. Harland Brandon. GST and N-terminally GST-tagged OLA1 were available from previous lab member Dr. Binod Pageni and newly purified by Fan Mo. StpA was purified previously by Jeremy Quiroga and LysRS and EF-Ts by Dr. Taylor Sheahan. BSA was purchased from Bio Basic Inc (Cat. No. AJ642).

All proteins were purified from *E. coli* BL21(DE3) cells using Ni^{2+}-Sepharose® 6Fast Flow column (GE Healthcare, Cat. No. 17–5318–02) followed by Superdex™ 75 XK26/100 column (GE Healthcare, Cat. No. 17–1044–02) size exclusion chromatography with a couple of exceptions. GST-hOLA1 was purified using Glutathione Sepharose® 4B (GE Healthcare, Cat. No. 17-0756-01) and purified with and without strong anion exchange before size exclusion chromatography.

N-terminally H_6-tagged wildtype *E. coli* OLA1 was purified similarly as described in Becker *et al.* (2012). The standard nucleic acid-binding protein purification protocol used in the Wieden lab for proteins such as *Ec*OLA1 is as follows. First, pET28a plasmids containing the *ola1* gene were transformed into competent *E. coli* BL21(DE3) cells and grown in LB supplemented with 50 µg/ml Kanamycin at 37°C and 220 rpm. Overexpression was induced with 1mM isopropyl-β-D-thiogalactopyranoside at an OD_{600} of 0.6. The cells were grown to stationary phase before being pelleted by centrifugation (10 min, 5000xg, 4°C, JLA 16.250), flash frozen, and stored at -80°C. The cells were opened in 7 ml of buffer A (50 mM Tris-Cl, 60 mM NH_4Cl, 7 mM $MgCl_2$, 300 mM KCl, 10 mM imidazole, 15% (v/v) glycerol, 7mM β-mercaptoethanol, 1mM PMSF, pH 8.0), with 1 mg/mL lysozyme, 12.5 mg sodium deoxycholate, and a few DNase I crystals per gram of cells. The resulting lysate was centrifuged twice (30 min, 5000xg and 45 min, 30000 xg, JA 25.50), and the final supernatant was incubated on a gravity-flow Ni^{2+}-Sepharose® 6Fast Flow column at 4°C with gentle rocking for 1 hr. An increasing concentration of imidazole, from 20 to 300 mM in buffer A, was used to elute the protein. Eluted protein (confirmed by 12% SDS-PAGE) was buffer exchanged into buffer QA (50 mM Tris-base, 10 mM $MgCl_2$, 0.5 mM EDTA, 1.0 mM dithiothreitol, pH 7.5) using

a Vivaspin® 20 30 kDa MWCO polyethersulfone centrifugal filter (GE Healthcare; Cat. No. 28–9323–61). OLA1 was separated from nucleic acid using Q-Sepharose® XK26/10 Fast Flow (GE Healthcare, Cat. No. 17–0510–10) anion-exchange chromatography on an Äkta FPLC purification system (GE Healthcare). A gradient of increasing salinity in buffer QA (0 to 1 M KCl) was used to elute the resin-bound protein. Fractions containing *Ec*OLA1 were pooled, concentrated, and further purified by size exclusion on a Superdex™ 75 XK26/100 column in $TAKM_7$-Cl (50 mM Tris-HCl, 70 mM NH_4Cl, 30 mM KCl, 7 mM $MgCl_2$, pH 7.5). Fractions containing pure *Ec*OLA1 were pooled, concentrated, flash-frozen, and stored at -80°C.

To monitor purity and nucleic acid contamination, the obtained protein samples were resolved using 12% SDS-PAGE and 15% 8M Urea-PAGE, and subsequently stained with Coomassie brilliant blue or ethidium bromide before being imaged using the Amersham™ Typhoon™ Laser-Scanner Platform Densitometry or Cy3 settings, respectively.

The concentration of GST-hOLA1 co-purifying with tRNA was determined using densitometry, with bovine serum albumin (BSA) and EF-G as standards. The concentrations of nucleic acid-free proteins were determined photometrically at 280 nm using theoretical extinction coefficients ε_{280}=29 910 M^{-1} cm^{-1} for GST (Uniprot Q1RBG0), ε_{280}=74 175 M^{-1} cm^{-1} for tRNA-free GST-hOLA1 (UniProt Q1RBG0 and Q9NTK5), ε_{280}=2 980 M^{-1} cm^{-1} for His_6-EF-Ts (UniProt O82851), ε_{280}=12490 M^{-1} cm^{-1} for His_6-StpA (UniProt P0ACG1), and ε_{280}=16305 M^{-1} cm^{-1} for His_6-*Ec*OLA1 (UniProt P0ABU2). All theoretical extinction coefficients were calculated using the Expasy ProtPram tool (Gasteiger et al., 2005).

Ribosome Isolation.

Vacant 70S ribosomes were purified from *E. coli* MRE600 cells using sucrose-gradient centrifugation as described in Milon *et al.* (2007) by H.-J. Wieden and lab members.

Nondenaturing Electrophoretic Mobility Shift Assays (EMSAs).

Electrophoretic mobility shift assays were used to analyze protein-RNA complex formation. First, $tRNA^{Phe}$ was refolded by heating at 65°C for 5 minutes and cooling at room temperature for 10 minutes in 1x$TAKM_7$-Ac buffer (50 mM Tris-Ac, 70 mM NH_4OAc, 30 mM KOAc, 7 mM $Mg(OAc)_2$,

pH 7.5). 10 µL reactions of 1 µM tRNA, 100 µM nucleotide (ATP or ADP), and 0-8 µM *Ec*OLA1, TruB, EF-Ts, or (0-3 µM) GST-hOLA1 were incubated at 37°C for 10 minutes before being combined with glycerol (4% (v/v), final), then resolved on nondenaturing acrylamide gels at 150 V for 30 minutes (8% acrylamide (19:1), 1xTAKM$_7$-Ac buffer). Protein concentrations were chosen based on known dissociation constants for tRNA^{Phe} (Keffer-Wilkes et al., 2016). Buffer composition and run time were optimized by monitoring the RNA and protein migration using silver-staining (described below, 2.7). To avoid the RNA and protein bands potentially obscuring one another, EMSAs were separately stained with ethidium bromide and Coomassie brilliant blue. The fraction of total tRNA shifted in each lane was quantified using ImageJ. The respective equilibrium dissociation constants were estimated from the concentration dependence of % tRNA shifted as the approximate protein concentration at half of the maximum.

Silver Staining of Proteins and Nucleic Acids.

Silver staining is a sensitive colorimetric technique for detecting proteins and nucleic acids. Here it was used to ensure that both the tRNA and protein were migrating into the acrylamide EMSA gels. First, each gel was incubated in Fix I (30% (v/v) EtOH, 10% (v/v) acetic acid) for 15 minutes, followed by a minimum 30 minutes in Fix II (30% (v/v) EtOH, 0.5% (v/v) acetic acid, 0.4 M $C_2H_3NaO_2$, 0.5 % (v/v) glutaraldehyde, and 1 mg/mL $Na_2SO_4O_3$). The gels were then washed thrice for 5 minutes with milliQ H_2O, incubated 30 minutes with silver stain solution (1.45 g/L $AgNO_3$, 9.25x10^3 % (v/v) formaldehyde), and briefly rinsed with milliQ H_2O. Finally, each gel was incubated in a developing solution (25 µg/mL Na_2CO_3, 1.48x10^2 % (v/v) formaldehyde) until both the nucleic and amino acids were visible, at which point the reaction was quenched with 5% (v/v) acetic acid. The protein stain appears black, whereas the nucleic acid stains brown (sfigure 2).

Aminoacylation of tRNA^{Lys} and tRNA^{Phe}.

The ability to aminoacylate tRNA with cognate aa can be used to assess correct tRNA folding (Bhaskaran et al., 2012; Gartland & Sueoka, 1966). Pure tRNA^{Phe} and tRNA^{Lys} were unfolded at 65°C for 5 minutes and allowed to refold at room temperature for 10 minutes in 1xTAKM$_7$-Ac buffer. For a small-scale (50 µL) aminoacylation, each reaction contained 0.6 µM cognate tRNA, 6 mM

ATP, 3 mM PEP (Sigma-Aldrich®; Cat. No. 860077), 0.002 U/µL pyruvate kinase (Roche; EC 2.7.1.40), 1 mM DTT, 0.03 U/µL inorganic pyrophosphatase, 0.3 U/µL RiboLock RNase inhibitor, and 40 µM [^{14}C Phe] in TAKM$_7$-Ac (pH 7.5). Control reactions used 37.5 or 20.2 µM total *E. coli* tRNA to achieve approximately 0.6 µM tRNA^{Phe} or tRNA^{Lys}. The amount of total *E. coli* tRNA required was calculated using an average tRNA extinction coefficient of ε_{260}=600 000 M^{-1} cm^{-1} and a contribution of 1.6% tRNA^{Phe} and 2.97% tRNA^{Lys} (Dong et al., 1996). To start the reaction, 5 µM of the corresponding synthetase was added and incubated at 37°C for 30 minutes. At 1, 5, 15, and 30 minutes, 10 µL were removed from the reaction and precipitated on 5% (w/v) trichloroacetic acid (TCA) presoaked Whatman™ papers. All filter papers were dried at 65°C, washed for 5 minutes with 5% (w/v) TCA thrice, washed once with absolute ethanol, and then dried at 65°C again. The amount of [^{14}C]Phe-tRNA^{Phe} was calculated based on the [^{14}C] activity retained on the filter, quantified using scintillation counting (PerkinElmer® Tri-Carb 4910TR 110 V Liquid Scintillation Counter). The fraction (%) of [^{14}C]aa-tRNA^{aa} formed was calculated relative to the total [^{14}C] activity in each reaction as measured by direct scintillation counting of the reaction mixtures. Total tRNA aminoacylation results were normalized to a maximum of 100% aminoacylation to correct for overestimation. The resulting aminoacylation time courses were plotted using GraphPad Prism 9 (n=2).

Nitrocellulose Filtration Assays.

Nitrocellulose filtration was carried out similarly to the protocol in Wright *et al.* (2011). TAKM$_7$-Ac buffer was used at all steps. First, tRNA was heated at 65°C for 5 minutes and allowed to fold for 10 minutes at room temperature. 50 µL reaction mixtures containing 200 µM nucleotide (ATP or ADP), 0.04 µM [^{3}H]-tRNA^{Phe}, and protein – *Ec*OLA1 (0, 0.5, 1, 2, 3, 5, 10, 15, 20, 35, 50, 65 µM), GST (0, 0.5, 1, 2, 3, 5, 10, 15, 20 µM), GST-hOLA1 (0, 0.5, 1, 2, 3, 5, 10, 15, 20 µM), 70S ribosomes (0, 0.2, 0.6, 1.0, 1.2 µM), EF-Ts (0, 0.5, 1, 2, 3, 5, 10, 15, 20, 30 µM), or tRNA-containing GST-hOLA1 (0, 0.04, 0.07, 0.15, 0.22, 0.37, 0.73, 1.10, 1.46, 2.19 µM) – were incubated for 10 minutes at 37°C. When monitoring the fraction of tRNA^{Phe} bound in the presence of the 70S ribosome and *Ec*OLA1, *Ec*OLA1 was added as the final component, allowing for a 10 minute pre-incubation of the 70S and tRNA. Following the incubation, the reactions were vacuum-filtered through buffer-

soaked cellulose nitrate membranes (Cytiva, Cat. No. 7182-002) and rapidly rinsed with 1 mL ice-cold buffer. The cellulose nitrate membranes were allowed to dissolve in 10 mL of EcoLite™ scintillation cocktail (MP Biomedical Cat. No. 882475) overnight. As a reference, 10 µL of tRNA premix was dissolved in 2 ml of scintillation cocktail to measure the total amount of [^{3}H]-tRNA^{Phe} in the respective reactions. The amount of tRNA bound by protein on each membrane was quantified by scintillation counting. All reactions were performed in triplicate. The data were fit with a hyperbolic equation 1 on GraphPad Prism 9:

$$Y = B_{max} \times [protein] / (K_D + [protein]) \quad (1)$$

Here, Y is the fraction bound, in other words, the percentage of tRNA retained by the protein on the membrane; B_{max} is the maximum specific binding in the same unit as Y; and K_D is the dissociation constant, reported in µM and corresponding to the protein concentration at which half-maximum binding is reached.

Microscale Thermophoresis Helicase Assays.

The secondary structures of the *E. coli* (PDB: 6BU8) rRNA sequences used as substrate in the helicase assays were predicted using RNAfold (figure 12A and sfigure 5) (Gruber et al., 2008). Chase DNA oligos were designed to complement the stem-structure-forming ribonucleotides of the RNA and synthesized with a 3' fluorescein label. RNA oligos were purchased from IDT (Coralville, IA, USA) and DNA oligos from AlphaDNA (Montreal, QC, Ca). The sequences for the *E. coli* SRL, ASF, and "RNA duplex" (RD) oligos are listed in table 2.

Table 2. SRL, ASF, and RD RNA and complementary DNA oligos

	Sequence (5' to 3')	**Notes**
SRL	GrGrCrUrGrCrUrCrCrUrArGrUrArCrGrArGrArGrGrArCrCrGrGrArGrUrGrGrArCr	RNA
	GTCCACTCCGGTCCTCTC	DNA, 3' fluorescein
ASF	ArGrGrArUrGrUrUrGrGrCrUrUrArGrArArGrCrArGrCrCrArUrCrArUrUrUrArArAr	RNA
	TAAATGATGGCTGCTTC	DNA, 3' fluorescein
RD	ArUrGrUrGrGrArArArArUrCrUrCrUrArGrCrArGrUr	RNA
	ACUGCUAGAGAUUUUCCACAU	DNA, 3' fluorescein

Helicase assays were performed similarly to Nelson et al. (2020). Reaction mixtures of 1 μM RNA, 0.06 μM complementary fluorescent DNA oligo, 1 μM protein, and 200 μM ATP/ADP or without nucleotide were incubated in TAKM$_7$-Ac buffer for 10 minutes at 37°C. To reduce background fluorescence interference, the fluorescent DNA oligo concentration was limiting and kept constant across all assays. The RNA unwinding activity of *Ec*OLA1 (the unknown), StpA (a known chaperone), and BSA (a protein with no known unwinding activity) was determined. Two reaction conditions (*e.g.,* +/- ATP) were compared per measurement. All reactions were performed fourfold. Monolith® NT.115 capillaries were loaded through capillary action. Measurements were taken in a NanoTemper Technologies Monolith® NT.115 MicroScale Thermophoresis with a temperature of 37°C.

Raw data was analyzed through NanoTemper MO. Affinity Analysis (x86 software). For each capillary, the initial fluorescence before turning on the IR laser is normalized to 1 (relative fluorescence). Here, the final fluorescence is the average fluorescence between 4-5 seconds after the IR laser has been turned on. F_{norm} is calculated by dividing the final fluorescence by the initial fluorescence and is represented in per mille (‰). Statistical significance between the F_{norm} for different conditions was calculated using unpaired t-tests as implemented in GraphPad Prism 9 ((0.1234 (ns), 0.0322 (*), 0.0021 (**), 0.0002 (***), 0.0001 (****)).

An additional parameter calculated by the NanoTemper MO. Affinity Analysis (x86 software) is the signal-to-noise ratio. Defined as the response amplitude divided by the standard deviation of the replicates, the signal-to-noise ratio indicates the quality of the assay. A signal-to-noise ratio above 5 is desirable, and above 12 suggests an exceptional assay.

Microscale Thermophoresis RNA and Protein Affinity Check.

The affinity between the DNA and proteins were determined using MST to address the significant change in fluorescence observed upon the addition of StpA, *Ec*OLA1, and BSA to the ASF DNA oligo. Proteins were serially diluted, with the highest concentrations being 20 μM for StpA and BSA, and 33 μM for *Ec*OLA1. To match MST conditions mentioned above, ASF DNA oligo and ADP were added to final concentrations of 0.06 μM and 200 μM, respectively. SRL DNA oligo,

ADP, and *Ec*OLA1 were combined as a negative control. All reactions were completed in triplicate. Reactions were incubated for 10 minutes at 37°C before being loaded into the Monolith® NT.115 capillaries and subsequently into the MST. Thermophoresis was measured at 37°C and performed using 20 or 60% excitation power and medium MST IR-laser power. F_{norm} from -1 to 0 and 4 to 5 seconds was plotted against the protein concentration. Using GraphPad Prism 9, these binding curves were fit with hyperbolic equation 1 (*vide supra*). In this case, Y is the change in normalized fluorescence upon addition of the protein; B_{max} is the maximum specific fluorescence change; and K_D is reported in µM, corresponding to the protein concentration at which half the maximum change in fluorescence is reached.

For affinity check experiments, the NanoTemper MO. Affinity Analysis (x86 software) calculates the signal-to-noise ratio (S/N) using the following equation (2):

$$\text{S/N} = \text{Response Amplitude} / \sqrt{\frac{\sum_i (r_i - \bar{r})^2}{n-1}} \quad (2)$$

Where r_i is the residual of the fit at a given data point, $\bar{r}$ is the average of all the residuals, and n is the number of data points.

CHAPTER 3: RESULTS

3.1 Objective 1: tRNA Binding

Aminoacylation of tRNA.

In vitro transcribed (IVT) $tRNA^{Lys}$ and $tRNA^{Phe}$ were purified as described in the methods (chapter 2). Despite both being 76 nt, the $tRNA^{Lys}$ *in vitro* transcription product migrates further than the respective $tRNA^{Phe}$ during electrophoresis, suggesting a difference in length (figure 8A). The ability of tRNA synthetases to aminoacylate their corresponding tRNA can be used to assess tRNA quality. To this end, the ability of the purified IVT $tRNA^{Phe}$ and $tRNA^{Lys}$ to be aminoacylated was quantified. Each of the purified aaRS used was active, as evidenced by their ability to aminoacylate the respective tRNA from *E. coli* total tRNA. The IVT $tRNA^{Phe}$ could be aminoacylated by PheRS up to 100%, but $tRNA^{Lys}$ aminoacylation by LysRS remained below 25% (Figure 8B-C). Thus, only $tRNA^{Phe}$ was used moving forward.

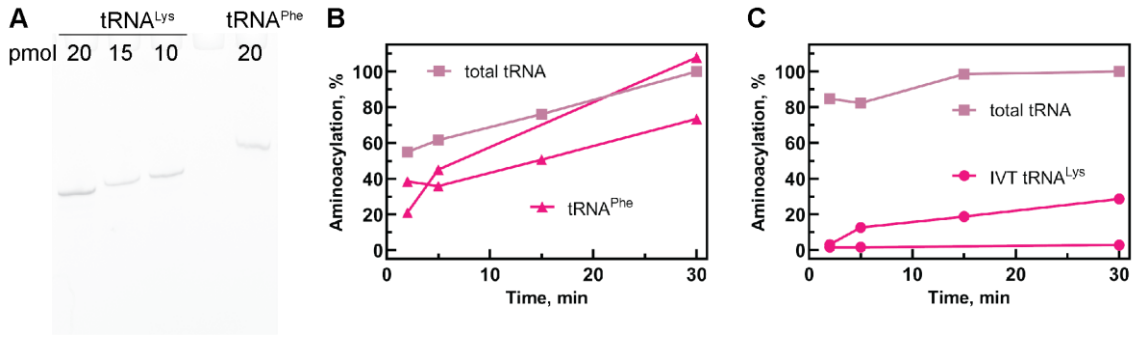

Figure 8. Aminoacylation of tRNA indicates correct folding of $tRNA^{Phe}$. (**A**) Purified IVT $tRNA^{Lys}$ and $tRNA^{Phe}$ were resolved on a 15% urea-PAGE and then checked for correct folding using aminoacylation time courses. (**B**) $tRNA^{Phe}$ aminoacylation is comparable to the native $tRNA^{Phe}$ control from *E. coli* total tRNA (n=1). (**C**) $tRNA^{Lys}$ aminoacylation is much less efficient than the $tRNA^{Lys}$ control from *E. coli* total tRNA (n=1).

Deacylated tRNA Forms a Complex with OLA1

The ability of GST-hOLA1 and *Ec*OLA1 to bind deacylated-tRNA was investigated using EMSAs. In such an assay, reaction components are equilibrated and resolved on a nondenaturing gel. A shift of either component when incubated together compared to that component alone is

representative of an interaction occurring. Because OLA1 is a nucleotide hydrolase whose functional cycle likely depends on the specific nucleotide bound, the experiments were conducted in the presence of saturating concentrations of ATP ($K_{D, ATP} \approx 1$ µM) (Becker *et al.*, 2012; Koller-Eichhorn *et al.*, 2007; Rosler *et al.*, 2015). To validate the experimental condition used in the EMSAs, I determined the ability of a known tRNA interaction partner, TruB (D48N), to shift the mobility of the IVT $tRNA^{Phe}$ used in my experiments.

Figure 9 clearly shows a shift of the tRNA band in the presence of TruB (D48N) (indicated by *), demonstrating the formation of a TruB•tRNA complex. The approximate K_D of 2 µM derived from the concentration dependence (measured using ImageJ) is close to the published value (Wright *et al.*, 2011). A similar shift is seen in the presence of GST-hOLA1•*Ec*tRNA in figure 9A (indicated by ¶), with an estimated K_D of ~1 µM (figure 9C), demonstrating the formation of a GST-hOLA1•$tRNA^{Phe}$ complex despite the presence of endogenous *E. coli* tRNA. However, no such shift in mobility can be observed in the presence of *Ec*OLA1 (figure 9B) independent of the presence of ATP (sfigure 3).

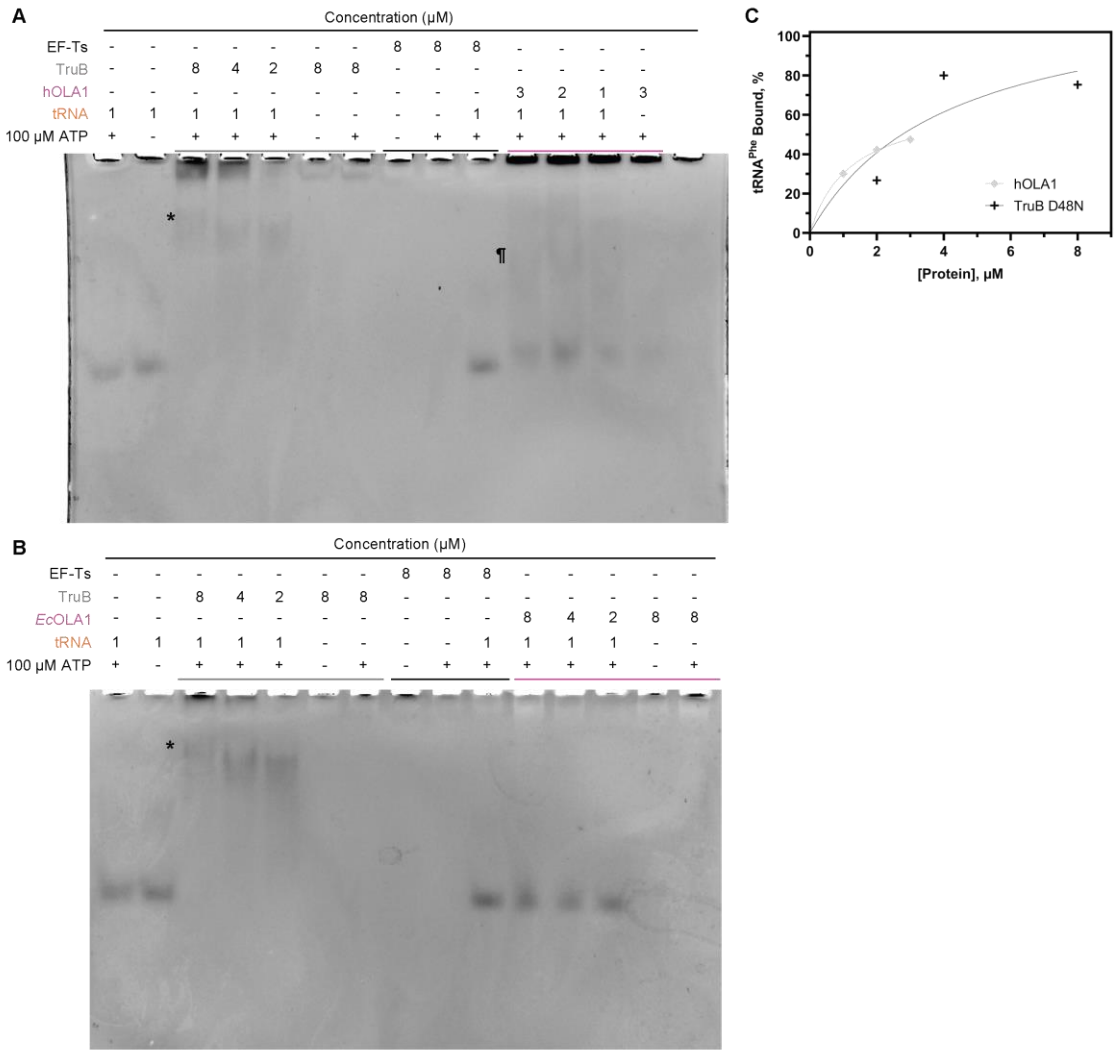

Figure 9. Comparison of tRNA^{Phe} binding to TruB, EF-Ts, and GST-hOLA1•*Ec*tRNA or *Ec*OLA1. Both EtBr-stained, 8% native acrylamide gels contain reactions of tRNA^{Phe} with EF-Ts as a negative control, TruB (D48N) as a positive control, and either (**A**) GST-hOLA1•*Ec*OLA1 or (**B**) *Ec*OLA1 equilibrated for 10 minutes at 37°C. The change in tRNA^{Phe} migration due to binding of TruB (D48N) is marked with an asterisk (*) in both assays. Complex formation between tRNA and GST-hOLA1 occurs (¶) despite the presence of hOLA1-bound endogenous *E. coli* tRNA. In contrast, tRNA^{Phe} migration does not change in the presence of EF-Ts or *Ec*OLA1. (**C**) The approximate protein-dependent fraction of tRNA^{Phe} bound in EMSA A is shown, facilitating K_D estimations of ~2 μM for TruB D48N (+) and ~1 μM for hOLA1 (◆).

To further assess the ability of *Ec*OLA1 and its human homolog GST-hOLA1 to bind deacylated tRNA, their affinity to $tRNA^{Phe}$ was determined using nitrocellulose filtration. A tritium-labelled *in vitro* transcribed $tRNA^{Phe}$ (*vide infra*) was incubated with varying concentrations of the respective protein and saturating concentrations of ADP or ATP. The catalytically inactive variant of TruB was again used as a tRNA-binding positive control. Here, TruB (D48N) bound $[^3H]$-$tRNA^{Phe}$ with a K_D of 0.52 ± 0.09 µM at 37°C (figure 10A), consistent with the previously reported values of 1.4 ± 0.3 µM (Wright *et al.*, 2011) and 0.10 ± 0.02 µM (Keffer-Wilkes *et al.*, 2016). The concentration dependence of GST-hOLA1 and *Ec*OLA1 towards binding $tRNA^{Phe}$ shown in figure 10B-C reveals K_D's in the range of 1-3 µM for GST-hOLA1 and 10-22 µM for *Ec*OLA1 (summarized in table 3). Interestingly, only a small fraction (below 15%) of $tRNA^{Phe}$ is bound by *Ec*OLA1•ATP/ADP. Although endogenous *E. coli* tRNA was present after affinity chromatography purification, GST-hOLA1•ATP(•*Ec*tRNA) did bind a small fraction of $[^3H]$-$tRNA^{Phe}$ but did not bind $[^3H]$-$tRNA^{Phe}$ in the presence of ADP (figure 10D). The nitrocellulose filter binding was performed with GST as a negative control to confirm that the interaction between GST-hOLA1 and tRNA is not due to the presence of the GST tag (figure 10B). The nucleotide release factor for EF-Tu, EF-Ts, was also used as a negative control because it is not capable of binding to tRNA (figure 10C). Neither GST nor EF-Ts exhibited tRNA binding activity, supporting that binding occurs between both OLA1 homologs and tRNA.

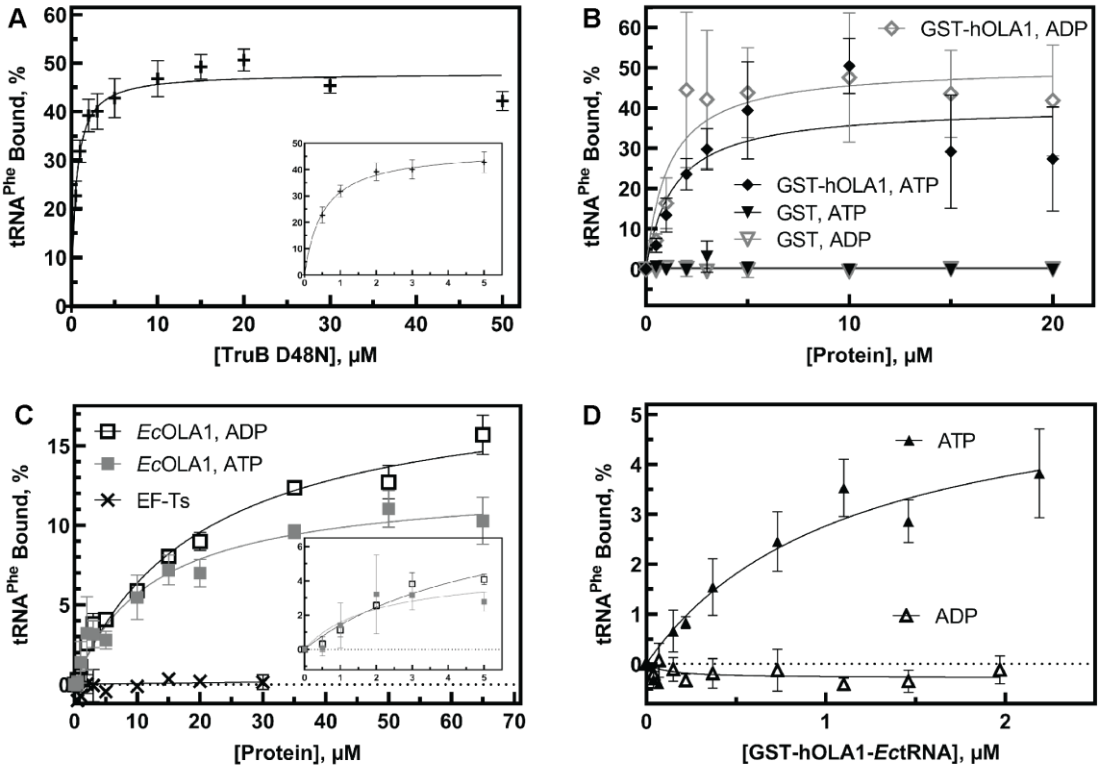

Figure 10. Concentration dependence of tRNA^{Phe} binding. Each line represents the hyperbolic fit for one site, specific binding kinetics used to obtain an equilibrium dissociation constant (K_D). For each reaction, 0.04 µM tRNA and 200 µM of each nucleotide were present. (**A**) TruB D48N (**+**), (**B**) GST-hOLA1 with ADP (◇)/ ATP (◆), GST with ATP (▼)/ ADP (▽), (**C**) EF-Ts (**x**), *Ec*OLA1 with ADP(□)/ ATP (■), and (**D**) GST-hOLA1-*Ec*tRNA with ATP (▲)/ ADP (Δ). "*Ec*tRNA" is used to denote the presence of endogenous *E. coli* tRNA bound to hOLA1.

Table 3. Dissociation constants (K_D's) of TruB (D48N), EF-Ts, *Ec*OLA1, GST-hOLA1, GST, and *E. coli* 70S ribosomes for tRNA^{Phe}.

Protein	Nucleotide	K_D (µM)	B_{Max} (%)	Purification Tag
TruB (D48N)	None	0.52 ± 0.09	47.9 ± 1.2	6xHis
EF-Ts		None	0	6xHis
*Ec*OLA1	ATP	12.3 ± 2.6	12.7 ± 0.9	6xHis
hOLA1		1.4 ± 0.6	40.4 ± 4.1	GST
GST		None	0	-
70S		0.28 ± 0.21	6.6 ± 1.4	-
*Ec*OLA1	ADP	20.0 ± 3.4	19.1 ± 1.3	6xHis
hOLA1		1.1 ± 0.4	50.5 ± 4.7	GST
GST		None	0	-

*Ec*OLA1 Does Not Increase the Fraction of Deacylated tRNA on Vacant Ribosomes.

Previous work has shown that OLA1 associates with ribosomes during polysome profiling (Chen et al., 2015; Gradia et al., 2009; Verstraeten et al., 2011) and co-elutes with translational RNA components like rRNA and tRNA (sfigure 1) (Cheung *et al.*, 2010), consistent with the *P. falciparum* OLA1•tRNA complex on the ribosome (A. Amunts, unpublished). To address the order of binding, nitrocellulose filtration was performed using *E. coli* 70S ribosomes and [^{3}H]-tRNA^{Phe} in the presence and the absence of *Ec*OLA1•ATP. The ability of vacant *E. coli* 70S ribosomes to bind tRNA^{Phe} is shown by retention of [^{3}H]-tRNA^{Phe} on the nitrocellulose membrane with a K_D of 0.28 ± 0.21 µM (figure 11A). From this data, a concentration of 1 µM 70S was chosen for testing the ability of *Ec*OLA1 to increase the fraction of tRNA^{Phe} retained by the ribosome. In theory, if OLA1 facilitates binding of tRNA to the A-site, the amount of tRNA bound should increase with increasing OLA1 concentrations. The tRNA^{Phe} retained in the presence of *Ec*OLA1 (figure 11B) is near the 6.6 ± 1.4% maximum observed for 1 µM of mRNA-free 70S without *Ec*OLA1 (figure 11A). When the percent values for tRNA bound by the 70S ribosome are subtracted from total tRNA binding in the presence of *Ec*OLA1, the percent tRNA returns to 0, indicating that *Ec*OLA1 does not stabilize tRNA on the ribosome as determined by nitrocellulose filtration.

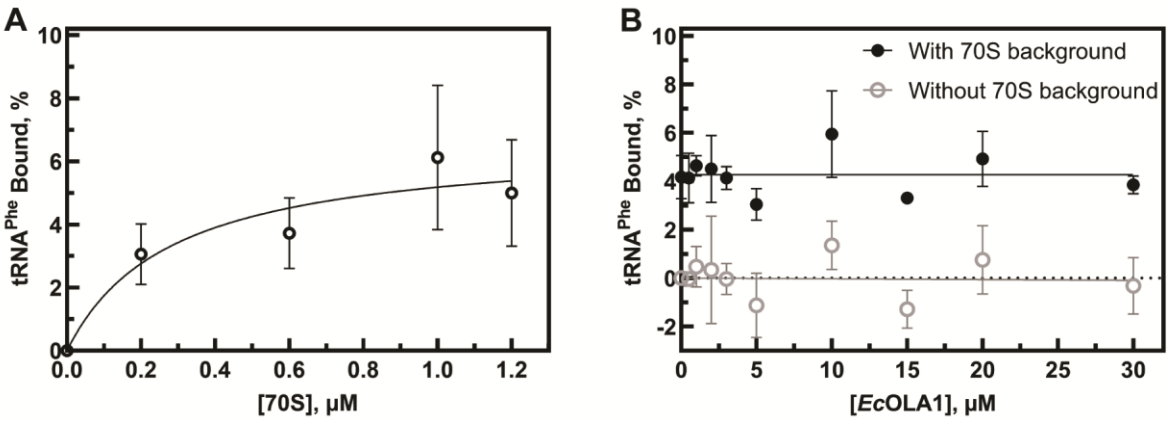

Figure 11. *Ec*OLA1 does not increase the fraction of tRNA^{Phe} retained by 70S ribosomes. The percentage of tRNA^{Phe} bound is shown in relation to the concentration of (**A**) 70S ribosomes (○) or (**B**) *Ec*OLA1 with the 70S background shown (•) and with the fraction bound by the 70S

ribosomes subtracted (○). Each reaction was performed with 0.04 µM tRNA, and 1 µM 70S ribosome was present in B.

3.2 Objective 2: RNA Remodeling

RNA Remodeling Activity on the *E. coli* Sarcin-Ricin Loop.

Preliminary results suggest that *Ec*OLA1 exhibits helicase activity (Brandon, 2021). To determine if RNA remodeling is part of *Ec*OLA1's role on the ribosome, ribosome-specific RNAs were selected as helicase assay substrates by identifying rRNA sequences that are within 4.2 Å of OLA1 in the *P. falciparum* ribosome cryo-EM structure (unpublished). The sarcin-ricin loop (SRL) and A-site finger (ASF) of the large ribosomal subunit and an interhelical sequence in the small subunit were identified as potential OLA1 interaction partners. Structure comparison of the *P. falciparum* 80S ribosome to the *E. coli* 70S ribosome (PDB 6BU8) was used to identify the corresponding *E. coli* SRL and ASF sequences, both of which maintain considerable structural conservation in their native conformations (RMSD of 1.14 Å for the SRL and 2.99 Å for the ASF; sfigure 4). The SRL 3D and 2D RNA structures are shown in figure 12A. An additional RNA construct consisting of two complementary RNA oligos (herein called RD) identical to the helicase assay substrate in Brandon (2021) was also used. The ASF and RD structures are shown in supplemental figure 5.

Helicase assays were carried out as described in the methods (chapter 2) and as illustrated in figure 12B. Following the experimental outline from Nelson *et al*., (2021), the fluorescent DNA oligo was kept at a limiting concentration, allowing binding events to produce signal changes over the background fluorescence. The RNA remodelling activity of *Ec*OLA1 was compared against a protein known not to affect RNA folding, BSA (Nelson et al., 2021), and a known RNA chaperone, StpA (Doetsch et al., 2010). RNA unfolding is required for the complementary DNA oligo to bind. Larger complexes containing the fluorescently labelled DNA oligos then move slower along the temperature gradient, theoretically leading to an increase in fluorescence in comparison to free DNA oligos. Therefore, protein binding to RNA without enabling the DNA oligo to anneal does not produce a measurable result. Although, changes in fluorescence can result from direct binding

between the protein and DNA or binding of all reaction components simultaneously. Controls for such scenarios were implemented.

Surprisingly, the DNA complementary to the ASF RNA bound directly to the proteins (sfigures 6A and 7). Additionally, there was no significant change in the normalized fluorescence for the positive controls when using the RD RNA (sfigure 6B). Therefore, only the SRL RNA was used moving forward. The ASF and RD results can be found in appendix I.

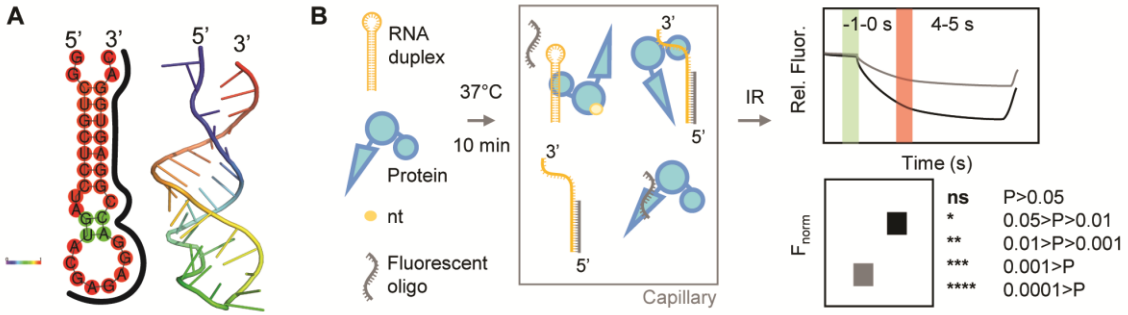

Figure 12. Helicase assay substrate and workflow. (**A**) A side-by-side comparison between the predicted 2D (left) and 3D (right) structures of the SRL rRNA shows potential nucleotide interactions within the stem. The SRL RNA secondary structure predicted by RNAfold has rainbow colour-coding denoting the base-pair probabilities, with red being most likely and blue being least likely. The black line marks the portion of RNA complementary to the fluorescent DNA-oligo. The tertiary structure present on the *E. coli* 70S ribosome (PDB: 6BU8) shown in cartoon form is rainbow coloured from the 3' to 5' ends. (**B**) A schematic overview of the MST helicase assay workflow (Nelson *et al.,* 2021). The fluorescently labelled DNA oligo must always be present, but the other components can be varied. A few different interactions are possible, including binding of the protein to RNA but not DNA; binding of the protein, DNA, and RNA; binding of the RNA and DNA; and binding of the protein to the DNA but not RNA. The relative fluorescence is measured both before and while the infrared (IR) laser is on, leading to a trace showing thermophoresis of the fluorophore. The change in fluorescence from the average at -1 to 0 seconds and the average at 4 to 5 seconds is calculated and plotted for each condition tested. Unpaired t-tests and signal-to-noise ratios are used to discern which conditions cause significant F_{norm} differences.

As a positive control for RNA remodelling activity, the RNA was allowed to refold in the presence of the complementary DNA oligo, thus replicating the effect of RNA unwinding in a protein-free way. As indicated in figure 13, the resulting change in normalized fluorescence was significant (P = 0.0006) with a signal-to-noise ratio of 5.3 (condition 0). According to the NanoTemper Technologies Dianthus NanoPedia, a signal-to-noise ratio above 5 is desirable and above 12 is exceptional. Notably, when comparing ATP or ADP in the absence of protein, there is no significant difference (P = 0.3489), and the signal-to-noise remains below 5 (condition 1). Interestingly, the addition of StpA, *Ec*OLA1, and BSA each resulted in significant F_{norm} changes ($P_{StpA/EcOLA1} < 0.0001$, $P_{BSA} = 0.0001$) and signal-to-noise ratios above 12 for StpA and *Ec*OLA1 (condition 2), although the directionality of the fluorescence change is reversed in comparison to the results under condition 0. The observed changes are not due to direct interactions with DNA ($P_{StpA} = 0.0703$, $P_{BSA} = 0.1938$, $P_{EcOLA1} = 0.1801$, condition 3). The absence of DNA binding is supported by MST binding affinity experiments (sfigure 7) and by comparing RNA presence and absence ($P = \leq 0.0001$ for all proteins, condition 4). In condition 4, the F_{norm} trend reflects the results under condition 2. It is conceivable that the protein remains bound to the RNA•DNA complex, reducing thermophoresis and increasing F_{norm}.

To differentiate between potential chaperone and helicase activity, the importance of ATP was addressed in two ways. First, the presence of ATP versus ADP was compared for all proteins. Figure 13 (condition 1) shows that there is a significant difference in the F_{norm} for StpA (P = 0.0014) supported by the signal-to-noise ratio (S/N = 5.8), but less so for *Ec*OLA1 (P = 0.0119, S/N = 3.2) and not at all for BSA (P = 0.1914, S/N = 1.3). Second, the presence and absence of either ATP or ADP were tested for StpA and *Ec*OLA1. The changes in fluorescent oligo migration in the presence of ATP for both proteins were statistically significant ($P_{StpA} = 0.0387$, $P_{EcOLA1} = 0.0071$), but the signal-to-noise ratios are below the threshold of 5 (condition 5). In contrast, there was no difference with or without ADP ($P_{StpA} = 0.2394$, $P_{EcOLA1} = 0.4788$, condition 6).

Altogether, the SRL RNA appears to be remodelled in the presence of *Ec*OLA1, StpA, and BSA. Furthermore, ATP provides a modest benefit to the RNA remodelling activity in the presence of StpA and *Ec*OLA1.

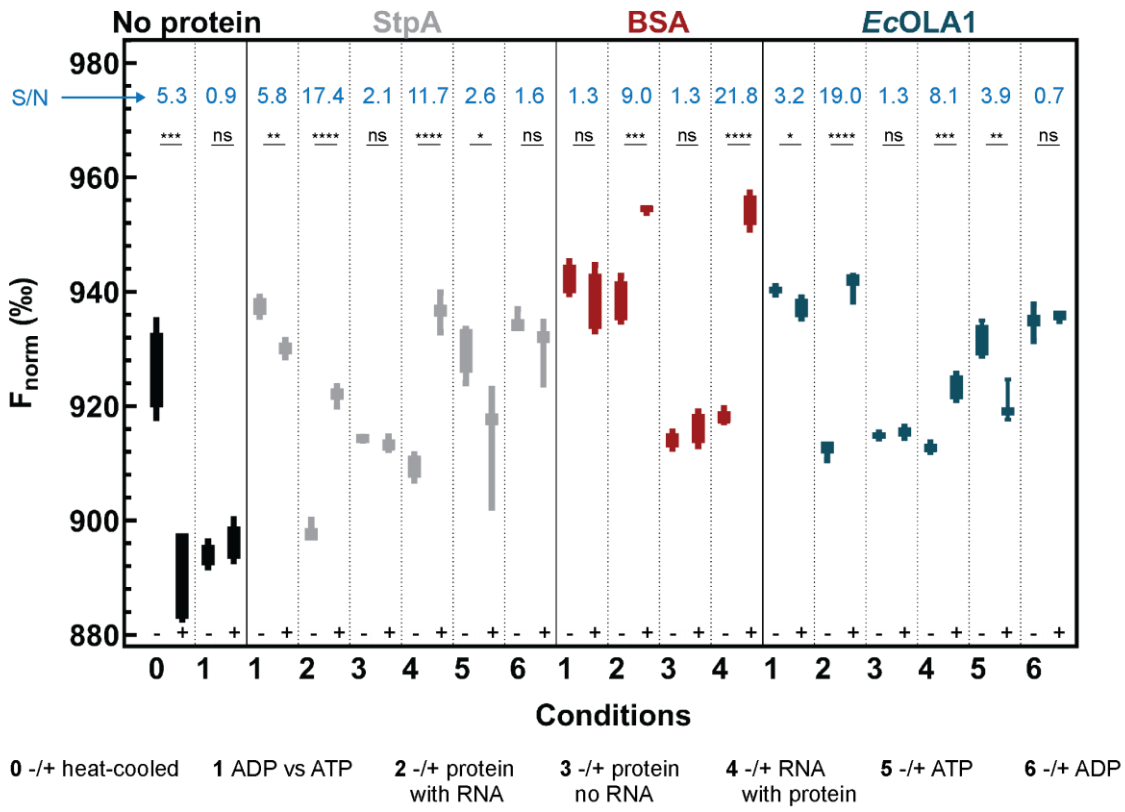

Figure 13. Changes in normalized fluorescence for different helicase assays with SRL RNA as substrate (n=4). The left box for each column represents the result for the absence of the variable component (-), and the right is the presence of the variable component (+) — dashed lines separate conditions. Results for the absence of protein (black), for StpA (gray), for BSA (red), and for *Ec*OLA1 (blue) are separated by solid lines. The significance between F_{norm} (per mille) for each condition comparison is indicated, as measured by unpaired t-tests on GraphPad Prism 9 ((0.1234 (ns), 0.0322 (*), 0.0021 (**), 0.0002 (***), 0.0001 (****)). The signal-to-noise ratio (S/N) is shown in blue text at the top of each data set.

CHAPTER 4: DISCUSSION

OLA1 is present in all domains of life (Caldon & March, 2003; Verstraeten *et al.*, 2011), but its cellular role has yet to be fully understood. OLA1 homologs are well conserved, suggesting that elucidating the molecular mechanisms of action in one homolog can reveal the cellular role across the domains of life. For example, the human and *E. coli* OLA1 share 47% sequence identity and 62% sequence similarity and are both preferentially ATPases (Becker *et al.*, 2012; Landwehr *et al.*, 2021; Sidlowski *et al.*, 2023). Perhaps the 38% difference in the amino acids sequence between OLA1 in pathogens versus humans could be exploited as antimicrobial targets, similar to how the tetrapeptide GE81112 inhibits the formation of the 30S initiation complex but not the 40S initiation complex (Brandi *et al.*, 2006).

OLA1 has been reported to interact with ribosomes in a variety of organisms, including humans, plants, *Trypanosoma*, yeast, and *E. coli* (Chen et al., 2015; Cheung et al., 2022; Dannenmaier et al., 2021; Gradia et al., 2009; Landwehr et al., 2021). More specifically, OLA1 homologs co-elute with rRNA (Cheung *et al.*, 2022; Cheung *et al.*, 2010), r-proteins (Gradia *et al.*, 2009; Landwehr *et al.*, 2021), and tRNA from *E. coli* during affinity chromatography purification (Brandon, 2021). Yet, the exact purpose and mechanistic details of OLA1's role in translation remain unknown. Therefore, I sought to reveal details on the intersection of the ribosomal and *Ec*OLA1 functional cycles, specifically looking at the interaction of *Ec*OLA1 and GST-hOLA1 with tRNA and rRNA.

This chapter is intended to comprehensively integrate my research findings into what has thus far been reported by others regarding the cellular and molecular mechanisms of OLA1.

4.1 Objective 1: tRNA Binding

It is not known if OLA1 binding to tRNA is facilitated by the ribosome or occurs prior to ribosome binding. Thus, binding of human and *E. coli* OLA1 to tRNA was investigated using EMSAs and nitrocellulose filtration assays in the absence of the ribosome. Both homologs are known to preferentially bind ATP, so experiments were carried out in the presence of ADP and ATP (Becker *et al.*, 2012; Koller-Eichhorn *et al.*, 2007; Sidlowski *et al.*, 2023).

Correlation Between tRNA Structure and Function

The dissociation constants reported here are for unmodified *in vitro* transcribed tRNA that have the propensity to fold differently than native, fully modified tRNA (for review, see Zavialov *et al.* (2001)). For example, using structural probing Helm *et al*. (1999) demonstrated that transcribed human $tRNA^{Lys}$ requires the modification m^1A9 to adopt a cloverleaf secondary structure. Posttranscriptional modifications of $tRNA^{Lys}$ are also essential for recognition by *E. coli* LysRS (Tamura et al., 1992). Of note, aminoacylation of unmodified tRNA can be slower without changing the ratio of properly versus misfolded populations (Bhaskaran *et al.*, 2012). However, much lower levels (~20%) of aminoacylation are reached when the tRNA is trapped in an unfavourable conformation. In line with this, the IVT $tRNA^{Lys}$ product barely reaches 20% aminoacylation (figure 8C) and appears smaller than IVT $tRNA^{Phe}$ when separated on a urea-page (figure 8A). Therefore, the unmodified IVT *E. coli* $tRNA^{Lys}$ is not a suitable aaRS substrate, possibly due to a combination of misfolding, or even truncation.

Modifications are not required for proper folding of all tRNA. Sampson and Uhlenbeck (1988) reported $tRNA^{Phe}$ aminoacylation of up to 90% both with and without modifications present. Additionally, Bhaskaran *et al.* (2012) revealed both native *E. coli* $tRNA_1^{Gln}$ (UUG) and unmodified IVT $tRNA_1^{Gln}$ to reach ~70% aminoacylation in under 5 min. When properly folded, a burst of aa-tRNA formation occurs within 1 minute, followed by slower accumulation (Bhaskaran *et al.*, 2012), as demonstrated in figure 8B. By these standards, the $tRNA^{Phe}$ used in the experiments herein was folded sufficiently, as its aminoacylation reached 100% (figure 8B).

Differences in tRNA Binding Between hOLA1 and *Ec*OLA1

EMSAs are used to visualize complex formation between proteins and RNA with low dissociation constants (K_D < 2 µM) and low dissociation rates relative to association rates ($\frac{k_a}{k_d} < 10^{10}\ M^{-1}$) (Cann, 1989; Ryder et al., 2008). Interestingly, tRNA binding to TruB (D48N) can be shown using an EMSA (figure 9) but binding to RelA cannot (Kudrin *et al.*, 2018; Kushwaha *et al.*, 2019), despite both proteins being known tRNA-interaction partners. TruB (D48N) has a K_D in the 0.1 µM range for tRNA, and wt TruB has a $k_{release}$ of 10.6 ± 0.3 s^{-1} for tRNA (k_a not determined), independent of other

binding partners (Keffer-Wilkes *et al.*, 2016). RelA has K_D in the 0.01 µM range, a "slow" dissociation rate (Kushwaha *et al.*, 2019), and recognizes tRNA both on and off the A-site (Arenz *et al.*, 2016). Similar to OLA1, whether RelA binds tRNA independently of the ribosome *in vivo* is a point of ongoing discussion.

Here, EMSAs show the formation of a GST-hOLA1•$tRNA^{Phe}$ complex, even in the presence of endogenous *E. coli* tRNA (figure 9A). Despite high sequence and structure conservation between OLA1 homologs, a complex between *Ec*OLA1 and *E. coli* IVT $tRNA^{Phe}$ was not visible using an EMSA (figure 9B) regardless of the nucleotide present (sfigure 3). Either the formation of an *Ec*OLA1•nt•tRNA complex is not possible under the conditions used, or the fraction bound is too low for detection. This is the first evidence suggesting a difference in the behaviour between human and *E. coli* OLA1.

Compared to EMSAs, nitrocellulose filtration is more sensitive for analyzing the binding between a radio-labelled ligand and protein. Based on my nitrocellulose filtration results, *Ec*OLA1 and GST-hOLA1 both bind tRNA *in vitro*, though with different affinity. GST-hOLA1•ATP/ADP binds $tRNA^{Phe}$ with a K_D < 2 µM, comparable to known tRNA binding proteins TruB (~0.5 µM) and EF-Tu (~0.9 µM) and 10x weaker than RelA (10^{-2} µM) (Kushwaha et al., 2019; Vorstenbosch et al., 2000; Winther et al., 2018). Additionally, this is comparable to HisRS, which binds its cognate tRNA with a K_D of ~4 µM, and IF2, which binds initiator tRNA with a K_D of ~1 µM (Bovee et al., 1999; Guenneugues et al., 2000). On the other hand, *Ec*OLA1 exhibits weak $tRNA^{Phe}$ binding, more comparable to HisRS binding to $tRNA^{Phe}$ (K_D ≈ 7 µM) (Bovee *et al.*, 1999). *Ec*OLA1 has approximately half the dissociation constant for tRNA in the presence of ATP (K_D ≈10 µM) than in the presence of ADP (K_D ≈20 µM), suggesting ATP-bound *Ec*OLA1 has a higher affinity for tRNA.

Adding to the results showing differences between GST-hOLA1 and *Ec*OLA1 tRNA-binding behaviours is the observation that GST-hOLA1 retains a higher percent of tRNA on the nitrocellulose membrane (~40%) than *Ec*OLA1 does (1-15%) as seen in figure 10. The small fraction of $tRNA^{Phe}$ bound by *Ec*OLA1•ATP/ADP is comparable to GST-hOLA1•ATP•*Ec*tRNA (figure 10D), even though *Ec*OLA1 is free of endogenous tRNA. Fast tRNA dissociation could

explain the low fraction bound. With nitrocellulose filtration being a non-equilibrium experiment, the tRNA can dissociate after filtration and be removed in the washing step, leading to a lower fraction bound on the filter.

Altogether, it is clear that hOLA1 and *Ec*OLA1 can bind to tRNA in the absence of the ribosome. This binding likely occurs *in vivo*. The abundance of *Ec*OLA1 in the cell is approximately 4 µM. The cellular concentration of different tRNAs range from 1 to 30 µM in *E. coli* cells depending on their growth phase (Dong et al., 1996); for example, $tRNA^{Phe}$ is present at ~3 µM at slow growth (0.4 doublings/hr) and ~5 µM at fast growth (2.5 doublings/hr). Considering these concentrations and the tRNA binding by *Ec*OLA1 (10-20 µM), *Ec*OLA1•ATP may bind a small fraction (~20%) of cellular tRNA. It is likely that *Ec*OLA1•ATP•tRNA forms *in vivo* in a way that is coupled to the growth phase of the cell. In contrast, tRNA concentrations in humans can range up to 100 µM depending on the specific tissue (Pan, 2018) and hOLA1 concentrations are around 0.2 µM (calculated from Beck *et al*., (2011)). The binding of hOLA1 to tRNA occurs with a higher affinity in comparison to *Ec*OLA1 (1 vs ~15 µM), suggesting a difference in OLA1's cellular function in the two organisms.

Ribosome-Aided Stabilization of OLA1-tRNA Complexes

OLA1 binds to tRNA at the A-site but it is unknown if the ribosome facilitates the interaction between *Ec*OLA1 and tRNA, or if a OLA1•ATP•tRNA complex forms before binding to the ribosome. Due to the addition of rRNA and r-protein contacts, *Ec*OLA1 may bind to tRNA on the ribosome with a higher affinity than to free tRNA. The rate of deacylated tRNA dissociation from the ribosomal A-site is higher than from the P-site, suggesting preferential binding of tRNA to the P-site of inactive ribosomes (Fahlman et al., 2004). Towards answering whether *Ec*OLA1 can increase and stabilize the binding of tRNA to the ribosomal A-site, nitrocellulose filtration experiments were performed with 1 µM 70S ribosomes, sub-stoichiometric [^{3}H]-$tRNA^{Phe}$ (0.04 µM) and increasing *Ec*OLA1 (0-30 µM). Interestingly, my filter binding results indicate that *Ec*OLA1 does not increase the fraction of tRNA retained during filtration. The results could be explained by excess *Ec*OLA1 binding to the empty ribosomal A-site and preventing rather than enhancing tRNA binding. If this experiment were to be redone, a higher concentration of tRNA should be used to prevent competitive binding inhibition.

Experimental Limitations

The role of nucleotide binding in the OLA1•tRNA interaction is not yet understood. For hOLA1, the K_D's describing the interaction towards tRNA in the presence of tri- or dinucleotide are nearly identical, but *Ec*OLA1 clearly has a higher affinity for tRNA in the presence of ATP. In the case of *Ec*OLA1, it is likely that the "on" conformation in the presence of ATP (not ADP•P_i) forms favourable contacts with tRNA. It is unknown if eukaryotic OLA1 hydrolyzes available ATP before binding to tRNA – hence favouring a diphosphate-bound ternary complex –, or if an ATP-bound complex forms equally well. The use of a nonhydrolyzable ATP analog could clarify between these possibilities. If the K_D is higher in the presence of ADPNP, then an "off" OLA1 conformation favours tRNA.

There is competition between endogenous tRNA and $tRNA^{Phe}$ to bind hOLA1, as the fraction of tRNA bound increased after purifying away endogenous tRNA (figure 10 B vs D). The observation that endogenous *E. coli* tRNA co-purifies with GST-hOLA1 led to another interesting conclusion: preliminary results suggest that GST-hOLA1•*Ec*tRNA binds radiolabelled $tRNA^{Phe}$ in the presence of ATP but not ADP (figure 10D). The low (4%) tRNA binding during nitrocellulose filtration in the presence of ATP (figure 10D) could be attributed to the low amount of GST-OLA1 used and the even lower amount not already bound to endogenous *E. coli* tRNA. hOLA1 likely has a higher affinity for native, modified tRNA than *in vitro* transcribed, unmodified tRNA. It is estimated that approximately 100% of GST-hOLA1 binds endogenous tRNA when isolated from the cell (sfigure 1). The absence of tRNA binding in the presence of ADP suggests that ATP hydrolysis facilitates the release of tRNA by hOLA1. However, a requirement for ATP hydrolysis to exchange tRNA is not in line with hOLA1 binding tRNA with similar K_D's in the presence of ADP and ATP. Ultimately, the experiment should be repeated with higher protein concentrations. A chase experiment between radio-labelled and non-labelled tRNA with OLA1 in the presence of ATP, ADPNP, and ADP would also provide a definitive answer. If nucleotide hydrolysis gates tRNA release, then a chase experiment would reveal tRNA exchange only in the presence of ATP.

4.2 Objective 2: RNA Remodeling

OLA1 has been shown to bind rRNA along with tRNA, specifically at the A-site. The fact that docking of EF-Tu and *Ec*OLA1 at the A-site must be asynchronous prompts an important question: How is OLA1 outcompeting EF-Tu? Preliminary data suggests OLA1 is capable of RNA remodelling (Brandon, 2021).

I decided to further test the ability of *Ec*OLA1 to remodel RNA using *E. coli* rRNA substrate from the vicinity of OLA1's binding site using MST. MST clearly reports a change in normalized fluorescence (F_{norm}) upon complexing of a fluorescently labelled DNA oligo with complementary RNA. The change in F_{norm} upon the addition of *Ec*OLA1 to SRL RNA and complementary DNA is among the largest in the data set ($P < 0.0001$, S/N = 19). However, the thermophoresis of the fluorescent DNA oligo changes upon the addition of all proteins tested, even BSA. With the SRL substrate, the addition of BSA in the presence of ATP (200 µM), RNA (1 µM), and DNA (0.06 µM) results in a significant change in F_{norm}. No such change occurs in the absence of RNA or when comparing ATP versus ADP, suggesting BSA directly interacts with the SRL RNA in a nucleotide-independent manner. This contradicts the results from similar assays using BSA (Hussain et al., 2013; Nelson et al., 2021; Nelson et al., 2020). For example, in Nelson et al. (2020), the addition of BSA was not shown to unwind RNA (74 nt in length) when compared to the absence of protein. I hypothesize that the helicase assays using the SRL rRNA did not work as intended because of the transient opening of the RNA structure, specifically at the U-A and G-C base pairs at the loop base (green nucleotides in figure 12A). Such transient RNA dynamics have been observed for other RNA, and the phenomenon is termed "RNA breathing" (Homan *et al.*, 2014). As a result of SRL "RNA breathing," the complementary DNA oligo could more easily base pair the loop region. Although generally considered inert, it is possible that BSA interacts with a few nucleotides from the SRL rRNA, stabilizing a DNA oligo-receptive conformation and producing the results seen here. Because of the likely RNA breathing, the results regarding the ability of OLA1 to unwind rRNA are inconclusive. However, the presence of *Ec*OLA1, StpA, and BSA facilitate SRL remodeling in some way, perhaps through molecular crowding. Ultimately, the assay should be redone with a shorter

fluorescent oligo that is only complementary to the base-paired segment of the SRL stem, not the loop, and perhaps with additional negative controls.

In the literature, StpA is reported to be an RNA chaperone, not requiring ATP for either RNA annealing or strand displacement (Rajkowitsch & Schroeder, 2007). Instead, "RNA crowding" promotes unspecific RNA annealing of StpA (Mayer et al., 2007). Interestingly, the results herein suggest that RNA unwinding by StpA differs in the presence of ATP versus ADP ($P = 0.0014$, S/N = 5.8). Yet, when comparing the presence or absence of ATP or ADP the signal-to-noise ratio does not indicate stimulation (S/N = 2.6 and 1.6, respectively). Similar results occur with *Ec*OLA1; although the presence of ATP significantly affects *Ec*OLA1 compared to the absence of nucleotide ($P = 0.0071$), the signal-to-noise ratio is below the threshold of 5. The same trend is observed when comparing the presence of ADP and ATP directly ($P = 0.0119$, S/N = 3.2). Considering that StpA is not known to behave in a nucleotide-specific manner and considering the contradictions within the helicase assay results presented here, I propose that the minor effects on fluorescence detection by the nucleotides are not representative of an influence on protein•RNA binding.

Even if OLA1 can remodel SRL rRNA, the *in vivo* relevance is not addressed by decoupling of the SRL and the 70S ribosome. The region of OLA1 nearest the SRL in the *P. falciparum* Cryo-EM structure is the G-domain (A. Amunts, unpublished), shared by other trNTPases. The sensitivity of the SRL to change conformations in the proximity of 3 different proteins and the high conservation of the G-domain suggests that other A-site-binding trNTPases could affect the SRL similarly. In fact, IF1 is known to exhibit RNA chaperone activity and binds at the A-site (Merrick & Pavitt, 2018; Semrad, 2011). Altogether, remodelling of the SRL by OLA1 is not disproven but it is unlikely for cells to maintain a protein with SRL remodeling as the primary role when other proteins are equally capable. Thus, OLA1's likely has an alternative role at the A-site, like transiently pausing translation.

Experimental Limitations

Decoupling the SRL rRNA from the 70S ribosome is a convenient technique for *in vitro* assays that has been used before (Mitkevich *et al.*, 2012), however, it does not allow for direct probing of

functional versus non-functional ribosome conformations Furthermore, it is unclear what region of OLA1 is contacting the SRL and what the exact nucleic acid recognition sequence is in the experimental design used here. *In vivo*, tRNA would be bound between OLA1 and the ribosome and the OLA1 C-terminal tail would be buried in the SSU rRNA. OLA1 is also known to bind dsDNA (Teplyakov *et al.*, 2003), suggesting relaxed nucleic acid sequence recognition. Measuring the K_D's of OLA1 towards the MST RNA substrate would aid in understanding OLA1's RNA binding specificity but an alternate experimental design is required to ascertain whether OLA1 performs rRNA maintenance.

The potential RNA chaperone activity by *Ec*OLA1 has implications on its tRNA binding that were not considered in the helicase assay design. Some tRNA binding proteins like TruB have RNA remodelling activity. TruB binds folded and misfolded tRNA with similar affinity (Keffer-Wilkes *et al.*, 2016). Of note, the chaperone activity of TruB is only observed with tRNA, not single-stranded or other "structured" RNA (Keffer-Wilkes *et al.*, 2016). Whether *Ec*OLA1 has inverse behaviour – only remodelling rRNA and not tRNA – remains to be seen. The TGS domain of RelA is not known to remodel RNA but binds tRNA indiscriminately through interactions with the RNA backbone (Brown *et al.*, 2016). Remodelling of tRNA by OLA1 should be considered in future experiments.

4.3 OLA1 and Translation: A Holistic View

Differences Between Bacteria and Eukaryotes: A Hybrid Hypothesis

The results herein demonstrate that hOLA1 forms a ternary complex off the ribosome. *Ec*OLA1 may also bind tRNA independent of the ribosome, but with weaker affinity than hOLA1 does. I propose a two-part explanation. In *E. coli*, ensuring that OLA1 is not outcompeting aaRS for deacylated tRNA theoretically benefits the rate of translation under ideal conditions. Therefore, *Ec*OLA1 may preferentially bind to tRNA already at the A-site of the ribosome, competing with RelA in a way that prevents stringent response. The stringent response rewires cells for slow growth under various hostile conditions, like nutrient limitation, heat stress, oxidative stress, and antibiotic exposure, ultimately enabling cell survival (Khakimova et al., 2013; Liu et al., 2015; VanBogelen et

al., 1987; Winther et al., 2018). OLA1 inhibiting the stringent response could explain the negative stress regulation observed in *E. coli*, where OLA1 overexpression causes hypersensitivity towards oxidative stress (Wenk *et al.*, 2012) and OLA1 deletion correlates to resistance against replication inhibitor hydroxyurea and the translational inhibitor fusidic acid (Landwehr *et al.*, 2021).

OLA1 ternary complex formation in humans would logically also require a benefit to offset the cost of potentially reducing tRNA charging. Note that alarmones are only present in bacteria and plant chloroplasts, so the stringent response is not relevant in the human cellular environment; there is no known RelA homolog for OLA1 to compete against in animals (Ito *et al.*, 2020). I propose that in humans, the OLA1 ternary complex formation is important for centrosome regulation. Evidence herein suggests that tRNA is the unidentified factor X that facilitates binding between hOLA1 and BRCA1 during centrosome regulation, a role not conserved for bacterial OLA1. Matsuzawa *et al.* (2014) were the first to mention unidentified factor X in the BARD1•OLA1•X•BRCA1•γ-tubulin•Y complex. Yoshino *et al.* (2019) later identified factor Y as RACK1 by analyzing co-eluting proteins with mass spectrometry but did not identify factor X. The GST-hOLA1 and FLAG-hOLA1 used in both studies were purified with glutathione Sepharose® and immunoprecipitation by anti-FLAG antibodies, respectively, neither of which removes RNA. In addition, there is no indication that the mass spectrometry analysis was tailored to include RNA; the proteins co-eluting with FLAG-hOLA1 were resolved by SDS-PAGE, and the recovered peptides were analyzed by mass spectrometry. Thus, factor X is likely an RNA. Factor X associates between BRCA1 and OLA1, unless OLA1 has the cancer-linked E168Q mutation. Interestingly, E168 is located next to a conserved lysine that likely binds tRNA in the *P. falciparum* structure (A. Amunts, unpublished), suggesting that factor X might specifically be a tRNA.

In the model I am proposing, OLA1 is incentivized to form a ternary complex in humans because of translation-pausing and centrosome regulation roles but lacks centrosome-related pressure in bacteria or in other eukaryotes like fungi or plants. BRCA1 and BARD1 homologs exist in plants but are involved in fixing DNA double-strand breaks rather than centrosome regulation (Reidt et al., 2006; Trapp et al., 2011). Therefore, OLA1 may participate in DNA repair in fungi and plants. Interestingly, plant chloroplasts contain RelA/Spot homologs (RSH) (Ochi *et al.*, 2012).

Members of the RSH1 group found in *A. thalia* and *O. sativa*, among others, contain a TGS domain and may compete with OLA1 for ribosome binding in plants (Dąbrowska et al., 2021; Ito et al., 2017). The role of OLA1 in plants and fungi may reflect what has been proposed for animals, while the role of OLA1 in plant chloroplasts may be more analogous to that of bacteria.

CHAPTER 5: CONCLUSIONS AND FUTURE DIRECTIONS

5.1 An Update to the Proposed Functional Cycle of OLA1.

My main finding is that OLA1 can bind deacylated tRNA without the ribosome. Together with the observation of an *Pf*OLA1•ADP•tRNA complex on the 80S ribosome (A. Amunts, unpublished), this data suggests that OLA1's role in translation involves tRNA. Interactions involving OLA1 outside of translation may also include tRNA, such as BRCA1 binding during centrosome regulation in human cells. The proposed functional cycle of OLA1 in relation to translation is depicted in figure 14.

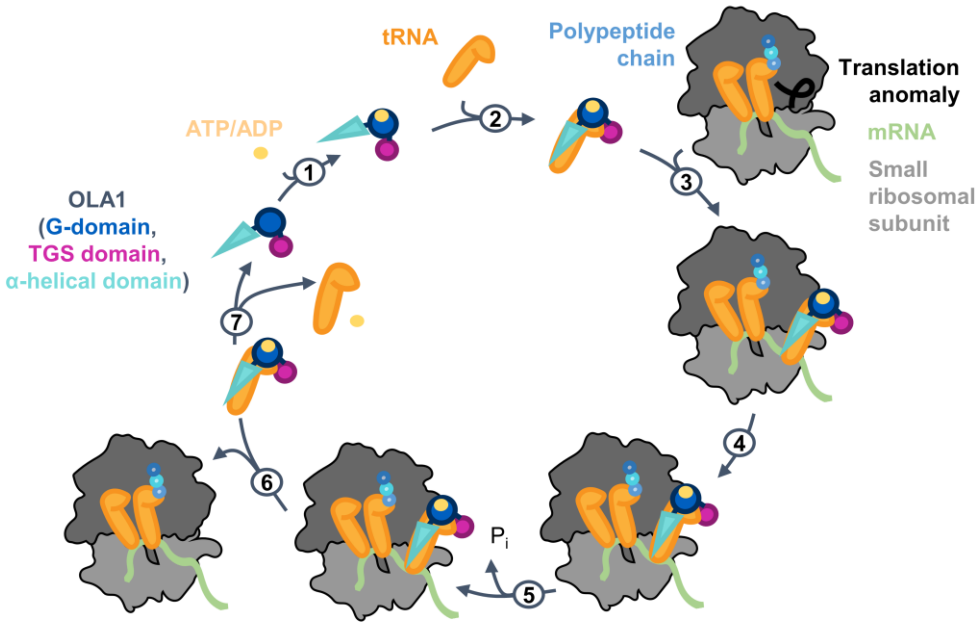

Figure 14. The proposed functional cycle of OLA1. OLA1 is likely bound to ATP/ADP (1) before binding tRNA (2). Under cellular stress, such as low amino acid abundance or oxidation that prevents EF-Tu from binding to the A-site, the OLA1 ternary complex binds instead (3). When at the A-site, OLA1 either modifies the ribosome in some way or acts as a placeholder during stress (4). ATP hydrolysis and inorganic phosphate release then occur (5), ultimately returning the ribosome and OLA1 to their respective functional cycles (6) as well as allowing for tRNA release, though tRNA release could theoretically happen earlier in the cycle (7).

The bound nucleotide's di- or triphosphate state is not specified in the proposed functional cycle of OLA1 for several reasons. While *Ec*OLA1 has a higher affinity for tRNA in the presence of ATP, hOLA1 does not. Also, *Ec*OLA1 can bind the ribosome in both its "on" and "off" states (Becker *et al.*, 2012). Coupled with the observation that ATP concentrations can decrease by over half in stressed cells (Bajerski *et al.*, 2018) and that OLA1 has moderate ADPNP and ADP binding (K_D's ≈ 9 and 10, respectively), it is plausible that the nucleotide can be exchanged at any point within the cycle, similar to EF-G.

Along with the specific role of nucleotide binding, many details of the OLA1 functional cycle are still unknown. For instance, although OLA1 likely utilizes deacylated tRNA rather than aa-tRNA based on apparent steric clashes with the amino acid and TGS domain noted in the structural analysis, OLA1's binding to aa-tRNA has yet to be tested biochemically. Furthermore, it remains to be seen whether *Ec*OLA1 binds tRNA transiently or only binds to A-site tRNA. The effect tRNA has on the ability of the ribosome to stimulate OLA1's ATPase activity is also unknown. These observations, the holistic overview of all OLA1-related hypotheses written above, and the investigation of two additional OLA1 structures (*P. falciparum* and *P. horikoshii*) provide some direction for future studies.

5.2 Future Directions: Advancing Our Understanding of the OLA1 Functional Cycle.

Avenues for future research include solidifying our understanding of the components involved in OLA1's interaction with the ribosome, ultimately allowing for detailed kinetic studies of the reconstituted system. I propose some recently developed techniques to identify the tRNA and mRNA necessary for OLA's function in translation.

To further address the potential tRNA preference of OLA1, I propose that filter-binding experiments are repeated with aa-tRNA^{Phe}. If OLA1 can bind aa-tRNA, a combination of reverse-transcription quantitative (q)PCR and individual tRNA acylation PCR (i-tRAP) can be used to differentiate between deacylated and aa-tRNA that co-elute with OLA1 during affinity chromatography (Tsukamoto et al., 2022). i-tRAP utilizes a periodate oxidation and beta-elimination step, removing the aa from acylated tRNA and the 3' adenine of deacylated tRNA. I

propose that the reactions used in i-tRAP can be combined with the optimized sequencing for reverse-transcribed tRNA by Lucas *et al.* (2023), which is reported to be sensitive enough to identify the absence of the tRNA 3' adenine resulting from oxidative stress. The results can be analyzed using an open-source computational pipeline called single-read analysis of crosstalks (SLAC) described by Hernandez-Alias *et al*. (2023). If OLA1 cannot bind aa-tRNA, steps from i-tRAP can be excluded, and native tRNA can be sequenced directly using nanopore-based tRNA sequencing (Nano-tRNAseq) (Lucas *et al.*, 2023). For direct sequencing of deacylated tRNA, Lucas *et al.* (2023) employ a 24-nt 5' RNA adapter complementary to the tRNA 3' CCA end, in addition to a 30-nt 3' RNA: DNA splint adapter pre-annealed to the 5' adapter. This extends the tRNA length above the ~100-nt sequencing threshold, allowing for recognition during a custom configuration of direct RNA sequencing (further detailed in Lucas *et al.* (2023)) or SLAC (Hernandez-Alias *et al*. 2023). Such an approach would enable the recognition of the tRNA that interact with OLA1 *in vivo* and the tRNA modifications present on interacting tRNA.

To address the question of mRNA sequence dependence of OLA1-targeted ribosomes and to address the hypothesis of OLA1 acting as a placeholder at the A-site, I propose that 5′ monophosphate sequencing (5P-Seq) is used to compare where ribosomes stall in the presence and absence OLA1 (Zeng *et al.*, 2021). 5P-Seq selects for ribosome footprints on mRNA undergoing 5′-to-3′ co-translational degradation, essentially capturing the *in vivo* footprint of the last translating ribosome's 5' position. This technique is used to identify the mRNA sequence of pause sites genome-wide and the rate of translation, and it can also identify ribosome collisions based on the footprint size (Zeng *et al.*, 2021).

When 5P-Seq was used for characterizing the cellular role of Rbg1, multiple-knockout strains were required to deconvolute the functional overlap of Rbg1 and Slh1. OLA1 has also been suggested to have functional redundancy with multiple proteins (Glass *et al.*, 2006; Samanfar *et al.*, 2014), indicating that multiple-knockout stains may be required to decouple its function from other proteins, as was done when studying Rbg1.

Filling in these knowledge gaps can expand our understanding of ribosome regulation, an essential process at the intersection of cellular biology and medicine. Understanding how the ribosomes of different organisms adapt to stress allows for better design of antimicrobials as well as ribosomopathy and cancer treatments (Adiga *et al.*, 2018; Barluenga *et al.*, 2004; Parmeggiani & Nissen, 2006; Poehlsgaard & Douthwaite, 2005; Qiu *et al.*, 2019).

BIBLIOGRAPHY

Adékambi, T., Butler, R. W., Hanrahan, F., Delcher, A. L., Drancourt, M., & Shinnick, T. M. (2011). Core gene set as the basis of multilocus sequence analysis of the subclass Actinobacteridae. *PLoS One*, *6*(3), e14792. https://doi.org/10.1371/journal.pone.0014792

Adiga, R., Al-Adhami, M., Andar, A., Borhani, S., Brown, S., Burgenson, D., Cooper, M. A., Deldari, S., Frey, D. D., Ge, X., Guo, H., Gurramkonda, C., Jensen, P., Kostov, Y., LaCourse, W., Liu, Y., Moreira, A., Mupparapu, K., Peñalber-Johnstone, C., . . . Zuber, A. (2018). Point-of-care production of therapeutic proteins of good-manufacturing-practice quality. *Nat Biomed Eng*, *2*(9), 675-686. https://doi.org/10.1038/s41551-018-0259-1

Adio, S., Sharma, H., Senyushkina, T., Karki, P., Maracci, C., Wohlgemuth, I., Holtkamp, W., Peske, F., & Rodnina, M. V. (2018). Dynamics of ribosomes and release factors during translation termination in E. coli. *Elife*, *7*. https://doi.org/10.7554/eLife.34252

Akulich, K. A., Andreev, D. E., Terenin, I. M., Smirnova, V. V., Anisimova, A. S., Makeeva, D. S., Arkhipova, V. I., Stolboushkina, E. A., Garber, M. B., Prokofjeva, M. M., Spirin, P. V., Prassolov, V. S., Shatsky, I. N., & Dmitriev, S. E. (2016). Four translation initiation pathways employed by the leaderless mRNA in eukaryotes. *Sci Rep*, *6*, 37905. https://doi.org/10.1038/srep37905

Aleksandrov, A., & Field, M. (2013). Mechanism of activation of elongation factor Tu by ribosome: catalytic histidine activates GTP by protonation. *Rna*, *19*(9), 1218-1225. https://doi.org/10.1261/rna.040097.113

Anand, B., Verma, S. K., & Prakash, B. (2006). Structural stabilization of GTP-binding domains in circularly permuted GTPases: implications for RNA binding. *Nucleic Acids Res*, *34*(8), 2196-2205. https://doi.org/10.1093/nar/gkl178

Arenz, S., Abdelshahid, M., Sohmen, D., Payoe, R., Starosta, A. L., Berninghausen, O., Hauryliuk, V., Beckmann, R., & Wilson, D. N. (2016). The stringent factor RelA adopts an open conformation on the ribosome to stimulate ppGpp synthesis. *Nucleic Acids Res*, *44*(13), 6471-6481. https://doi.org/10.1093/nar/gkw470

Assmann, S. M., Chou, H. L., & Bevilacqua, P. C. (2023). Rock, scissors, paper: How RNA structure informs function. *Plant Cell*. https://doi.org/10.1093/plcell/koad026

Aze, A., & Maiorano, D. (2018). Recent advances in understanding DNA replication: cell type-specific adaptation of the DNA replication program. *F1000Res*, *7*. https://doi.org/10.12688/f1000research.15408.1

Bajerski, F., Stock, J., Hanf, B., Darienko, T., Heine-Dobbernack, E., Lorenz, M., Naujox, L., Keller, E. R. J., Schumacher, H. M., Friedl, T., Eberth, S., Mock, H. P., Kniemeyer, O., & Overmann, J. (2018). ATP Content and Cell Viability as Indicators for Cryostress Across the Diversity of Life. *Front Physiol*, *9*, 921. https://doi.org/10.3389/fphys.2018.00921

Bakshi, S., Siryaporn, A., Goulian, M., & Weisshaar, J. C. (2012). Superresolution imaging of ribosomes and RNA polymerase in live Escherichia coli cells. *Mol Microbiol*, *85*(1), 21-38. https://doi.org/10.1111/j.1365-2958.2012.08081.x

Balasingam, N., Brandon, H. E., Ross, J. A., Wieden, H. J., & Thakor, N. (2020). Cellular roles of the human Obg-like ATPase 1 (hOLA1) and its YchF homologs. *Biochem Cell Biol*, *98*(1), 1-11. https://doi.org/10.1139/bcb-2018-0353

Ban, N., Beckmann, R., Cate, J. H., Dinman, J. D., Dragon, F., Ellis, S. R., Lafontaine, D. L., Lindahl, L., Liljas, A., Lipton, J. M., McAlear, M. A., Moore, P. B., Noller, H. F., Ortega, J., Panse, V. G., Ramakrishnan, V., Spahn, C. M., Steitz, T. A., Tchorzewski, M., . . . Yusupov, M. (2014).

A new system for naming ribosomal proteins. *Curr Opin Struct Biol*, *24*, 165-169. https://doi.org/10.1016/j.sbi.2014.01.002

Barluenga, S., Simonsen, K. B., Littlefield, E. S., Ayida, B. K., Vourloumis, D., Winters, G. C., Takahashi, M., Shandrick, S., Zhao, Q., Han, Q., & Hermann, T. (2004). Rational design of azepane-glycoside antibiotics targeting the bacterial ribosome. *Bioorg Med Chem Lett*, *14*(3), 713-718. https://doi.org/10.1016/j.bmcl.2003.11.028

Basu, R. S., Sherman, M. B., & Gagnon, M. G. (2022). Compact IF2 allows initiator tRNA accommodation into the P site and gates the ribosome to elongation. *Nat Commun*, *13*(1), 3388. https://doi.org/10.1038/s41467-022-31129-2

Beck, M., Schmidt, A., Malmstroem, J., Claassen, M., Ori, A., Szymborska, A., Herzog, F., Rinner, O., Ellenberg, J., & Aebersold, R. (2011). The quantitative proteome of a human cell line. *Mol Syst Biol*, *7*, 549. https://doi.org/10.1038/msb.2011.82

Becker, M., Gzyl, K. E., Altamirano, A. M., Vuong, A., Urban, K., & Wieden, H. J. (2012). The 70S ribosome modulates the ATPase activity of Escherichia coli YchF. *RNA Biol*, *9*(10), 1288-1301. https://doi.org/10.4161/rna.22131

Bentley, D. L. (2014). Coupling mRNA processing with transcription in time and space. *Nat Rev Genet*, *15*(3), 163-175. https://doi.org/10.1038/nrg3662

Bessho, Y., Shibata, R., Sekine, S., Murayama, K., Higashijima, K., Hori-Takemoto, C., Shirouzu, M., Kuramitsu, S., & Yokoyama, S. (2007). Structural basis for functional mimicry of long-variable-arm tRNA by transfer-messenger RNA. *Proc Natl Acad Sci U S A*, *104*(20), 8293-8298. https://doi.org/10.1073/pnas.0700402104

Bhaskaran, H., Rodriguez-Hernandez, A., & Perona, J. J. (2012). Kinetics of tRNA folding monitored by aminoacylation. *Rna*, *18*(3), 569-580. https://doi.org/10.1261/rna.030080.111

Bian, R., Zhao, J., Yao, Z., Cai, Y., Shou, C., Lou, D., Zhou, L., & Qian, Y. (2022). Knockdown of Obg-like ATPase 1 enhances sorafenib sensitivity by inhibition of GSK-3β/β-catenin signaling in hepatocellular carcinoma cells. *J Gastrointest Oncol*, *13*(3), 1255-1265. https://doi.org/10.21037/jgo-22-458

Biou, V., Yaremchuk, A., Tukalo, M., & Cusack, S. (1994). The 2.9 A crystal structure of T. thermophilus seryl-tRNA synthetase complexed with tRNA(Ser). *Science*, *263*(5152), 1404-1410. https://doi.org/10.1126/science.8128220

Bovee, M. L., Yan, W., Sproat, B. S., & Francklyn, C. S. (1999). tRNA discrimination at the binding step by a class II aminoacyl-tRNA synthetase. *Biochemistry*, *38*(41), 13725-13735. https://doi.org/10.1021/bi991182g

Bowman, J. C., Petrov, A. S., Frenkel-Pinter, M., Penev, P. I., & Williams, L. D. (2020). Root of the Tree: The Significance, Evolution, and Origins of the Ribosome. *Chem Rev*, *120*(11), 4848-4878. https://doi.org/10.1021/acs.chemrev.9b00742

Brandi, L., Fabbretti, A., La Teana, A., Abbondi, M., Losi, D., Donadio, S., & Gualerzi, C. O. (2006). Specific, efficient, and selective inhibition of prokaryotic translation initiation by a novel peptide antibiotic. *Proc Natl Acad Sci U S A*, *103*(1), 39-44. https://doi.org/10.1073/pnas.0507740102

Brandman, O., & Hegde, R. S. (2016). Ribosome-associated protein quality control. *Nat Struct Mol Biol*, *23*(1), 7-15. https://doi.org/10.1038/nsmb.3147

Brandon, H. E. (2021). *Biophysical studies of the universally conserved NTPases HflX and YchF* University of Lethbridge]. https://hdl.handle.net/10133/6013

Brazier, A. J., Avril, M., Bernabeu, M., Benjamin, M., & Smith, J. D. (2017). Pathogenicity Determinants of the Human Malaria Parasite Plasmodium falciparum Have Ancient Origins. *mSphere*, *2*(1). https://doi.org/10.1128/mSphere.00348-16

Brock, S., Szkaradkiewicz, K., & Sprinzl, M. (1998). Initiation factors of protein biosynthesis in bacteria and their structural relationship to elongation and termination factors. *Mol Microbiol*, *29*(2), 409-417. https://doi.org/10.1046/j.1365-2958.1998.00893.x

Brosius, J., & Raabe, C. A. (2016). What is an RNA? A top layer for RNA classification. *RNA Biol*, *13*(2), 140-144. https://doi.org/10.1080/15476286.2015.1128064

Brown, A., Fernández, I. S., Gordiyenko, Y., & Ramakrishnan, V. (2016). Ribosome-dependent activation of stringent control. *Nature*, *534*(7606), 277-280. https://doi.org/10.1038/nature17675

Buckstein, M. H., He, J., & Rubin, H. (2008). Characterization of nucleotide pools as a function of physiological state in Escherichia coli. *J Bacteriol*, *190*(2), 718-726. https://doi.org/10.1128/jb.01020-07

Buglino, J., Shen, V., Hakimian, P., & Lima, C. D. (2002). Structural and biochemical analysis of the Obg GTP binding protein. *Structure*, *10*(11), 1581-1592. https://doi.org/10.1016/s0969-2126(02)00882-1

Buskirk, A. R., & Green, R. (2017). Ribosome pausing, arrest and rescue in bacteria and eukaryotes. *Philos Trans R Soc Lond B Biol Sci*, *372*(1716). https://doi.org/10.1098/rstb.2016.0183

Byrgazov, K., Vesper, O., & Moll, I. (2013). Ribosome heterogeneity: another level of complexity in bacterial translation regulation. *Curr Opin Microbiol*, *16*(2), 133-139. https://doi.org/10.1016/j.mib.2013.01.009

Caldon, C. E., & March, P. E. (2003). Function of the universally conserved bacterial GTPases. *Curr Opin Microbiol*, *6*(2), 135-139. https://doi.org/10.1016/s1369-5274(03)00037-7

Caldon, C. E., Yoong, P., & March, P. E. (2001). Evolution of a molecular switch: universal bacterial GTPases regulate ribosome function. *Mol Microbiol*, *41*(2), 289-297. https://doi.org/10.1046/j.1365-2958.2001.02536.x

Cann, J. R. (1989). Phenomenological theory of gel electrophoresis of protein-nucleic acid complexes. *J Biol Chem*, *264*(29), 17032-17040.

Carbone, C. E., Demo, G., Madireddy, R., Svidritskiy, E., & Korostelev, A. A. (2020). ArfB can displace mRNA to rescue stalled ribosomes. *Nat Commun*, *11*(1), 5552. https://doi.org/10.1038/s41467-020-19370-z

Carbone, C. E., Loveland, A. B., Gamper, H. B., Jr., Hou, Y. M., Demo, G., & Korostelev, A. A. (2021). Time-resolved cryo-EM visualizes ribosomal translocation with EF-G and GTP. *Nat Commun*, *12*(1), 7236. https://doi.org/10.1038/s41467-021-27415-0

Carlson, M. A., Haddad, B. G., Weis, A. J., Blackwood, C. S., Shelton, C. D., Wuerth, M. E., Walter, J. D., & Spiegel, P. C., Jr. (2017). Ribosomal protein L7/L12 is required for GTPase translation factors EF-G, RF3, and IF2 to bind in their GTP state to 70S ribosomes. *Febs j*, *284*(11), 1631-1643. https://doi.org/10.1111/febs.14067

Chadani, Y., Matsumoto, E., Aso, H., Wada, T., Kutsukake, K., Sutou, S., & Abo, T. (2011). trans-translation-mediated tight regulation of the expression of the alternative ribosome-rescue factor ArfA in Escherichia coli. *Genes Genet Syst*, *86*(3), 151-163. https://doi.org/10.1266/ggs.86.151

Chapeville, F., Lipmann, F., Von Ehrenstein, G., Weisblum, B., Ray, W. J., Jr., & Benzer, S. (1962). On the role of soluble ribonucleic acid in coding for amino acids. *Proc Natl Acad Sci U S A*, *48*(6), 1086-1092. https://doi.org/10.1073/pnas.48.6.1086

Chen, A. H., & Silver, P. A. (2012). Designing biological compartmentalization. *Trends Cell Biol*, *22*(12), 662-670. https://doi.org/10.1016/j.tcb.2012.07.002

Chen, H., Song, R., Wang, G., Ding, Z., Yang, C., Zhang, J., Zeng, Z., Rubio, V., Wang, L., Zu, N., Weiskoff, A. M., Minze, L. J., Jeyabal, P. V., Mansour, O. C., Bai, L., Merrick, W. C., Zheng,

S., & Shi, Z. Z. (2015). OLA1 regulates protein synthesis and integrated stress response by inhibiting eIF2 ternary complex formation. *Sci Rep*, *5*, 13241. https://doi.org/10.1038/srep13241

Chen, T., Yeh, H. W., Chen, P. P., Huang, W. T., Wu, C. Y., Liao, T. C., Lin, S. L., Chen, Y. Y., Lin, K. T., Hsu, S. D., & Cheng, H. C. (2022). BARD1 is an ATPase activating protein for OLA1. *Biochim Biophys Acta Gen Subj*, *1866*(5), 130099. https://doi.org/10.1016/j.bbagen.2022.130099

Chen, Y. C., & Chung, Y. T. (2011). A conserved GTPase YchF of Vibrio vulnificus is involved in macrophage cytotoxicity, iron acquisition, and mouse virulence. *Int J Med Microbiol*, *301*(6), 469-474. https://doi.org/10.1016/j.ijmm.2011.02.002

Cherkasov, V., Grousl, T., Theer, P., Vainshtein, Y., Glässer, C., Mongis, C., Kramer, G., Stoecklin, G., Knop, M., Mogk, A., & Bukau, B. (2015). Systemic control of protein synthesis through sequestration of translation and ribosome biogenesis factors during severe heat stress. *FEBS Lett*, *589*(23), 3654-3664. https://doi.org/10.1016/j.febslet.2015.10.010

Cheung, M. Y., Li, X., Ku, Y. S., Chen, Z., & Lam, H. M. (2022). Co-crystalization reveals the interaction between AtYchF1 and ppGpp. *Front Mol Biosci*, *9*, 1061350. https://doi.org/10.3389/fmolb.2022.1061350

Cheung, M. Y., Li, X., Miao, R., Fong, Y. H., Li, K. P., Yung, Y. L., Yu, M. H., Wong, K. B., Chen, Z., & Lam, H. M. (2016). ATP binding by the P-loop NTPase OsYchF1 (an unconventional G protein) contributes to biotic but not abiotic stress responses. *Proc Natl Acad Sci U S A*, *113*(10), 2648-2653. https://doi.org/10.1073/pnas.1522966113

Cheung, M. Y., Xue, Y., Zhou, L., Li, M. W., Sun, S. S., & Lam, H. M. (2010). An ancient P-loop GTPase in rice is regulated by a higher plant-specific regulatory protein. *J Biol Chem*, *285*(48), 37359-37369. https://doi.org/10.1074/jbc.M110.172080

Cheung, M. Y., Zeng, N. Y., Tong, S. W., Li, W. F., Xue, Y., Zhao, K. J., Wang, C., Zhang, Q., Fu, Y., Sun, Z., Sun, S. S., & Lam, H. M. (2008). Constitutive expression of a rice GTPase-activating protein induces defense responses. *New Phytol*, *179*(2), 530-545. https://doi.org/10.1111/j.1469-8137.2008.02473.x

Clementi, N., Chirkova, A., Puffer, B., Micura, R., & Polacek, N. (2010). Atomic mutagenesis reveals A2660 of 23S ribosomal RNA as key to EF-G GTPase activation. *Nat Chem Biol*, *6*(5), 344-351. https://doi.org/10.1038/nchembio.341

Copeland, P. R., & Howard, M. T. (2021). Ribosome Fate during Decoding of UGA-Sec Codons. *Int J Mol Sci*, *22*(24). https://doi.org/10.3390/ijms222413204

Cretel, E., Pierres, A., Benoliel, A. M., & Bongrand, P. (2008). How Cells feel their environment: a focus on early dynamic events. *Cell Mol Bioeng*, *1*(1), 5-14. https://doi.org/10.1007/s12195-008-0009-7

Cruz-Vera, L. R., Galindo, J. M., & Guarneros, G. (2002). Transcriptional analysis of the gene encoding peptidyl-tRNA hydrolase in Escherichia coli. *Microbiology (Reading)*, *148*(Pt 11), 3457-3466. https://doi.org/10.1099/00221287-148-11-3457

Dąbrowska, G. B., Turkan, S., Tylman-Mojżeszek, W., & Mierek-Adamska, A. (2021). In Silico Study of the RSH (RelA/SpoT Homologs) Gene Family and Expression Analysis in Response to PGPR Bacteria and Salinity in Brassica napus. *Int J Mol Sci*, *22*(19). https://doi.org/10.3390/ijms221910666

Danese, I., Haine, V., Delrue, R. M., Tibor, A., Lestrate, P., Stevaux, O., Mertens, P., Paquet, J. Y., Godfroid, J., De Bolle, X., & Letesson, J. J. (2004). The Ton system, an ABC transporter, and a universally conserved GTPase are involved in iron utilization by Brucella melitensis 16M. *Infect Immun*, *72*(10), 5783-5790. https://doi.org/10.1128/iai.72.10.5783-5790.2004

Dannenmaier, S., Desroches Altamirano, C., Schüler, L., Zhang, Y., Hummel, J., Milanov, M., Oeljeklaus, S., Koch, H. G., Rospert, S., Alberti, S., & Warscheid, B. (2021). Quantitative proteomics identifies the universally conserved ATPase Ola1p as a positive regulator of heat shock response in Saccharomyces cerevisiae. *J Biol Chem*, *297*(5), 101050. https://doi.org/10.1016/j.jbc.2021.101050

Das, G., & Varshney, U. (2006). Peptidyl-tRNA hydrolase and its critical role in protein biosynthesis. *Microbiology (Reading)*, *152*(Pt 8), 2191-2195. https://doi.org/10.1099/mic.0.29024-0

Dassain, M., Leroy, A., Colosetti, L., Carolé, S., & Bouché, J. P. (1999). A new essential gene of the 'minimal genome' affecting cell division. *Biochimie*, *81*(8-9), 889-895. https://doi.org/10.1016/s0300-9084(99)00207-2

Daugeron, M. C., Prouteau, M., Lacroute, F., & Séraphin, B. (2011). The highly conserved eukaryotic DRG factors are required for efficient translation in a manner redundant with the putative RNA helicase Slh1. *Nucleic Acids Res*, *39*(6), 2221-2233. https://doi.org/10.1093/nar/gkq898

Demo, G., Svidritskiy, E., Madireddy, R., Diaz-Avalos, R., Grant, T., Grigorieff, N., Sousa, D., & Korostelev, A. A. (2017). Mechanism of ribosome rescue by ArfA and RF2. *Elife*, *6*. https://doi.org/10.7554/eLife.23687

Diaconu, M., Kothe, U., Schlünzen, F., Fischer, N., Harms, J. M., Tonevitsky, A. G., Stark, H., Rodnina, M. V., & Wahl, M. C. (2005). Structural basis for the function of the ribosomal L7/12 stalk in factor binding and GTPase activation. *Cell*, *121*(7), 991-1004. https://doi.org/10.1016/j.cell.2005.04.015

Diez, S., Ryu, J., Caban, K., Gonzalez, R. L., Jr., & Dworkin, J. (2020). The alarmones (p)ppGpp directly regulate translation initiation during entry into quiescence. *Proc Natl Acad Sci U S A*, *117*(27), 15565-15572. https://doi.org/10.1073/pnas.1920013117

Ding, Z., Liu, Y., Rubio, V., He, J., Minze, L. J., & Shi, Z. Z. (2016). OLA1, a Translational Regulator of p21, Maintains Optimal Cell Proliferation Necessary for Developmental Progression. *Mol Cell Biol*, *36*(20), 2568-2582. https://doi.org/10.1128/mcb.00137-16

Doetsch, M., Gstrein, T., Schroeder, R., & Fürtig, B. (2010). Mechanisms of StpA-mediated RNA remodeling. *RNA Biol*, *7*(6), 735-743. https://doi.org/10.4161/rna.7.6.13882

Dong, H., Nilsson, L., & Kurland, C. G. (1996). Co-variation of tRNA abundance and codon usage in Escherichia coli at different growth rates. *J Mol Biol*, *260*(5), 649-663. https://doi.org/10.1006/jmbi.1996.0428

Dong, Y., Yin, A., Xu, C., Jiang, H., Wang, Q., Wu, W., & Guo, S. (2021). OLA1 is a potential prognostic molecular biomarker for endometrial cancer and promotes tumor progression. *Oncol Lett*, *22*(2), 576. https://doi.org/10.3892/ol.2021.12837

Dörner, K., Ruggeri, C., Zemp, I., & Kutay, U. (2023). Ribosome biogenesis factors-from names to functions. *Embo j*, *42*(7), e112699. https://doi.org/10.15252/embj.2022112699

Drummond, D. A., & Wilke, C. O. (2009). The evolutionary consequences of erroneous protein synthesis. *Nat Rev Genet*, *10*(10), 715-724. https://doi.org/10.1038/nrg2662

Dworkin, J. (2023). Understanding the Stringent Response: Experimental Context Matters. *mBio*, *14*(1), e0340422. https://doi.org/10.1128/mbio.03404-22

Eddy, S. R. (2001). Non-coding RNA genes and the modern RNA world. *Nat Rev Genet*, *2*(12), 919-929. https://doi.org/10.1038/35103511

Fahlman, R. P., Dale, T., & Uhlenbeck, O. C. (2004). Uniform binding of aminoacylated transfer RNAs to the ribosomal A and P sites. *Mol Cell*, *16*(5), 799-805. https://doi.org/10.1016/j.molcel.2004.10.030

Fernebro, J., Blomberg, C., Morfeldt, E., Wolf-Watz, H., Normark, S., & Normark, B. H. (2008). The influence of in vitro fitness defects on pneumococcal ability to colonize and to cause invasive disease. *BMC Microbiol*, *8*, 65. https://doi.org/10.1186/1471-2180-8-65

Fishbein, S. R. S., Tomasi, F. G., Wolf, I. D., Dulberger, C. L., Wang, A., Keshishian, H., Wallace, L., Carr, S. A., Ioerger, T. R., Rego, E. H., & Rubin, E. J. (2020). The conserved translation factor LepA is required for optimal synthesis of a porin family in Mycobacterium smegmatis. *J Bacteriol*, *203*(6). https://doi.org/10.1128/jb.00604-20

Fong, J. J., & Fujita, M. K. (2011). Evaluating phylogenetic informativeness and data-type usage for new protein-coding genes across Vertebrata. *Mol Phylogenet Evol*, *61*(2), 300-307. https://doi.org/10.1016/j.ympev.2011.06.016

Forsyth, R. A., Haselbeck, R. J., Ohlsen, K. L., Yamamoto, R. T., Xu, H., Trawick, J. D., Wall, D., Wang, L., Brown-Driver, V., Froelich, J. M., C, K. G., King, P., McCarthy, M., Malone, C., Misiner, B., Robbins, D., Tan, Z., Zhu Zy, Z. Y., Carr, G., . . . Zyskind, J. W. (2002). A genome-wide strategy for the identification of essential genes in Staphylococcus aureus. *Mol Microbiol*, *43*(6), 1387-1400. https://doi.org/10.1046/j.1365-2958.2002.02832.x

Francis, S. M., Gas, M. E., Daugeron, M. C., Bravo, J., & Séraphin, B. (2012). Rbg1-Tma46 dimer structure reveals new functional domains and their role in polysome recruitment. *Nucleic Acids Res*, *40*(21), 11100-11114. https://doi.org/10.1093/nar/gks867

Fraser, C. M., Gocayne, J. D., White, O., Adams, M. D., Clayton, R. A., Fleischmann, R. D., Bult, C. J., Kerlavage, A. R., Sutton, G., Kelley, J. M., Fritchman, R. D., Weidman, J. F., Small, K. V., Sandusky, M., Fuhrmann, J., Nguyen, D., Utterback, T. R., Saudek, D. M., Phillips, C. A., . . . Venter, J. C. (1995). The minimal gene complement of Mycoplasma genitalium. *Science*, *270*(5235), 397-403. https://doi.org/10.1126/science.270.5235.397

Fukai, S., Nureki, O., Sekine, S., Shimada, A., Vassylyev, D. G., & Yokoyama, S. (2003). Mechanism of molecular interactions for tRNA(Val) recognition by valyl-tRNA synthetase. *Rna*, *9*(1), 100-111. https://doi.org/10.1261/rna.2760703

Furano, A. V. (1975). Content of elongation factor Tu in Escherichia coli. *Proc Natl Acad Sci U S A*, *72*(12), 4780-4784. https://doi.org/10.1073/pnas.72.12.4780

Gagliardi, D., & Dziembowski, A. (2018). 5' and 3' modifications controlling RNA degradation: from safeguards to executioners. *Philos Trans R Soc Lond B Biol Sci*, *373*(1762). https://doi.org/10.1098/rstb.2018.0160

Gagnon, M. G., Seetharaman, S. V., Bulkley, D., & Steitz, T. A. (2012). Structural basis for the rescue of stalled ribosomes: structure of YaeJ bound to the ribosome. *Science*, *335*(6074), 1370-1372. https://doi.org/10.1126/science.1217443

Galperin, M. Y., & Koonin, E. V. (2004). 'Conserved hypothetical' proteins: prioritization of targets for experimental study. *Nucleic Acids Res*, *32*(18), 5452-5463. https://doi.org/10.1093/nar/gkh885

Gartland, W. J., & Sueoka, N. (1966). Two interconvertible forms of tryptophanyl sRNA in E. coli. *Proc Natl Acad Sci U S A*, *55*(4), 948-956. https://doi.org/10.1073/pnas.55.4.948

Gasteiger, E., Hoogland, C., Gattiker, A., Duvaud, S. e., Wilkins, M. R., Appel, R. D., & Bairoch, A. (2005). Protein Identification and Analysis Tools on the ExPASy Server. In J. M. Walker (Ed.), *The Proteomics Protocols Handbook* (pp. 571-607). Humana Press. https://doi.org/10.1385/1-59259-890-0:571

Gavin, A. C., Bösche, M., Krause, R., Grandi, P., Marzioch, M., Bauer, A., Schultz, J., Rick, J. M., Michon, A. M., Cruciat, C. M., Remor, M., Höfert, C., Schelder, M., Brajenovic, M., Ruffner, H., Merino, A., Klein, K., Hudak, M., Dickson, D., . . . Superti-Furga, G. (2002). Functional organization of the yeast proteome by systematic analysis of protein complexes. *Nature*, *415*(6868), 141-147. https://doi.org/10.1038/415141a

Ge, X., Mandava, C. S., Lind, C., Åqvist, J., & Sanyal, S. (2018). Complementary charge-based interaction between the ribosomal-stalk protein L7/12 and IF2 is the key to rapid subunit association. *Proc Natl Acad Sci U S A*, *115*(18), 4649-4654. https://doi.org/10.1073/pnas.1802001115

Geggier, P., Dave, R., Feldman, M. B., Terry, D. S., Altman, R. B., Munro, J. B., & Blanchard, S. C. (2010). Conformational sampling of aminoacyl-tRNA during selection on the bacterial ribosome. *J Mol Biol*, *399*(4), 576-595. https://doi.org/10.1016/j.jmb.2010.04.038

Gibbs, M. R., Moon, K. M., Warner, B. R., Chen, M., Bundschuh, R., Foster, L. J., & Fredrick, K. (2020). Functional Analysis of BipA in E. coli Reveals the Natural Plasticity of 50S Subunit Assembly. *J Mol Biol*, *432*(19), 5259-5272. https://doi.org/10.1016/j.jmb.2020.07.013

Gil, R., Silva, F. J., Peretó, J., & Moya, A. (2004). Determination of the core of a minimal bacterial gene set. *Microbiol Mol Biol Rev*, *68*(3), 518-537, table of contents. https://doi.org/10.1128/mmbr.68.3.518-537.2004

Glass, J. I., Assad-Garcia, N., Alperovich, N., Yooseph, S., Lewis, M. R., Maruf, M., Hutchison, C. A., 3rd, Smith, H. O., & Venter, J. C. (2006). Essential genes of a minimal bacterium. *Proc Natl Acad Sci U S A*, *103*(2), 425-430. https://doi.org/10.1073/pnas.0510013103

Gradia, D. F., Rau, K., Umaki, A. C., de Souza, F. S., Probst, C. M., Correa, A., Holetz, F. B., Avila, A. R., Krieger, M. A., Goldenberg, S., & Fragoso, S. P. (2009). Characterization of a novel Obg-like ATPase in the protozoan Trypanosoma cruzi. *Int J Parasitol*, *39*(1), 49-58. https://doi.org/10.1016/j.ijpara.2008.05.019

Graf, M., Huter, P., Maracci, C., Peterek, M., Rodnina, M. V., & Wilson, D. N. (2018). Visualization of translation termination intermediates trapped by the Apidaecin 137 peptide during RF3-mediated recycling of RF1. *Nat Commun*, *9*(1), 3053. https://doi.org/10.1038/s41467-018-05465-1

Grill, S., Gualerzi, C. O., Londei, P., & Bläsi, U. (2000). Selective stimulation of translation of leaderless mRNA by initiation factor 2: evolutionary implications for translation. *Embo j*, *19*(15), 4101-4110. https://doi.org/10.1093/emboj/19.15.4101

Grosjean, H., Breton, M., Sirand-Pugnet, P., Tardy, F., Thiaucourt, F., Citti, C., Barré, A., Yoshizawa, S., Fourmy, D., de Crécy-Lagard, V., & Blanchard, A. (2014). Predicting the minimal translation apparatus: lessons from the reductive evolution of mollicutes. *PLoS Genet*, *10*(5), e1004363. https://doi.org/10.1371/journal.pgen.1004363

Gruber, A. R., Lorenz, R., Bernhart, S. H., Neuböck, R., & Hofacker, I. L. (2008). The Vienna RNA websuite. *Nucleic Acids Res*, *36*(Web Server issue), W70-74. https://doi.org/10.1093/nar/gkn188

Guenneugues, M., Caserta, E., Brandi, L., Spurio, R., Meunier, S., Pon, C. L., Boelens, R., & Gualerzi, C. O. (2000). Mapping the fMet-tRNA(f)(Met) binding site of initiation factor IF2. *Embo j*, *19*(19), 5233-5240. https://doi.org/10.1093/emboj/19.19.5233

Guerrero, C., Tagwerker, C., Kaiser, P., & Huang, L. (2006). An integrated mass spectrometry-based proteomic approach: quantitative analysis of tandem affinity-purified in vivo cross-linked protein complexes (QTAX) to decipher the 26 S proteasome-interacting network. *Mol Cell Proteomics*, *5*(2), 366-378. https://doi.org/10.1074/mcp.M500303-MCP200

Hannemann, L., Suppanz, I., Ba, Q., MacInnes, K., Drepper, F., Warscheid, B., & Koch, H. G. (2016). Redox Activation of the Universally Conserved ATPase YchF by Thioredoxin 1. *Antioxid Redox Signal*, *24*(3), 141-156. https://doi.org/10.1089/ars.2015.6272

Harding, S. E. (2018). The Svedberg Lecture 2017. From nano to micro: the huge dynamic range of the analytical ultracentrifuge for characterising the sizes, shapes and interactions of molecules and assemblies in Biochemistry and Polymer Science. *Eur Biophys J*, *47*(7), 697-707. https://doi.org/10.1007/s00249-018-1321-3

Hatfield, D. L., & Gladyshev, V. N. (2002). How selenium has altered our understanding of the genetic code. *Mol Cell Biol*, *22*(11), 3565-3576. https://doi.org/10.1128/mcb.22.11.3565-3576.2002

Hauryliuk, V., Mitkevich, V. A., Draycheva, A., Tankov, S., Shyp, V., Ermakov, A., Kulikova, A. A., Makarov, A. A., & Ehrenberg, M. (2009). Thermodynamics of GTP and GDP binding to bacterial initiation factor 2 suggests two types of structural transitions. *J Mol Biol*, *394*(4), 621-626. https://doi.org/10.1016/j.jmb.2009.10.015

Hauryliuk, V., Mitkevich, V. A., Eliseeva, N. A., Petrushanko, I. Y., Ehrenberg, M., & Makarov, A. A. (2008). The pretranslocation ribosome is targeted by GTP-bound EF-G in partially activated form. *Proc Natl Acad Sci U S A*, *105*(41), 15678-15683. https://doi.org/10.1073/pnas.0807912105

Helgstrand, M., Mandava, C. S., Mulder, F. A., Liljas, A., Sanyal, S., & Akke, M. (2007). The ribosomal stalk binds to translation factors IF2, EF-Tu, EF-G and RF3 via a conserved region of the L12 C-terminal domain. *J Mol Biol*, *365*(2), 468-479. https://doi.org/10.1016/j.jmb.2006.10.025

Helm, M., Giegé, R., & Florentz, C. (1999). A Watson-Crick base-pair-disrupting methyl group (m1A9) is sufficient for cloverleaf folding of human mitochondrial tRNALys. *Biochemistry*, *38*(40), 13338-13346. https://doi.org/10.1021/bi991061g

Hernandez-Alias, X., Katanski, C. D., Zhang, W., Assari, M., Watkins, C. P., Schaefer, M. H., Serrano, L., & Pan, T. (2023). Single-read tRNA-seq analysis reveals coordination of tRNA modification and aminoacylation and fragmentation. *Nucleic Acids Res*, *51*(3), e17. https://doi.org/10.1093/nar/gkac1185

Hofmann, S., Kedersha, N., Anderson, P., & Ivanov, P. (2021). Molecular mechanisms of stress granule assembly and disassembly. *Biochim Biophys Acta Mol Cell Res*, *1868*(1), 118876. https://doi.org/10.1016/j.bbamcr.2020.118876

Homan, P. J., Favorov, O. V., Lavender, C. A., Kursun, O., Ge, X., Busan, S., Dokholyan, N. V., & Weeks, K. M. (2014). Single-molecule correlated chemical probing of RNA. *Proc Natl Acad Sci U S A*, *111*(38), 13858-13863. https://doi.org/10.1073/pnas.1407306111

Houston, L., Platten, E. M., Connelly, S. M., Wang, J., & Grayhack, E. J. (2022). Frameshifting at collided ribosomes is modulated by elongation factor eEF3 and by integrated stress response regulators Gcn1 and Gcn20. *Rna*, *28*(3), 320-339. https://doi.org/10.1261/rna.078964.121

Huang, S., Zhang, C., Sun, C., Hou, Y., Zhang, Y., Tam, N. L., Wang, Z., Yu, J., Huang, B., Zhuang, H., Zhou, Z., Ma, Z., Sun, Z., He, X., Zhou, Q., Hou, B., & Wu, L. (2020). Obg-like ATPase 1 (OLA1) overexpression predicts poor prognosis and promotes tumor progression by regulating P21/CDK2 in hepatocellular carcinoma. *Aging (Albany NY)*, *12*(3), 3025-3041. https://doi.org/10.18632/aging.102797

Hubé, F., & Francastel, C. (2018). Coding and Non-coding RNAs, the Frontier Has Never Been So Blurred. *Front Genet*, *9*, 140. https://doi.org/10.3389/fgene.2018.00140

Huber, M., Faure, G., Laass, S., Kolbe, E., Seitz, K., Wehrheim, C., Wolf, Y. I., Koonin, E. V., & Soppa, J. (2019). Translational coupling via termination-reinitiation in archaea and bacteria. *Nat Commun*, *10*(1), 4006. https://doi.org/10.1038/s41467-019-11999-9

Hummels, K. R., & Kearns, D. B. (2020). Translation elongation factor P (EF-P). *FEMS Microbiol Rev*, *44*(2), 208-218. https://doi.org/10.1093/femsre/fuaa003

Hussain, R. H., Zawawi, M., & Bayfield, M. A. (2013). Conservation of RNA chaperone activity of the human La-related proteins 4, 6 and 7. *Nucleic Acids Res*, *41*(18), 8715-8725. https://doi.org/10.1093/nar/gkt649

Hutchison, C. A., Peterson, S. N., Gill, S. R., Cline, R. T., White, O., Fraser, C. M., Smith, H. O., & Venter, J. C. (1999). Global transposon mutagenesis and a minimal Mycoplasma genome. *Science*, *286*(5447), 2165-2169. https://doi.org/10.1126/science.286.5447.2165

Imai, H., Abe, T., Miyoshi, T., Nishikawa, S. I., Ito, K., & Uchiumi, T. (2018). The ribosomal stalk protein is crucial for the action of the conserved ATPase ABCE1. *Nucleic Acids Res*, *46*(15), 7820-7830. https://doi.org/10.1093/nar/gky619

Ingolia, N. T., Lareau, L. F., & Weissman, J. S. (2011). Ribosome profiling of mouse embryonic stem cells reveals the complexity and dynamics of mammalian proteomes. *Cell*, *147*(4), 789-802. https://doi.org/10.1016/j.cell.2011.10.002

Ishihama, Y., Schmidt, T., Rappsilber, J., Mann, M., Hartl, F. U., Kerner, M. J., & Frishman, D. (2008). Protein abundance profiling of the Escherichia coli cytosol. *BMC Genomics*, *9*, 102. https://doi.org/10.1186/1471-2164-9-102

Ito, D., Ihara, Y., Nishihara, H., & Masuda, S. (2017). Phylogenetic analysis of proteins involved in the stringent response in plant cells. *J Plant Res*, *130*(4), 625-634. https://doi.org/10.1007/s10265-017-0922-8

Ito, D., Kawamura, H., Oikawa, A., Ihara, Y., Shibata, T., Nakamura, N., Asano, T., Kawabata, S. I., Suzuki, T., & Masuda, S. (2020). ppGpp functions as an alarmone in metazoa. *Commun Biol*, *3*(1), 671. https://doi.org/10.1038/s42003-020-01368-4

Ivanova, N., Pavlov, M. Y., Felden, B., & Ehrenberg, M. (2004). Ribosome rescue by tmRNA requires truncated mRNAs. *J Mol Biol*, *338*(1), 33-41. https://doi.org/10.1016/j.jmb.2004.02.043

Jain, S., Wheeler, J. R., Walters, R. W., Agrawal, A., Barsic, A., & Parker, R. (2016). ATPase-Modulated Stress Granules Contain a Diverse Proteome and Substructure. *Cell*, *164*(3), 487-498. https://doi.org/10.1016/j.cell.2015.12.038

Jiang, M., Sullivan, S. M., Walker, A. K., Strahler, J. R., Andrews, P. C., & Maddock, J. R. (2007). Identification of novel Escherichia coli ribosome-associated proteins using isobaric tags and multidimensional protein identification techniques. *J Bacteriol*, *189*(9), 3434-3444. https://doi.org/10.1128/jb.00090-07

Jüttner, M., & Ferreira-Cerca, S. (2022). A Comparative Perspective on Ribosome Biogenesis: Unity and Diversity Across the Tree of Life. *Methods Mol Biol*, *2533*, 3-22. https://doi.org/10.1007/978-1-0716-2501-9_1

Kabsch, W., Gast, W. H., Schulz, G. E., & Leberman, R. (1977). Low resolution structure of partially trypsin-degraded polypeptide elongation factor, EF-TU, from Escherichia coli. *J Mol Biol*, *117*(4), 999-1012. https://doi.org/10.1016/s0022-2836(77)80009-0

Karamyshev, A. L., & Karamysheva, Z. N. (2018). Lost in Translation: Ribosome-Associated mRNA and Protein Quality Controls. *Front Genet*, *9*, 431. https://doi.org/10.3389/fgene.2018.00431

Karousis, E. D., & Mühlemann, O. (2019). Nonsense-Mediated mRNA Decay Begins Where Translation Ends. *Cold Spring Harb Perspect Biol*, *11*(2). https://doi.org/10.1101/cshperspect.a032862

Kedersha, N., Cho, M. R., Li, W., Yacono, P. W., Chen, S., Gilks, N., Golan, D. E., & Anderson, P. (2000). Dynamic shuttling of TIA-1 accompanies the recruitment of mRNA to mammalian stress granules. *J Cell Biol*, *151*(6), 1257-1268. https://doi.org/10.1083/jcb.151.6.1257

Keffer-Wilkes, L. C., Veerareddygari, G. R., & Kothe, U. (2016). RNA modification enzyme TruB is a tRNA chaperone. *Proc Natl Acad Sci U S A*, *113*(50), 14306-14311. https://doi.org/10.1073/pnas.1607512113

Khakimova, M., Ahlgren, H. G., Harrison, J. J., English, A. M., & Nguyen, D. (2013). The stringent response controls catalases in Pseudomonas aeruginosa and is required for hydrogen

peroxide and antibiotic tolerance. *J Bacteriol*, *195*(9), 2011-2020. https://doi.org/10.1128/jb.02061-12

Kisly, I., & Tamm, T. (2023). Archaea/eukaryote-specific ribosomal proteins - guardians of a complex structure. *Comput Struct Biotechnol J*, *21*, 1249-1261. https://doi.org/10.1016/j.csbj.2023.01.037

Kobayashi, K., Kikuno, I., Kuroha, K., Saito, K., Ito, K., Ishitani, R., Inada, T., & Nureki, O. (2010). Structural basis for mRNA surveillance by archaeal Pelota and GTP-bound EF1α complex. *Proc Natl Acad Sci U S A*, *107*(41), 17575-17579. https://doi.org/10.1073/pnas.1009598107

Kobayashi, K., Saito, K., Ishitani, R., Ito, K., & Nureki, O. (2012). Structural basis for translation termination by archaeal RF1 and GTP-bound EF1α complex. *Nucleic Acids Res*, *40*(18), 9319-9328. https://doi.org/10.1093/nar/gks660

Koch, M., Flür, S., Kreutz, C., Ennifar, E., Micura, R., & Polacek, N. (2015). Role of a ribosomal RNA phosphate oxygen during the EF-G-triggered GTP hydrolysis. *Proc Natl Acad Sci U S A*, *112*(20), E2561-2568. https://doi.org/10.1073/pnas.1505231112

Kolberg, J., Høiby, E. A., Lopez, R., & Sletten, K. (1997). Monoclonal antibodies against Streptococcus pneumoniae detect epitopes on eubacterial ribosomal proteins L7/L12 and on streptococcal elongation factor Ts. *Microbiology (Reading)*, *143 (Pt 1)*, 55-61. https://doi.org/10.1099/00221287-143-1-55

Koller-Eichhorn, R., Marquardt, T., Gail, R., Wittinghofer, A., Kostrewa, D., Kutay, U., & Kambach, C. (2007). Human OLA1 defines an ATPase subfamily in the Obg family of GTP-binding proteins. *J Biol Chem*, *282*(27), 19928-19937. https://doi.org/10.1074/jbc.M700541200

Koller, T. O., Turnbull, K. J., Vaitkevicius, K., Crowe-McAuliffe, C., Roghanian, M., Bulvas, O., Nakamoto, J. A., Kurata, T., Julius, C., Atkinson, G. C., Johansson, J., Hauryliuk, V., & Wilson, D. N. (2022). Structural basis for HflXr-mediated antibiotic resistance in Listeria monocytogenes. *Nucleic Acids Res*, *50*(19), 11285-11300. https://doi.org/10.1093/nar/gkac934

Komoda, T., Sato, N. S., Phelps, S. S., Namba, N., Joseph, S., & Suzuki, T. (2006). The A-site finger in 23 S rRNA acts as a functional attenuator for translocation. *J Biol Chem*, *281*(43), 32303-32309. https://doi.org/10.1074/jbc.M607058200

Koonin, E. V. (2012). Does the central dogma still stand? *Biol Direct*, *7*, 27. https://doi.org/10.1186/1745-6150-7-27

Kudla, G., Murray, A. W., Tollervey, D., & Plotkin, J. B. (2009). Coding-sequence determinants of gene expression in Escherichia coli. *Science*, *324*(5924), 255-258. https://doi.org/10.1126/science.1170160

Kudrin, P., Dzhygyr, I., Ishiguro, K., Beljantseva, J., Maksimova, E., Oliveira, S. R. A., Varik, V., Payoe, R., Konevega, A. L., Tenson, T., Suzuki, T., & Hauryliuk, V. (2018). The ribosomal A-site finger is crucial for binding and activation of the stringent factor RelA. *Nucleic Acids Res*, *46*(4), 1973-1983. https://doi.org/10.1093/nar/gky023

Kunzmann, A., Brennicke, A., & Marchfelder, A. (1998). 5' end maturation and RNA editing have to precede tRNA 3' processing in plant mitochondria. *Proc Natl Acad Sci U S A*, *95*(1), 108-113. https://doi.org/10.1073/pnas.95.1.108

Kushwaha, G. S., Bange, G., & Bhavesh, N. S. (2019). Interaction studies on bacterial stringent response protein RelA with uncharged tRNA provide evidence for its prerequisite complex for ribosome binding. *Curr Genet*, *65*(5), 1173-1184. https://doi.org/10.1007/s00294-019-00966-y

Landwehr, V., Milanov, M., Angebauer, L., Hong, J., Jüngert, G., Hiersemenzel, A., Siebler, A., Schmit, F., Öztürk, Y., Dannenmaier, S., Drepper, F., Warscheid, B., & Koch, H. G. (2021).

The Universally Conserved ATPase YchF Regulates Translation of Leaderless mRNA in Response to Stress Conditions. *Front Mol Biosci*, *8*, 643696. https://doi.org/10.3389/fmolb.2021.643696

LaRiviere, F. J., Wolfson, A. D., & Uhlenbeck, O. C. (2001). Uniform binding of aminoacyl-tRNAs to elongation factor Tu by thermodynamic compensation. *Science*, *294*(5540), 165-168. https://doi.org/10.1126/science.1064242

Lechler, A., & Kreutzer, R. (1998). The phenylalanyl-tRNA synthetase specifically binds DNA. *J Mol Biol*, *278*(5), 897-901. https://doi.org/10.1006/jmbi.1998.1744

Leipe, D. D., Wolf, Y. I., Koonin, E. V., & Aravind, L. (2002). Classification and evolution of P-loop GTPases and related ATPases. *J Mol Biol*, *317*(1), 41-72. https://doi.org/10.1006/jmbi.2001.5378

Lescot, M., Hingamp, P., Kojima, K. K., Villar, E., Romac, S., Veluchamy, A., Boccara, M., Jaillon, O., Iudicone, D., Bowler, C., Wincker, P., Claverie, J. M., & Ogata, H. (2016). Reverse transcriptase genes are highly abundant and transcriptionally active in marine plankton assemblages. *Isme j*, *10*(5), 1134-1146. https://doi.org/10.1038/ismej.2015.192

Lin, Z., Li, R., Han, Z., Liu, Y., Gao, L., Huang, S., Miao, Y., & Miao, R. (2023). The Universally Conserved Unconventional G Protein YchF Is Critical for Growth and Stress Response. *Life (Basel)*, *13*(4). https://doi.org/10.3390/life13041058

Liu, K., Bittner, A. N., & Wang, J. D. (2015). Diversity in (p)ppGpp metabolism and effectors. *Curr Opin Microbiol*, *24*, 72-79. https://doi.org/10.1016/j.mib.2015.01.012

Liu, Q., & Fredrick, K. (2016). Intersubunit Bridges of the Bacterial Ribosome. *J Mol Biol*, *428*(10 Pt B), 2146-2164. https://doi.org/10.1016/j.jmb.2016.02.009

Liu, Y., Kong, X. X., He, J. J., Xu, Y. B., Zhang, J. K., Zou, L. Y., Ding, K. F., & Xu, D. (2022). OLA1 promotes colorectal cancer tumorigenesis by activation of HIF1α/CA9 axis. *BMC Cancer*, *22*(1), 424. https://doi.org/10.1186/s12885-022-09508-1

Lokanath, N. K., Yamamoto, H., Matsunaga, E., Sugahara, M., & Kunishima, N. (2005). Purification, crystallization and initial X-ray crystallographic analysis of the putative GTPase PH0525 from Pyrococcus horikoshii OT3. *Acta Crystallogr Sect F Struct Biol Cryst Commun*, *61*(Pt 10), 892-894. https://doi.org/10.1107/s1744309105027752

Lorenz, C., Lünse, C. E., & Mörl, M. (2017). tRNA Modifications: Impact on Structure and Thermal Adaptation. *Biomolecules*, *7*(2). https://doi.org/10.3390/biom7020035

Lu, J., Jia, J., Zhang, J., & Liu, X. (2021). HIV p17 enhances T cell proliferation by suppressing autophagy through the p17-OLA1-GSK3β axis under nutrient starvation. *J Med Virol*, *93*(6), 3607-3620. https://doi.org/10.1002/jmv.26423

Lu, S., Han, L., Hu, X., Sun, T., Xu, D., Li, Y., Chen, Q., Yao, W., He, M., Wang, Z., Wu, H., & Wei, M. (2021). N6-methyladenosine reader IMP2 stabilizes the ZFAS1/OLA1 axis and activates the Warburg effect: implication in colorectal cancer. *J Hematol Oncol*, *14*(1), 188. https://doi.org/10.1186/s13045-021-01204-0

Lucas, M. C., Pryszcz, L. P., Medina, R., Milenkovic, I., Camacho, N., Marchand, V., Motorin, Y., Ribas de Pouplana, L., & Novoa, E. M. (2023). Quantitative analysis of tRNA abundance and modifications by nanopore RNA sequencing. *Nat Biotechnol*. https://doi.org/10.1038/s41587-023-01743-6

Madeira, F., Pearce, M., Tivey, A. R. N., Basutkar, P., Lee, J., Edbali, O., Madhusoodanan, N., Kolesnikov, A., & Lopez, R. (2022). Search and sequence analysis tools services from EMBL-EBI in 2022. *Nucleic Acids Res*, *50*(W1), W276-w279. https://doi.org/10.1093/nar/gkac240

Mao, R. F., Rubio, V., Chen, H., Bai, L., Mansour, O. C., & Shi, Z. Z. (2013). OLA1 protects cells in heat shock by stabilizing HSP70. *Cell Death Dis*, *4*(2), e491. https://doi.org/10.1038/cddis.2013.23

Mateyak, M. K., & Kinzy, T. G. (2010). eEF1A: thinking outside the ribosome. *J Biol Chem*, *285*(28), 21209-21213. https://doi.org/10.1074/jbc.R110.113795

Matsuzawa, A., Kanno, S., Nakayama, M., Mochiduki, H., Wei, L., Shimaoka, T., Furukawa, Y., Kato, K., Shibata, S., Yasui, A., Ishioka, C., & Chiba, N. (2014). The BRCA1/BARD1-interacting protein OLA1 functions in centrosome regulation. *Mol Cell*, *53*(1), 101-114. https://doi.org/10.1016/j.molcel.2013.10.028

Mayer, O., Rajkowitsch, L., Lorenz, C., Konrat, R., & Schroeder, R. (2007). RNA chaperone activity and RNA-binding properties of the E. coli protein StpA. *Nucleic Acids Res*, *35*(4), 1257-1269. https://doi.org/10.1093/nar/gkl1143

Melnikov, S., Manakongtreecheep, K., & Söll, D. (2018). Revising the Structural Diversity of Ribosomal Proteins Across the Three Domains of Life. *Mol Biol Evol*, *35*(7), 1588-1598. https://doi.org/10.1093/molbev/msy021

Meng, K., Chung, C. Z., Söll, D., & Krahn, N. (2022). Unconventional genetic code systems in archaea. *Front Microbiol*, *13*, 1007832. https://doi.org/10.3389/fmicb.2022.1007832

Merrick, W. C., & Pavitt, G. D. (2018). Protein Synthesis Initiation in Eukaryotic Cells. *Cold Spring Harb Perspect Biol*, *10*(12). https://doi.org/10.1101/cshperspect.a033092

Milon, P., Konevega, A. L., Peske, F., Fabbretti, A., Gualerzi, C. O., & Rodnina, M. V. (2007). Transient kinetics, fluorescence, and FRET in studies of initiation of translation in bacteria. *Methods Enzymol*, *430*, 1-30. https://doi.org/10.1016/s0076-6879(07)30001-3

Milón, P., & Rodnina, M. V. (2012). Kinetic control of translation initiation in bacteria. *Crit Rev Biochem Mol Biol*, *47*(4), 334-348. https://doi.org/10.3109/10409238.2012.678284

Mitkevich, V. A., Ermakov, A., Kulikova, A. A., Tankov, S., Shyp, V., Soosaar, A., Tenson, T., Makarov, A. A., Ehrenberg, M., & Hauryliuk, V. (2010). Thermodynamic characterization of ppGpp binding to EF-G or IF2 and of initiator tRNA binding to free IF2 in the presence of GDP, GTP, or ppGpp. *J Mol Biol*, *402*(5), 838-846. https://doi.org/10.1016/j.jmb.2010.08.016

Mitkevich, V. A., Shyp, V., Petrushanko, I. Y., Soosaar, A., Atkinson, G. C., Tenson, T., Makarov, A. A., & Hauryliuk, V. (2012). GTPases IF2 and EF-G bind GDP and the SRL RNA in a mutually exclusive manner. *Sci Rep*, *2*, 843. https://doi.org/10.1038/srep00843

Mohr, D., Wintermeyer, W., & Rodnina, M. V. (2002). GTPase activation of elongation factors Tu and G on the ribosome. *Biochemistry*, *41*(41), 12520-12528. https://doi.org/10.1021/bi026301y

Moor, N., Kotik-Kogan, O., Tworowski, D., Sukhanova, M., & Safro, M. (2006). The crystal structure of the ternary complex of phenylalanyl-tRNA synthetase with tRNAPhe and a phenylalanyl-adenylate analogue reveals a conformational switch of the CCA end. *Biochemistry*, *45*(35), 10572-10583. https://doi.org/10.1021/bi060491l

Moore, P. B. (1995). Molecular mimicry in protein synthesis? *Science*, *270*(5241), 1453-1454. https://doi.org/10.1126/science.270.5241.1453

Morikawa, K., la Cour, T. F., Nyborg, J., Rasmussen, K. M., Miller, D. L., & Clark, B. F. (1978). High resolution x-ray crystallographic analysis of a modified form of the elongation factor Tu: guanosine diphosphate complex. *J Mol Biol*, *125*(3), 325-338. https://doi.org/10.1016/0022-2836(78)90406-0

Morimoto, T., Loh, P. C., Hirai, T., Asai, K., Kobayashi, K., Moriya, S., & Ogasawara, N. (2002). Six GTP-binding proteins of the Era/Obg family are essential for cell growth in Bacillus

subtilis. *Microbiology (Reading)*, *148*(Pt 11), 3539-3552. https://doi.org/10.1099/00221287-148-11-3539

Morse, J. C., Girodat, D., Burnett, B. J., Holm, M., Altman, R. B., Sanbonmatsu, K. Y., Wieden, H. J., & Blanchard, S. C. (2020). Elongation factor-Tu can repetitively engage aminoacyl-tRNA within the ribosome during the proofreading stage of tRNA selection. *Proc Natl Acad Sci U S A*, *117*(7), 3610-3620. https://doi.org/10.1073/pnas.1904469117

Mushegian, A. R., & Koonin, E. V. (1996). A minimal gene set for cellular life derived by comparison of complete bacterial genomes. *Proc Natl Acad Sci U S A*, *93*(19), 10268-10273. https://doi.org/10.1073/pnas.93.19.10268

Narayan, A., Gopi, S., Fushman, D., & Naganathan, A. N. (2019). A binding cooperativity switch driven by synergistic structural swelling of an osmo-regulatory protein pair. *Nat Commun*, *10*(1), 1995. https://doi.org/10.1038/s41467-019-10002-9

Nelson, C., Mrozowich, T., Gemmill, D. L., Park, S. M., & Patel, T. R. (2021). Human DDX3X Unwinds Japanese Encephalitis and Zika Viral 5' Terminal Regions. *Int J Mol Sci*, *22*(1). https://doi.org/10.3390/ijms22010413

Nelson, C. R., Mrozowich, T., Park, S. M., D'Souza, S., Henrickson, A., Vigar, J. R. J., Wieden, H. J., Owens, R. J., Demeler, B., & Patel, T. R. (2020). Human DDX17 Unwinds Rift Valley Fever Virus Non-Coding RNAs. *Int J Mol Sci*, *22*(1). https://doi.org/10.3390/ijms22010054

Nissen, P., Kjeldgaard, M., Thirup, S., Polekhina, G., Reshetnikova, L., Clark, B. F., & Nyborg, J. (1995). Crystal structure of the ternary complex of Phe-tRNAPhe, EF-Tu, and a GTP analog. *Science*, *270*(5241), 1464-1472. https://doi.org/10.1126/science.270.5241.1464

Nürenberg-Goloub, E., Kratzat, H., Heinemann, H., Heuer, A., Kötter, P., Berninghausen, O., Becker, T., Tampé, R., & Beckmann, R. (2020). Molecular analysis of the ribosome recycling factor ABCE1 bound to the 30S post-splitting complex. *Embo j*, *39*(9), e103788. https://doi.org/10.15252/embj.2019103788

Nyborg, J., Nissen, P., Kjeldgaard, M., Thirup, S., Polekhina, G., & Clark, B. F. (1996). Structure of the ternary complex of EF-Tu: macromolecular mimicry in translation. *Trends Biochem Sci*, *21*(3), 81-82.

Nyborg, J., Nissen, P., Kjeldgaard, M., Thirup, S., Polekhina, G., Clark, B. F., & Reshetnikova, L. (1997). Macromolecular mimicry in protein biosynthesis. *Fold Des*, *2*(3), S7-11. https://doi.org/10.1016/s1359-0278(97)00056-4

Ochi, K., Nishizawa, T., Inaoka, T., Yamada, A., Hashimoto, K., Hosaka, T., Okamoto, S., & Ozeki, Y. (2012). Heterologous expression of a plant RelA-SpoT homologue results in increased stress tolerance in Saccharomyces cerevisiae by accumulation of the bacterial alarmone ppGpp. *Microbiology (Reading)*, *158*(Pt 8), 2213-2224. https://doi.org/10.1099/mic.0.057638-0

Oh, J. E., Freilinger, A., Gelpi, E., Pollak, A., Hengstschläger, M., & Lubec, G. (2007). Proteins involved in neuronal differentiation of neuroblastoma cell line N1E-115. *Electrophoresis*, *28*(12), 2009-2017. https://doi.org/10.1002/elps.200600833

Olinares, P. D., Ponnala, L., & van Wijk, K. J. (2010). Megadalton complexes in the chloroplast stroma of Arabidopsis thaliana characterized by size exclusion chromatography, mass spectrometry, and hierarchical clustering. *Mol Cell Proteomics*, *9*(7), 1594-1615. https://doi.org/10.1074/mcp.M000038-MCP201

Otsuka, K., Yoshino, Y., Qi, H., & Chiba, N. (2020). The Function of BARD1 in Centrosome Regulation in Cooperation with BRCA1/OLA1/RACK1. *Genes (Basel)*, *11*(8). https://doi.org/10.3390/genes11080842

Pabo, C. O., & Sauer, R. T. (1984). Protein-DNA recognition. *Annu Rev Biochem*, *53*, 293-321. https://doi.org/10.1146/annurev.bi.53.070184.001453

Paduch, M., Jeleń, F., & Otlewski, J. (2001). Structure of small G proteins and their regulators. *Acta Biochim Pol*, *48*(4), 829-850.

Pan, T. (2018). Modifications and functional genomics of human transfer RNA. *Cell Res*, *28*(4), 395-404. https://doi.org/10.1038/s41422-018-0013-y

Pape, T., Wintermeyer, W., & Rodnina, M. V. (1998). Complete kinetic mechanism of elongation factor Tu-dependent binding of aminoacyl-tRNA to the A site of the E. coli ribosome. *Embo j*, *17*(24), 7490-7497. https://doi.org/10.1093/emboj/17.24.7490

Parmeggiani, A., & Nissen, P. (2006). Elongation factor Tu-targeted antibiotics: four different structures, two mechanisms of action. *FEBS Lett*, *580*(19), 4576-4581. https://doi.org/10.1016/j.febslet.2006.07.039

Peterson, E. T., & Uhlenbeck, O. C. (1992). Determination of recognition nucleotides for Escherichia coli phenylalanyl-tRNA synthetase. *Biochemistry*, *31*(42), 10380-10389. https://doi.org/10.1021/bi00157a028

Phizicky, E. M., & Hopper, A. K. (2010). tRNA biology charges to the front. *Genes Dev*, *24*(17), 1832-1860. https://doi.org/10.1101/gad.1956510

Pisarev, A. V., Skabkin, M. A., Pisareva, V. P., Skabkina, O. V., Rakotondrafara, A. M., Hentze, M. W., Hellen, C. U., & Pestova, T. V. (2010). The role of ABCE1 in eukaryotic posttermination ribosomal recycling. *Mol Cell*, *37*(2), 196-210. https://doi.org/10.1016/j.molcel.2009.12.034

Poehlsgaard, J., & Douthwaite, S. (2005). The bacterial ribosome as a target for antibiotics. *Nat Rev Microbiol*, *3*(11), 870-881. https://doi.org/10.1038/nrmicro1265

Polkinghorne, A., Hogan, R. J., Vaughan, L., Summersgill, J. T., & Timms, P. (2006). Differential expression of chlamydial signal transduction genes in normal and interferon gamma-induced persistent Chlamydophila pneumoniae infections. *Microbes Infect*, *8*(1), 61-72. https://doi.org/10.1016/j.micinf.2005.05.018

Porat, J., Kothe, U., & Bayfield, M. A. (2021). Revisiting tRNA chaperones: New players in an ancient game. *Rna*, *27*(5), 543-559. https://doi.org/10.1261/rna.078428.120

Qiu, Y., Chan, S. T., Lin, L., Shek, T. L., Tsang, T. F., Zhang, Y., Ip, M., Chan, P. K., Blanchard, N., Hanquet, G., Zuo, Z., Yang, X., & Ma, C. (2019). Nusbiarylins, a new class of antimicrobial agents: Rational design of bacterial transcription inhibitors targeting the interaction between the NusB and NusE proteins. *Bioorg Chem*, *92*, 103203. https://doi.org/10.1016/j.bioorg.2019.103203

Radman, M. (2020). Dysfunction and toxicity of damaged proteins in the etiology of aging and age-related degenerative and malignant diseases. *Croat Med J*, *61*(2), 159-166. https://doi.org/10.3325/cmj.2020.61.159

Rajkowitsch, L., & Schroeder, R. (2007). Dissecting RNA chaperone activity. *Rna*, *13*(12), 2053-2060. https://doi.org/10.1261/rna.671807

Ramakrishnan, V. (2002). Ribosome structure and the mechanism of translation. *Cell*, *108*(4), 557-572. https://doi.org/10.1016/s0092-8674(02)00619-0

Reeve, B., Hargest, T., Gilbert, C., & Ellis, T. (2014). Predicting translation initiation rates for designing synthetic biology. *Front Bioeng Biotechnol*, *2*, 1. https://doi.org/10.3389/fbioe.2014.00001

Reidt, W., Wurz, R., Wanieck, K., Chu, H. H., & Puchta, H. (2006). A homologue of the breast cancer-associated gene BARD1 is involved in DNA repair in plants. *Embo j*, *25*(18), 4326-4337. https://doi.org/10.1038/sj.emboj.7601313

Roberts, L., & Wieden, H. J. (2022). The prokaryotic activity of the IGR IRESs is mediated by ribosomal protein S1. *Nucleic Acids Res*, *50*(16), 9355-9367. https://doi.org/10.1093/nar/gkac697

Rodnina, M. V. (2018). Translation in Prokaryotes. *Cold Spring Harb Perspect Biol*, *10*(9). https://doi.org/10.1101/cshperspect.a032664

Rodnina, M. V., Peske, F., Peng, B. Z., Belardinelli, R., & Wintermeyer, W. (2019). Converting GTP hydrolysis into motion: versatile translational elongation factor G. *Biol Chem*, *401*(1), 131-142. https://doi.org/10.1515/hsz-2019-0313

Rojas, A. M., Ehrenberg, M., Andersson, S. G., & Kurland, C. G. (1984). ppGpp inhibition of elongation factors Tu, G and Ts during polypeptide synthesis. *Mol Gen Genet*, *197*(1), 36-45. https://doi.org/10.1007/bf00327920

Rosler, K. S., Mercier, E., Andrews, I. C., & Wieden, H. J. (2015). Histidine 114 Is Critical for ATP Hydrolysis by the Universally Conserved ATPase YchF. *J Biol Chem*, *290*(30), 18650-18661. https://doi.org/10.1074/jbc.M114.598227

Rubio Gomez, M. A., & Ibba, M. (2020). Aminoacyl-tRNA synthetases. *Rna*, *26*(8), 910-936. https://doi.org/10.1261/rna.071720.119

Rudra, P., Hurst-Hess, K. R., Cotten, K. L., Partida-Miranda, A., & Ghosh, P. (2020). Mycobacterial HflX is a ribosome splitting factor that mediates antibiotic resistance. *Proc Natl Acad Sci U S A*, *117*(1), 629-634. https://doi.org/10.1073/pnas.1906748117

Rundlet, E. J., Holm, M., Schacherl, M., Natchiar, S. K., Altman, R. B., Spahn, C. M. T., Myasnikov, A. G., & Blanchard, S. C. (2021). Structural basis of early translocation events on the ribosome. *Nature*, *595*(7869), 741-745. https://doi.org/10.1038/s41586-021-03713-x

Ryder, S. P., Recht, M. I., & Williamson, J. R. (2008). Quantitative analysis of protein-RNA interactions by gel mobility shift. *Methods Mol Biol*, *488*, 99-115. https://doi.org/10.1007/978-1-60327-475-3_7

Saito, K., Kratzat, H., Campbell, A., Buschauer, R., Burroughs, A. M., Berninghausen, O., Aravind, L., Green, R., Beckmann, R., & Buskirk, A. R. (2022). Ribosome collisions induce mRNA cleavage and ribosome rescue in bacteria. *Nature*, *603*(7901), 503-508. https://doi.org/10.1038/s41586-022-04416-7

Samanfar, B., Tan le, H., Shostak, K., Chalabian, F., Wu, Z., Alamgir, M., Sunba, N., Burnside, D., Omidi, K., Hooshyar, M., Galván Márquez, I., Jessulat, M., Smith, M. L., Babu, M., Azizi, A., & Golshani, A. (2014). A global investigation of gene deletion strains that affect premature stop codon bypass in yeast, Saccharomyces cerevisiae. *Mol Biosyst*, *10*(4), 916-924. https://doi.org/10.1039/c3mb70501c

Sampson, J. R., & Uhlenbeck, O. C. (1988). Biochemical and physical characterization of an unmodified yeast phenylalanine transfer RNA transcribed in vitro. *Proc Natl Acad Sci U S A*, *85*(4), 1033-1037. https://doi.org/10.1073/pnas.85.4.1033

Sankaranarayanan, R., Dock-Bregeon, A. C., Romby, P., Caillet, J., Springer, M., Rees, B., Ehresmann, C., Ehresmann, B., & Moras, D. (1999). The structure of threonyl-tRNA synthetase-tRNA(Thr) complex enlightens its repressor activity and reveals an essential zinc ion in the active site. *Cell*, *97*(3), 371-381. https://doi.org/10.1016/s0092-8674(00)80746-1

Saraste, M., Sibbald, P. R., & Wittinghofer, A. (1990). The P-loop--a common motif in ATP- and GTP-binding proteins. *Trends Biochem Sci*, *15*(11), 430-434. https://doi.org/10.1016/0968-0004(90)90281-f

Schmitt, E., Coureux, P. D., Kazan, R., Bourgeois, G., Lazennec-Schurdevin, C., & Mechulam, Y. (2020). Recent Advances in Archaeal Translation Initiation. *Front Microbiol*, *11*, 584152. https://doi.org/10.3389/fmicb.2020.584152

Schultz, A., Olorundami, O. A., Teng, R. J., Jarzembowski, J., Shi, Z. Z., Kumar, S. N., Pritchard, K., Jr., Konduri, G. G., & Afolayan, A. J. (2019). Decreased OLA1 (Obg-Like ATPase-1) Expression Drives Ubiquitin-Proteasome Pathways to Downregulate Mitochondrial SOD2

(Superoxide Dismutase) in Persistent Pulmonary Hypertension of the Newborn. *Hypertension*, *74*(4), 957-966. https://doi.org/10.1161/hypertensionaha.119.13430

Schultz, S. K., & Kothe, U. (2020). tRNA elbow modifications affect the tRNA pseudouridine synthase TruB and the methyltransferase TrmA. *Rna*, *26*(9), 1131-1142. https://doi.org/10.1261/rna.075473.120

Semrad, K. (2011). Proteins with RNA chaperone activity: a world of diverse proteins with a common task-impediment of RNA misfolding. *Biochem Res Int*, *2011*, 532908. https://doi.org/10.1155/2011/532908

Shah, P., Ding, Y., Niemczyk, M., Kudla, G., & Plotkin, J. B. (2013). Rate-limiting steps in yeast protein translation. *Cell*, *153*(7), 1589-1601. https://doi.org/10.1016/j.cell.2013.05.049

Shi, X., Khade, P. K., Sanbonmatsu, K. Y., & Joseph, S. (2012). Functional role of the sarcin-ricin loop of the 23S rRNA in the elongation cycle of protein synthesis. *J Mol Biol*, *419*(3-4), 125-138. https://doi.org/10.1016/j.jmb.2012.03.016

Shin, J. H., Gulesserian, T., Weitzdoerfer, R., Fountoulakis, M., & Lubec, G. (2004). Derangement of hypothetical proteins in fetal Down's syndrome brain. *Neurochem Res*, *29*(6), 1307-1316. https://doi.org/10.1023/b:nere.0000023617.49590.19

Shine, J., & Dalgarno, L. (1975). Determinant of cistron specificity in bacterial ribosomes. *Nature*, *254*(5495), 34-38. https://doi.org/10.1038/254034a0

Sidlowski, P., Czerwinski, A., Liu, Y., Liu, P., Teng, R. J., Kumar, S., Wells, C., Pritchard, K., Jr., Konduri, G. G., & Afolayan, A. J. (2023). OLA1 Phosphorylation Governs the Mitochondrial Bioenergetic Function of Pulmonary Vascular Cells. *Am J Respir Cell Mol Biol*, *68*(4), 395-405. https://doi.org/10.1165/rcmb.2022-0186OC

Sonenberg, N., & Hinnebusch, A. G. (2009). Regulation of translation initiation in eukaryotes: mechanisms and biological targets. *Cell*, *136*(4), 731-745. https://doi.org/10.1016/j.cell.2009.01.042

Sonneveld, S., Verhagen, B. M. P., & Tanenbaum, M. E. (2020). Heterogeneity in mRNA Translation. *Trends Cell Biol*, *30*(8), 606-618. https://doi.org/10.1016/j.tcb.2020.04.008

Sprang, S. R. (1997). G protein mechanisms: insights from structural analysis. *Annu Rev Biochem*, *66*, 639-678. https://doi.org/10.1146/annurev.biochem.66.1.639

Steitz, T. A. (1999). DNA polymerases: structural diversity and common mechanisms. *J Biol Chem*, *274*(25), 17395-17398. https://doi.org/10.1074/jbc.274.25.17395

Sun, H., Luo, X., Montalbano, J., Jin, W., Shi, J., Sheikh, M. S., & Huang, Y. (2010). DOC45, a novel DNA damage-regulated nucleocytoplasmic ATPase that is overexpressed in multiple human malignancies. *Mol Cancer Res*, *8*(1), 57-66. https://doi.org/10.1158/1541-7786.Mcr-09-0278

Takada, H., Roghanian, M., Caballero-Montes, J., Van Nerom, K., Jimmy, S., Kudrin, P., Trebini, F., Murayama, R., Akanuma, G., Garcia-Pino, A., & Hauryliuk, V. (2021). Ribosome association primes the stringent factor Rel for tRNA-dependent locking in the A-site and activation of (p)ppGpp synthesis. *Nucleic Acids Res*, *49*(1), 444-457. https://doi.org/10.1093/nar/gkaa1187

Tamura, K., Himeno, H., Asahara, H., Hasegawa, T., & Shimizu, M. (1992). In vitro study of E.coli tRNA(Arg) and tRNA(Lys) identity elements. *Nucleic Acids Res*, *20*(9), 2335-2339. https://doi.org/10.1093/nar/20.9.2335

Tamura, T., Matsuzawa, T., Oji, S., Ichikawa, N., Hosoyama, A., Katsumata, H., Yamazoe, A., Hamada, M., Suzuki, K., Gonoi, T., & Fujita, N. (2012). A genome sequence-based approach to taxonomy of the genus Nocardia. *Antonie Van Leeuwenhoek*, *102*(3), 481-491. https://doi.org/10.1007/s10482-012-9780-5

Tawde, M., Bior, A., Feiss, M., Teng, F., & Freimuth, P. (2022). A polypeptide model for toxic aberrant proteins induced by aminoglycoside antibiotics. *PLoS One*, *17*(4), e0258794. https://doi.org/10.1371/journal.pone.0258794

Temin, H. M. (1985). Reverse transcription in the eukaryotic genome: retroviruses, pararetroviruses, retrotransposons, and retrotranscripts. *Mol Biol Evol*, *2*(6), 455-468. https://doi.org/10.1093/oxfordjournals.molbev.a040365

Teplyakov, A., Obmolova, G., Chu, S. Y., Toedt, J., Eisenstein, E., Howard, A. J., & Gilliland, G. L. (2003). Crystal structure of the YchF protein reveals binding sites for GTP and nucleic acid. *J Bacteriol*, *185*(14), 4031-4037. https://doi.org/10.1128/jb.185.14.4031-4037.2003

Tomar, S. K., Kumar, P., & Prakash, B. (2011). Deciphering the catalytic machinery in a universally conserved ribosome binding ATPase YchF. *Biochem Biophys Res Commun*, *408*(3), 459-464. https://doi.org/10.1016/j.bbrc.2011.04.052

Trapp, O., Seeliger, K., & Puchta, H. (2011). Homologs of breast cancer genes in plants. *Front Plant Sci*, *2*, 19. https://doi.org/10.3389/fpls.2011.00019

Tsukamoto, Y., Nakamura, Y., Hirata, M., Sakate, R., & Kimura, T. (2022). i-tRAP (individual tRNA acylation PCR): A convenient method for selective quantification of tRNA charging. *Rna*, *29*(1), 111-122. https://doi.org/10.1261/rna.079323.122

Tweedie, A., & Nissan, T. (2021). Hiding in Plain Sight: Formation and Function of Stress Granules During Microbial Infection of Mammalian Cells. *Front Mol Biosci*, *8*, 647884. https://doi.org/10.3389/fmolb.2021.647884

Udagawa, T., Shimizu, Y., & Ueda, T. (2004). Evidence for the translation initiation of leaderless mRNAs by the intact 70 S ribosome without its dissociation into subunits in eubacteria. *J Biol Chem*, *279*(10), 8539-8546. https://doi.org/10.1074/jbc.M308784200

Ude, S., Lassak, J., Starosta, A. L., Kraxenberger, T., Wilson, D. N., & Jung, K. (2013). Translation elongation factor EF-P alleviates ribosome stalling at polyproline stretches. *Science*, *339*(6115), 82-85. https://doi.org/10.1126/science.1228985

VanBogelen, R. A., Kelley, P. M., & Neidhardt, F. C. (1987). Differential induction of heat shock, SOS, and oxidation stress regulons and accumulation of nucleotides in Escherichia coli. *J Bacteriol*, *169*(1), 26-32. https://doi.org/10.1128/jb.169.1.26-32.1987

Vasilyev, N., Gao, A., & Serganov, A. (2019). Noncanonical features and modifications on the 5'-end of bacterial sRNAs and mRNAs. *Wiley Interdiscip Rev RNA*, *10*(2), e1509. https://doi.org/10.1002/wrna.1509

Verstraeten, N., Fauvart, M., Versées, W., & Michiels, J. (2011). The universally conserved prokaryotic GTPases. *Microbiol Mol Biol Rev*, *75*(3), 507-542, second and third pages of table of contents. https://doi.org/10.1128/mmbr.00009-11

Vetter, I. R., & Wittinghofer, A. (2001). The guanine nucleotide-binding switch in three dimensions. *Science*, *294*(5545), 1299-1304. https://doi.org/10.1126/science.1062023

Voorhees, R. M., Schmeing, T. M., Kelley, A. C., & Ramakrishnan, V. (2010). The mechanism for activation of GTP hydrolysis on the ribosome. *Science*, *330*(6005), 835-838. https://doi.org/10.1126/science.1194460

Vorstenbosch, E. L., Potapov, A. P., de Graaf, J. M., & Kraal, B. (2000). The effect of mutations in EF-Tu on its affinity for tRNA as measured by two novel and independent methods of general applicability. *J Biochem Biophys Methods*, *42*(1-2), 1-14. https://doi.org/10.1016/s0165-022x(99)00032-9

Wallace, E. W., Kear-Scott, J. L., Pilipenko, E. V., Schwartz, M. H., Laskowski, P. R., Rojek, A. E., Katanski, C. D., Riback, J. A., Dion, M. F., Franks, A. M., Airoldi, E. M., Pan, T., Budnik, B. A., & Drummond, D. A. (2015). Reversible, Specific, Active Aggregates of Endogenous

Proteins Assemble upon Heat Stress. *Cell*, *162*(6), 1286-1298. https://doi.org/10.1016/j.cell.2015.08.041

Wang, Y., Cao, P., Sun, P., Zhao, J., Sun, X., Zhang, J., Li, C., Xiang, W., & Wang, X. (2019). Cryobacterium tepidiphilum sp. nov., isolated from rhizosphere soil of lettuce (var. ramosa Hort.). *Antonie Van Leeuwenhoek*, *112*(11), 1611-1621. https://doi.org/10.1007/s10482-019-01287-3

Weisser, M., & Ban, N. (2019). Extensions, Extra Factors, and Extreme Complexity: Ribosomal Structures Provide Insights into Eukaryotic Translation. *Cold Spring Harb Perspect Biol*, *11*(9). https://doi.org/10.1101/cshperspect.a032367

Wendrich, T. M., Blaha, G., Wilson, D. N., Marahiel, M. A., & Nierhaus, K. H. (2002). Dissection of the mechanism for the stringent factor RelA. *Mol Cell*, *10*(4), 779-788. https://doi.org/10.1016/s1097-2765(02)00656-1

Wenk, M., Ba, Q., Erichsen, V., MacInnes, K., Wiese, H., Warscheid, B., & Koch, H. G. (2012). A universally conserved ATPase regulates the oxidative stress response in Escherichia coli. *J Biol Chem*, *287*(52), 43585-43598. https://doi.org/10.1074/jbc.M112.413070

Wieden, H. J., Gromadski, K., Rodnin, D., & Rodnina, M. V. (2002). Mechanism of elongation factor (EF)-Ts-catalyzed nucleotide exchange in EF-Tu. Contribution of contacts at the guanine base. *J Biol Chem*, *277*(8), 6032-6036. https://doi.org/10.1074/jbc.M110888200

Wieden, H. J., Wintermeyer, W., & Rodnina, M. V. (2001). A common structural motif in elongation factor Ts and ribosomal protein L7/12 may be involved in the interaction with elongation factor Tu. *J Mol Evol*, *52*(2), 129-136. https://doi.org/10.1007/s002390010141

Wilson, D. N. (2009). The A-Z of bacterial translation inhibitors. *Crit Rev Biochem Mol Biol*, *44*(6), 393-433. https://doi.org/10.3109/10409230903307311

Wilson, D. N. (2014). Ribosome-targeting antibiotics and mechanisms of bacterial resistance. *Nat Rev Microbiol*, *12*(1), 35-48. https://doi.org/10.1038/nrmicro3155

Winther, K. S., Roghanian, M., & Gerdes, K. (2018). Activation of the Stringent Response by Loading of RelA-tRNA Complexes at the Ribosomal A-Site. *Mol Cell*, *70*(1), 95-105.e104. https://doi.org/10.1016/j.molcel.2018.02.033

Wittinghofer, A., & Vetter, I. R. (2011). Structure-function relationships of the G domain, a canonical switch motif. *Annu Rev Biochem*, *80*, 943-971. https://doi.org/10.1146/annurev-biochem-062708-134043

Wohlgemuth, I., Pohl, C., Mittelstaet, J., Konevega, A. L., & Rodnina, M. V. (2011). Evolutionary optimization of speed and accuracy of decoding on the ribosome. *Philos Trans R Soc Lond B Biol Sci*, *366*(1580), 2979-2986. https://doi.org/10.1098/rstb.2011.0138

World Health Organization. (2021, 17 November 2021). *Antimicrobial resistance*. Retrieved 01 June, 2023 from https://www.who.int/news-room/fact-sheets/detail/antimicrobial-resistance

Wright, J. R., Keffer-Wilkes, L. C., Dobing, S. R., & Kothe, U. (2011). Pre-steady-state kinetic analysis of the three Escherichia coli pseudouridine synthases TruB, TruA, and RluA reveals uniformly slow catalysis. *Rna*, *17*(12), 2074-2084. https://doi.org/10.1261/rna.2905811

Xie, D., Zhang, J., Ding, J., Yang, J., & Zhang, Y. (2020). OLA1 is responsible for normal spindle assembly and SAC activation in mouse oocytes. *PeerJ*, *8*, e8180. https://doi.org/10.7717/peerj.8180

Xu, B., Liu, L., & Song, G. (2021). Functions and Regulation of Translation Elongation Factors. *Front Mol Biosci*, *8*, 816398. https://doi.org/10.3389/fmolb.2021.816398

Xu, D., Song, R., Wang, G., Jeyabal, P. V., Weiskoff, A. M., Ding, K., & Shi, Z. Z. (2016). Obg-like ATPase 1 regulates global protein serine/threonine phosphorylation in cancer cells by

suppressing the GSK3β-inhibitor 2-PP1 positive feedback loop. *Oncotarget*, *7*(3), 3427-3439. https://doi.org/10.18632/oncotarget.6496

Yamamoto, H., Wittek, D., Gupta, R., Qin, B., Ueda, T., Krause, R., Yamamoto, K., Albrecht, R., Pech, M., & Nierhaus, K. H. (2016). 70S-scanning initiation is a novel and frequent initiation mode of ribosomal translation in bacteria. *Proc Natl Acad Sci U S A*, *113*(9), E1180-1189. https://doi.org/10.1073/pnas.1524554113

Yoshino, Y., Qi, H., Kanazawa, R., Sugamata, M., Suzuki, K., Kobayashi, A., Shindo, K., Matsuzawa, A., Shibata, S., Endo, S., Miyanishi, Y., Shimaoka, T., Ishioka, C., Kanno, S. I., Yasui, A., & Chiba, N. (2019). RACK1 regulates centriole duplication by controlling localization of BRCA1 to the centrosome in mammary tissue-derived cells. *Oncogene*, *38*(16), 3077-3092. https://doi.org/10.1038/s41388-018-0647-8

Yuan, H. X., Xiong, Y., & Guan, K. L. (2013). Nutrient sensing, metabolism, and cell growth control. *Mol Cell*, *49*(3), 379-387. https://doi.org/10.1016/j.molcel.2013.01.019

Yusupova, G., & Yusupov, M. (2015). Ribosome biochemistry in crystal structure determination. *Rna*, *21*(4), 771-773. https://doi.org/10.1261/rna.050039.115

Zavialov, A. V., Buckingham, R. H., & Ehrenberg, M. (2001). A posttermination ribosomal complex is the guanine nucleotide exchange factor for peptide release factor RF3. *Cell*, *107*(1), 115-124. https://doi.org/10.1016/s0092-8674(01)00508-6

Zeng, F., Li, X., Pires-Alves, M., Chen, X., Hawk, C. W., & Jin, H. (2021). Conserved heterodimeric GTPase Rbg1/Tma46 promotes efficient translation in eukaryotic cells. *Cell Rep*, *37*(4), 109877. https://doi.org/10.1016/j.celrep.2021.109877

Zhang, J. W., Rubio, V., Zheng, S., & Shi, Z. Z. (2009). Knockdown of OLA1, a regulator of oxidative stress response, inhibits motility and invasion of breast cancer cells. *J Zhejiang Univ Sci B*, *10*(11), 796-804. https://doi.org/10.1631/jzus.B0910009

Zhou, X., Liao, W. J., Liao, J. M., Liao, P., & Lu, H. (2015). Ribosomal proteins: functions beyond the ribosome. *J Mol Cell Biol*, *7*(2), 92-104. https://doi.org/10.1093/jmcb/mjv014

Zhu, M., Kuechler, E. R., Zhang, J., Matalon, O., Dubreuil, B., Hofmann, A., Loewen, C., Levy, E. D., Gsponer, J., & Mayor, T. (2020). Proteomic analysis reveals the direct recruitment of intrinsically disordered regions to stress granules in S. cerevisiae. *J Cell Sci*, *133*(13). https://doi.org/10.1242/jcs.244657

APPENDIX I. SUPPLEMENTAL MATERIALS TO CHAPTER 3

Objective 1: tRNA Binding

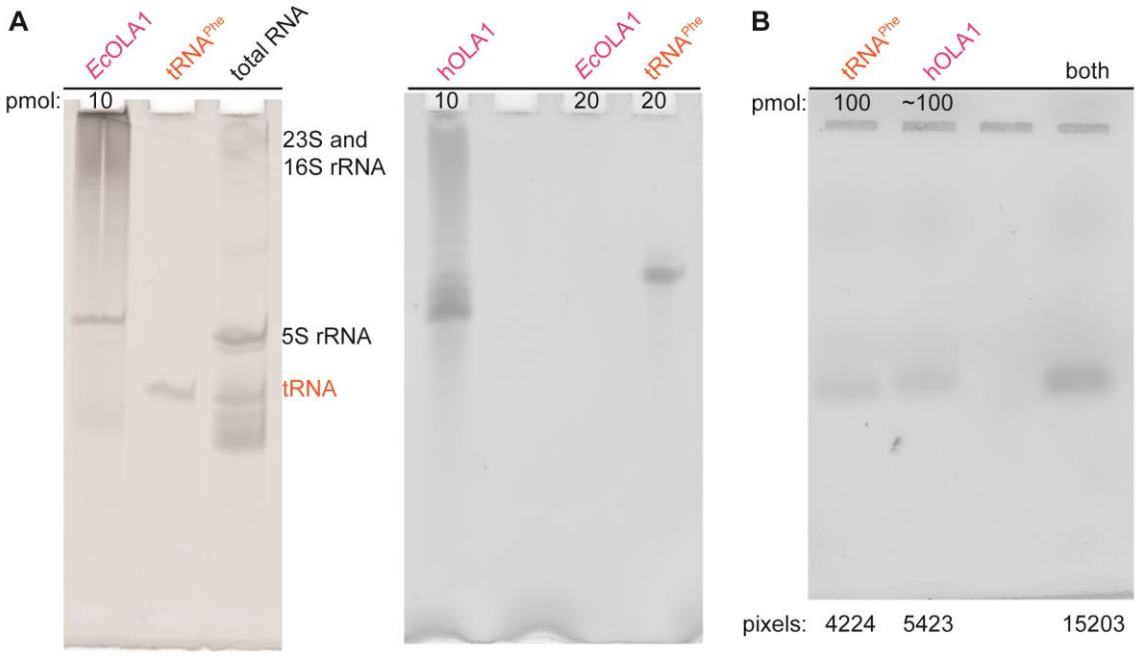

SFigure 1. Human and *E. coli* OLA1 co-elute with rRNA and tRNA during affinity chromatography purification. (**A**) Shown on 15% 8M urea polyacrylamide gels are IVT $tRNA^{Phe}$ and total RNA from *E. coli* K12 MG6155 as migration references along-side RNA that co-elutes with *Ec*OLA1 (L: 50 min, R: 37 min, 300V each). Anion exchange removes the bound RNA (L: *Ec*OLA1). (**B**) Without anion exchange, hOLA1 is roughly 100% tRNA-bound, as shown on a 1% agarose gel.

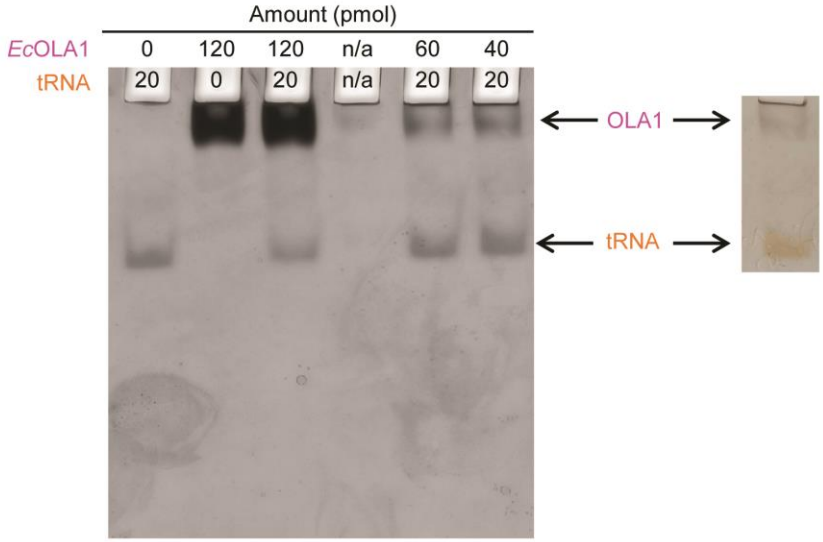

SFigure 2. Silver staining of RNA and protein. *Ec*OLA1 and IVT $tRNA^{Phe}$ are resolved on an 8% acrylamide native-PAGE (1xTAKM7-Ac, 125 V, 30 min). RNA stains brown and protein stains black.

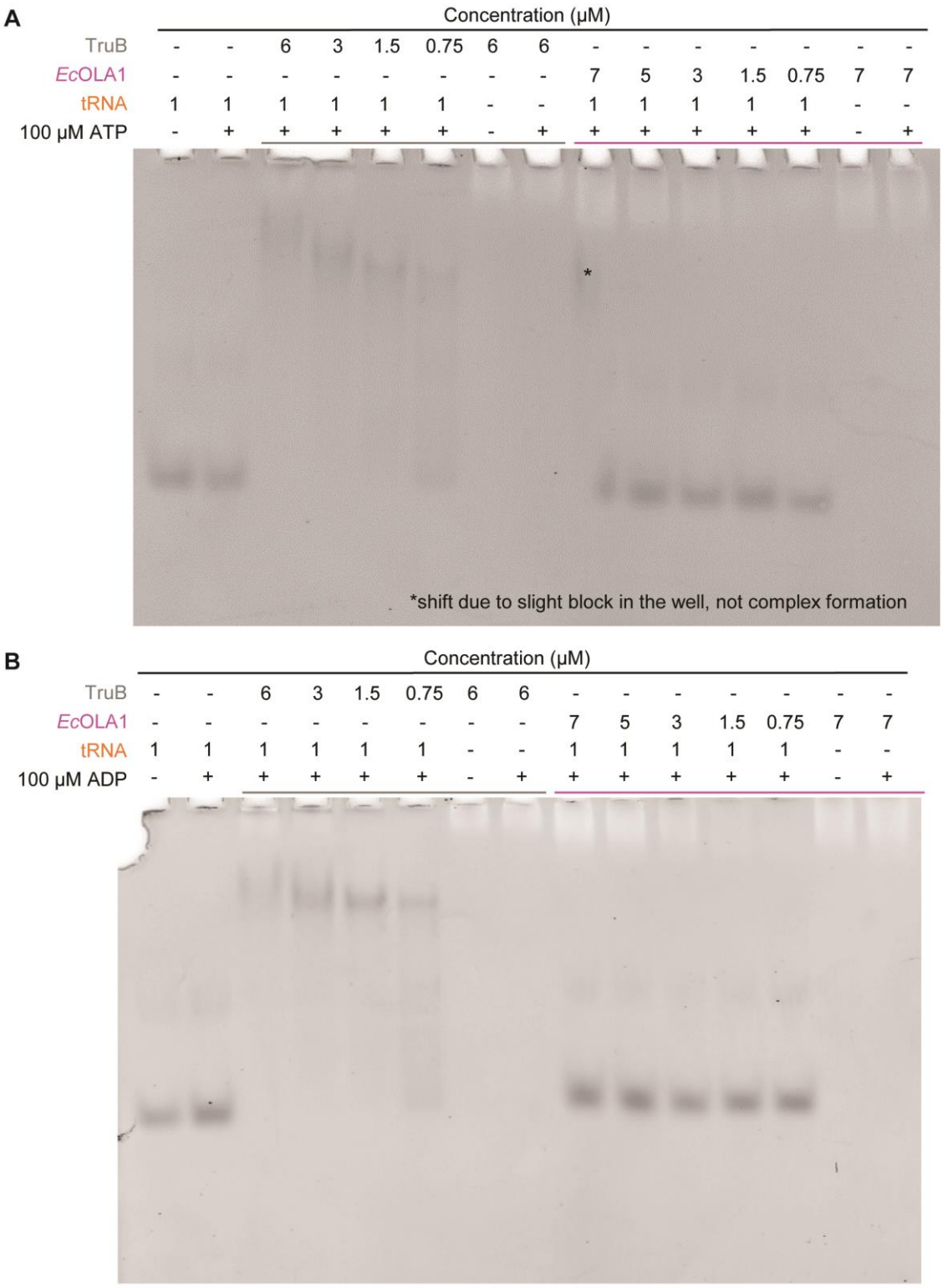

SFigure 3. *Ec*OLA1 does not shift the migration of IVT tRNA^{Phe} in the presence of (A) ATP or (B) ADP. In contrast, there is clearly a shift in tRNA migration with increasing concentration of TruB. Proteins are visible (white bands) as a result of Coomassie staining before EtBr staining.

Objective 2: RNA Remodeling

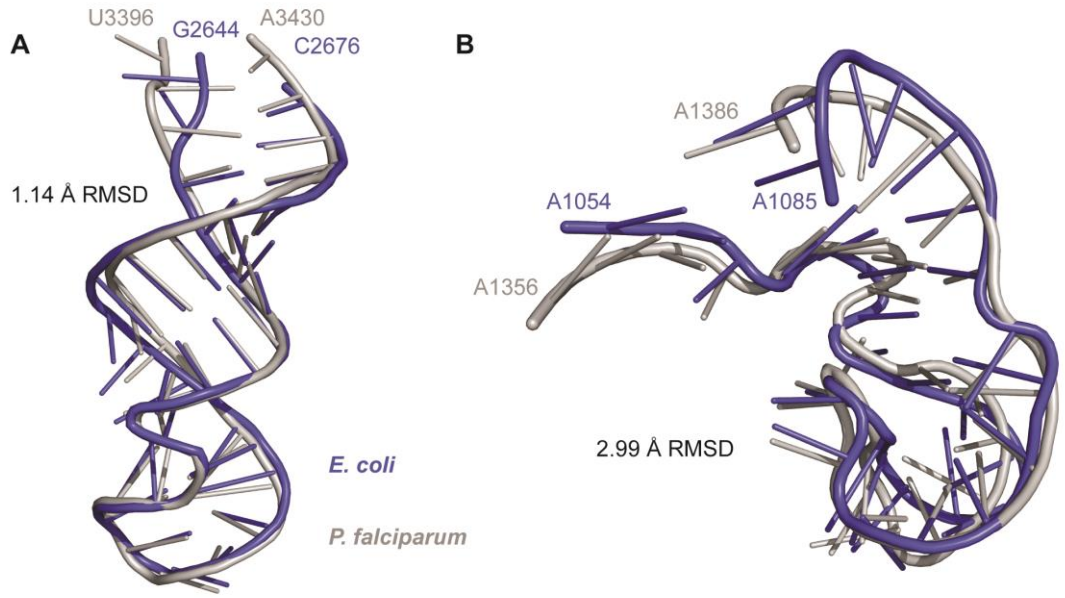

SFigure 4. The (A) SRL and (B) ASF conformations in *P. falciparum* (grey) and *E. coli* (blue, PDB 6BU8) are similar. The RMSD between the SRL structures and ASF structures is 1.14 Å and 2.99 Å, respectively. "Cealign" structural alignments were performed on Pymol.

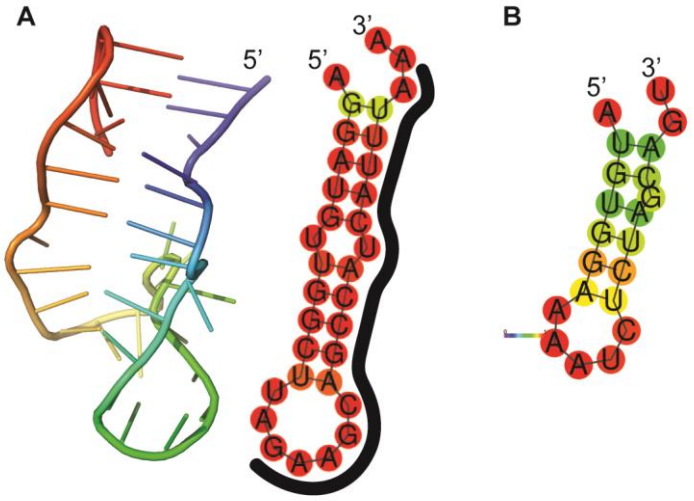

SFigure 5. Alternate helicase assay substrate. (A) The 3D (left) and predicted 2D (right) structures of the ASF rRNA shows potential nucleotide interactions within the stem. The tertiary structure of the ASF rRNA from the *E. coli* 70S ribosome (PDB: 6BU8) is shown in cartoon form and coloured rainbow from the 3' to 5' ends. The RNA secondary structure predicted by RNAfold has rainbow color-coding denoting the likeliness of an interaction, red being most likely and blue being least likely. The black line represents the portion of the ASF rRNA complementary to the fluorescent DNA-oligo. (B) The predicted 2D structure of one half of the RD RNA, which is entirely complementary to the fluorescent DNA oligo reporter sequence.

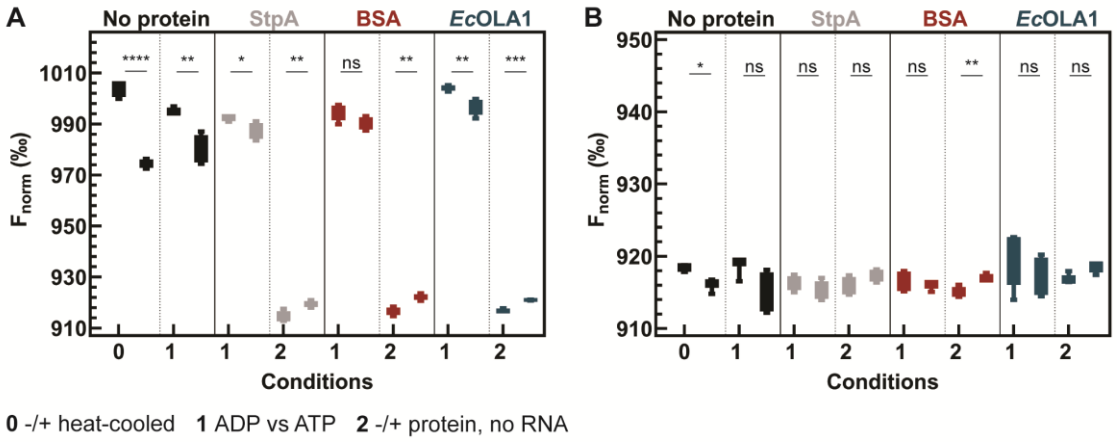

SFigure 6. Helicase assay results using the (A) A-site finger RNA and the (B) RNA-duplex RNA as substrate. A change in fluorescence is observed in the absence of ASF RNA and there is no change in signal for the RD positive controls. Each set of conditions tested is separated by dashed lines. The left box for each condition represents the result for the absence of the variable component and the right is the presence of the variable component. Results for absence of protein (black), for StpA (gray), for BSA (red), and for *Ec*OLA1 (blue) are separated by solid lines. The significance between F_{norm} (per mille) for each condition comparison is indicated, as measured by unpaired t-tests on GraphPad Prism 9 ((0.1234 (ns), 0.0322 (*), 0.0021 (**), 0.0002 (***), 0.0001 (****)).

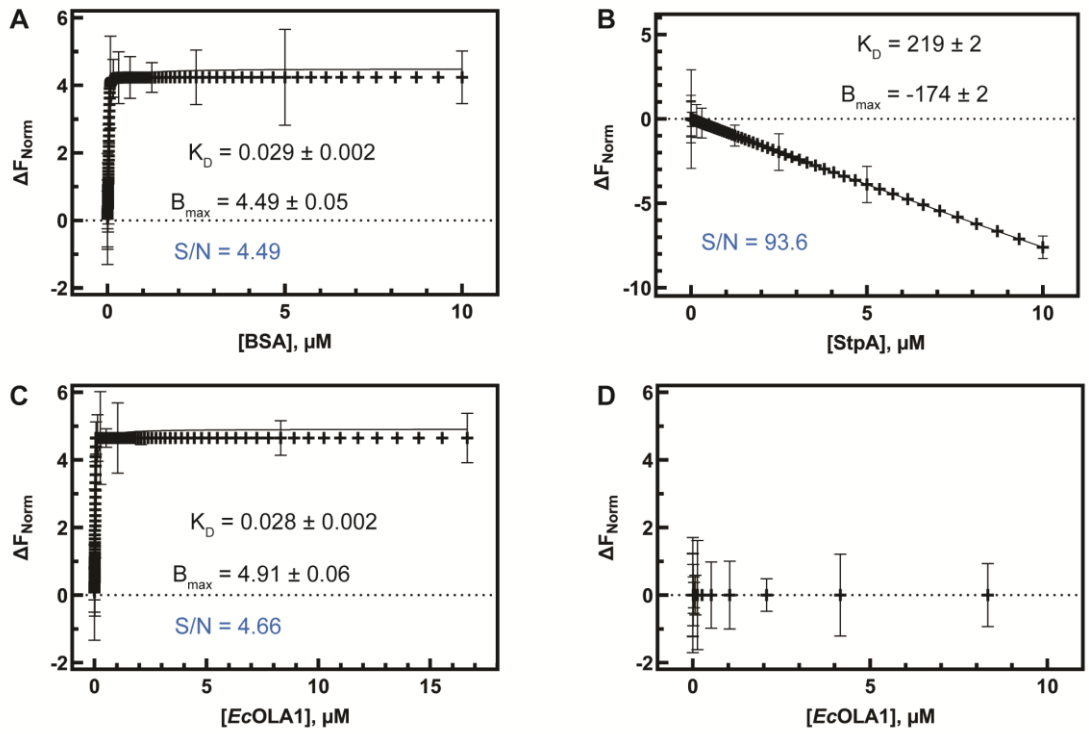

SFigure 7. MST binding affinity results suggest that (A) BSA, (B) StpA, and (C) *Ec*OLA1 interact with the DNA complementary for the ASF. (D) In contrast, *Ec*OLA1 does not interact with the DNA oligo complementary to the SRL.

SRL-complementary DNA did not change migration upon addition of proteins (figure 13, sfigure 7D), but ASF DNA did (sfigure 6A). MST binding affinity experiments further showed interactions of the ASF DNA with *Ec*OLA1, BSA, and StpA (sfigure 7A-C). Although the signal-to-noise ratio is high (93.6), suggesting an excellent assay, the K_D of StpA for ASF DNA was not experimentally relevant (218.696 ± 2.122 µM). The K_D's for *Ec*OLA1 and BSA binding to ASF DNA are 0.028 ± 0.002 and 0.029 ± 0.002 µM, respectively. Despite the tight binding, the signal-to-noise ratios are below 5. While more data is required to characterize the interaction between StpA, *Ec*OLA1, and BSA with this DNA, the results presented herein clearly show that this ASF construct is not appropriate helicase assay substrate.

In contrast to observing unexpected changes in F_{norm} with the ASF RNA/DNA, using the RD construct resulted in insignificant ΔF_{norm} for both positive controls: in the presence of StpA and when folding the RNA and DNA together. It is likely that if DNA-RNA annealing did occur the change in oligo size was too small to affect the thermophoresis.

No interaction was detectable between *Ec*OLA1 and the SRL DNA oligo (sfigure 7D), and the positive controls were a success, so this was the only substrate tested under other additional conditions.